Adaptive Façade

For Windload Reduction in High-rise

Graduation report
Sustainable design graduation studio (2014-2015)
MSc in Architecture, Urbanism and Building Sciences
Building Technology Track
Delft University of Technology

Student
Puttakhun Vongsingha
Student number: 4314395

Mentors
Peter Eigenraam
Prof.dr.ing. Ulrich Knaack

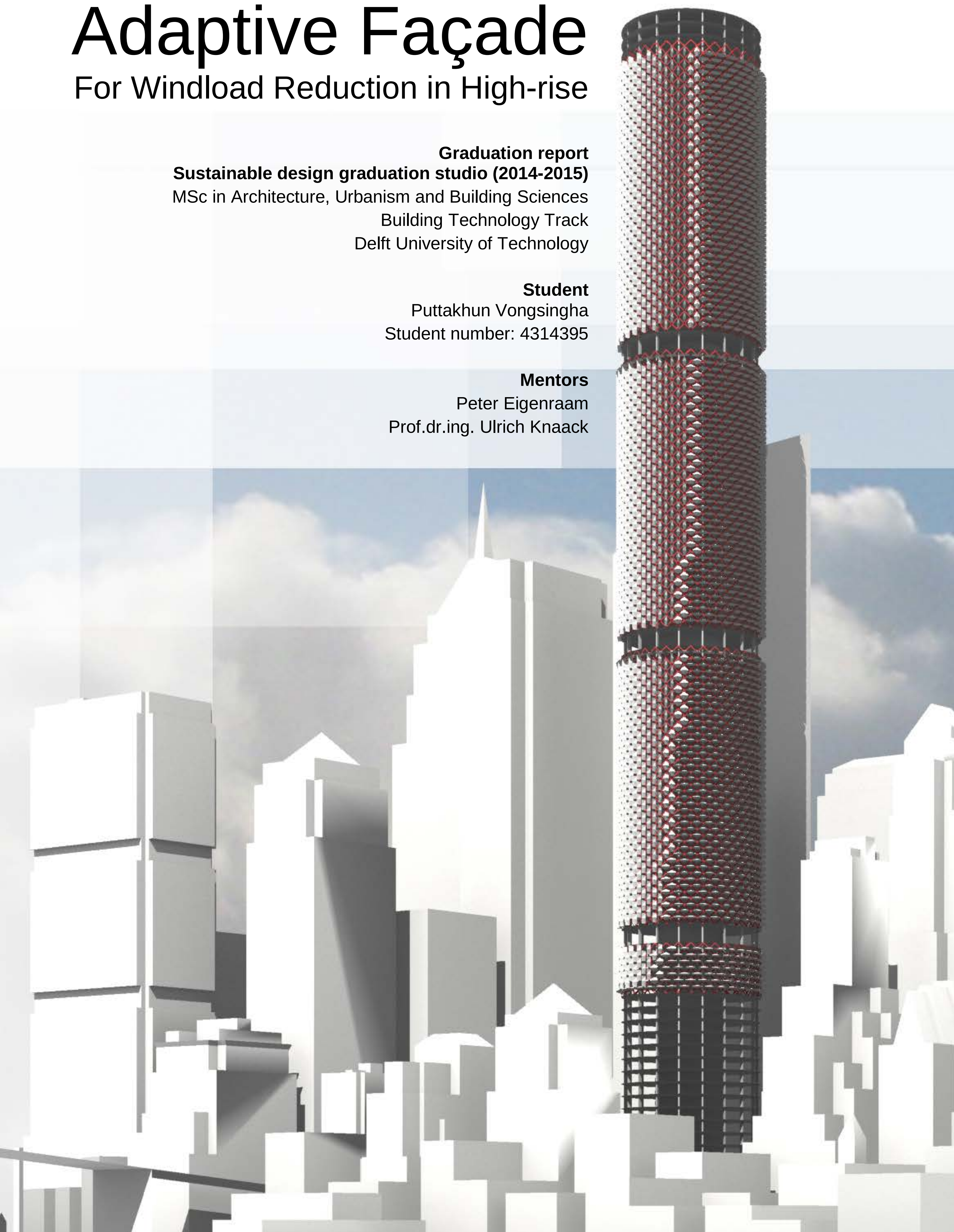

Graduation report
Sustainable design graduation studio (2014-2015)
MSc in Architecture, Urbanism and Building Sciences
Building Technology Track
Delft University of Technology

Project Title
Adaptive Façade for Windload Reduction in High-rise

Student
Puttakhun Vongsingha
Student number: 4314395

Mentors
Peter Eigenraam
Prof.dr.ing. Ulrich Knaack

Date
23 June 2015

Acknowledgement

Adaptive façade for windload reduction in high-rise building graduation project would not be possible without the support and trust from both of my mentors, Peter Eigenraam, who is always provide useful information of technical solution and make all the calculation possible, and Prof.dr.ing. Ulrich Knaack, who inspired and encouraged me to create this graduation project and challenge me to the level I never expect to be able to reach, By their inspiration and technical advices, push this challenge project to be far more advance that it could possibly be if it was done only by my own. Thanks to Dr Patrick TEUFFEL for information of EVOLO tower that formed the beginning and direction of this project. Thanks to Dr. -Ing. Marcel Bilow, Dr. Buckylab, for providing the essential equipments for wind tunnel experiment. Thanks to all my friends for all the support and enjoyment during this stressful time. And finally, for my parents who always support and believe in me.

Puttakhun Vongsingha

Adaptive Façade

for Windload Reduction in High-rise

Table of contents **Page**

1

Master thesis curriculum

Adaptive Façade for Windload Reduction in High-rise

1.1 Introduction

The nineteenth century was one of the most technically inventive centuries. Since then, it witnessed the application of new techniques and of new mechanical means in virtually every human activity. Also in architectural field, the new methods of construction were introduced which bring world architecture to reach another level with bigger buildings, faster construction, more sustainable buildings and also taller building. Before 1974 there were only a handful of high-rises that are taller than 300m, then Sears Building (Willis Tower) reached the height at 442 m in that year, Taipei 101 reached the highest point in the world at 509 m in 2004. Afterward, there are a number of designs being conducted to create a building in range of 500-1500 m(Emil Simiu, 1996). The finished Burj Dubai stands as the highest building in the world in 2009 at 828 m height. It can be easily seen that there are tendency of high-rise construction to be higher which it is a part of human challenge nowadays.

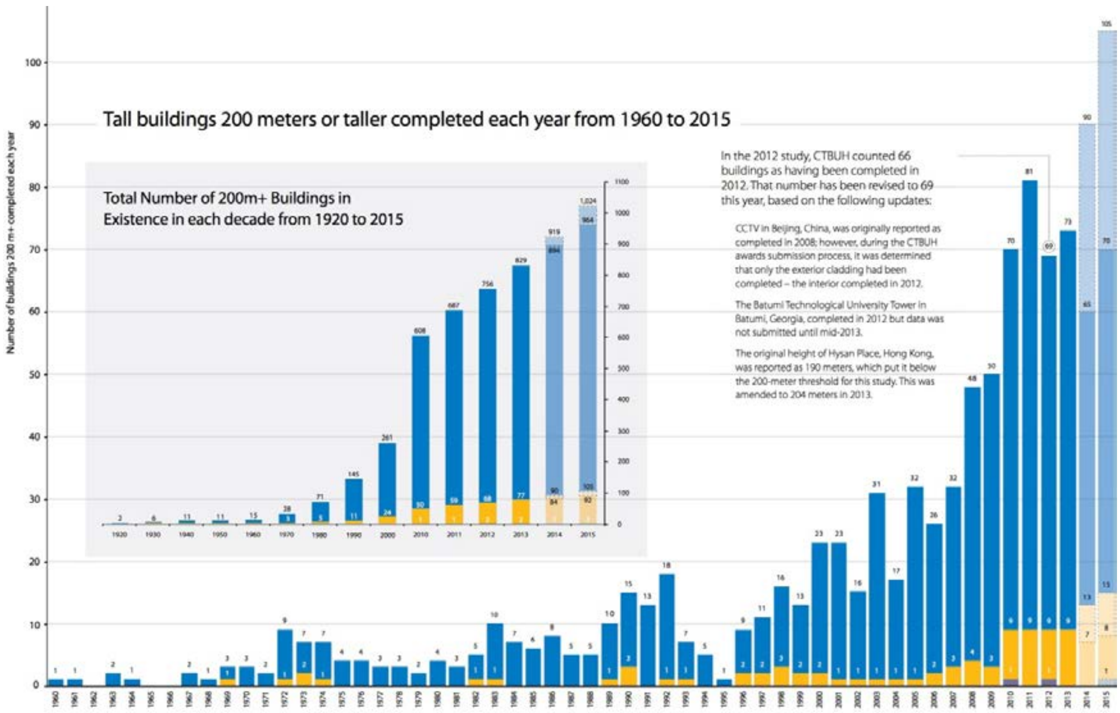

Fig 1.1: Growth in number of tall building from 1960-2015(the survey was made in 2013) (CTBUH, 2015)

Blue:	Number of 200 m+ buildings
Yellow:	Number of supertall buildings (300 m+)
Purple:	Number of megatall buildings (600 m+)

“We practically designed the tower in wind tunnel”
The structural engineer for Burj Dubai: Bill Baker of Skidmore Owings Merrill

Higher the building stands, the wind loads will become more critical to the stability of the building structure. Preventing wind loads, there are many different systems were used. Three main methods are normally applied to the design which are stiffen the building, increase the building mass and supplement the damping (Irwin, 2009). However, recently, adaptive system was introduced as the new method to offer the most effective solution in many difficulty that occur to a building, such as unwanted sunlight, lack of privacy, thermal bridge and wind loads.

In 2007, Braun Associates Architekten (architects) and Teuffel Engineering Consultant (structural engineering) proposed a 1080 m height tower – EVOLO Tower (Dr Patrick TEUFFEL, 2007). The tower is covered with adaptive envelope that can be changed in its shape freely according to wind direction. The main idea is to deal and cope with power of nature but not against it. The aim for the design is to reduce drag force, cross wind movement and prevent organization of big wind vortexes. Since then, there were some studies in adaptive façade to reduce the effect of wind load. Some of them that are interesting to be mentioned are the studies that prove that not only shape but the roughness of the façade can possibly reduce drag force and under-pressure to the facade surface.

The aim for this project is to study and research about wind behavior and its effect by literature study and self-investigation. The final product will be a design of wind adaptive façade that reduce loads from the wind to building structure.

1.2 Problem statement

Nature of the wind in term of high-rise designing is that wind at high altitude creates high bending stress to the structure, and also, in this level the wind has higher velocity than the wind in the near ground level because it occurs to be less friction to the earth surface or objects, such as trees or buildings. In an urban area, there are two different type of wind, first is high altitude wind which has constant velocity and direction, Most of the time, it is depended on the seasonal wind in the area. Second is the wind at low attitude which normally has lower velocity but because of the obstacles, the direction and flow of the wind can be manipulated and changed all the time. The wind in lower altitude always approaches the building in form of gust wind.

Four sides of the building will receive different kinds of loads according to the wind direction, which are, front façade receives the wind positive pressure, and side façades handle vortexes and under-pressure force, while back façade has to resists pull force. Building shape and surface that are placed in the correct location will play a big role in reducing wind effect.

Most of the time, wind direction is unpredictable and the effect from the wind starts at the moment when the building get the impact, which the adaptive system needs to be able to adjust itself in a short period of time. The façade can finally be control by a complex command script which cooperates with detecting sensors, or it can be mechanism or smart material that can realize surrounding and change itself according to the influence of its environment.

1.3 Research objective

<u>Main objective:</u>

Design an innovative adaptive façade system for high-rise building that can adapt its shape or surface to reduce wind effect from any direction in the range of predicted velocity in order to reduce the needs in structure material to handle lateral load.

<u>Sub objective:</u>

Create an understanding in wind effect to a building with different shapes and surfaces.
Create possible options of how a building can deal with wind load by façade adaptive system.

1.4 Research questions

<u>Main question</u>

In what extend that adaptive shape and surface of the building can reduce wind loads in a high-rise building with highest efficiency in reduction of structure material?

<u>Sub question</u>

What are the effects of the wind to a building and how shape and surface of a building alter those effects?
What kind of loads and effect from wind that occurred at different sides of the building?
What is the most suitable envelope shape or surface that is best to deal with different wind effect in each side of the building?
What are the criteria or values that indicate the load from the wind to a building?
What is the main aspect to define if small façade components or big façade system is the most suitable system?
What type of control and wind detecting system that is has fast reaction, less maintenance, easy to control and suitable for wind adaptive façade?
How is this additional building envelop connect to building main structure?

1.5 Scope of study

Building definition:	300+ m height
	~50x50 m^2 floor plate
	Multi-function used
	Width and length ratio = 1 (square or circular) for floor plate shape
Location:	High density city,
	Equatorial zone
	No seismic load (earthquake)
	No snowload
Wind speed:	Maximum Typhoon wind speed
	118-156km/h (32.78-43.33m/s)
Wind behavior:	Non uniform according area roughness length
	Unpredictable direction
	Vortex shedding is possible
	Higher velocity in higher altitude

1.6 Methodology & Time planning

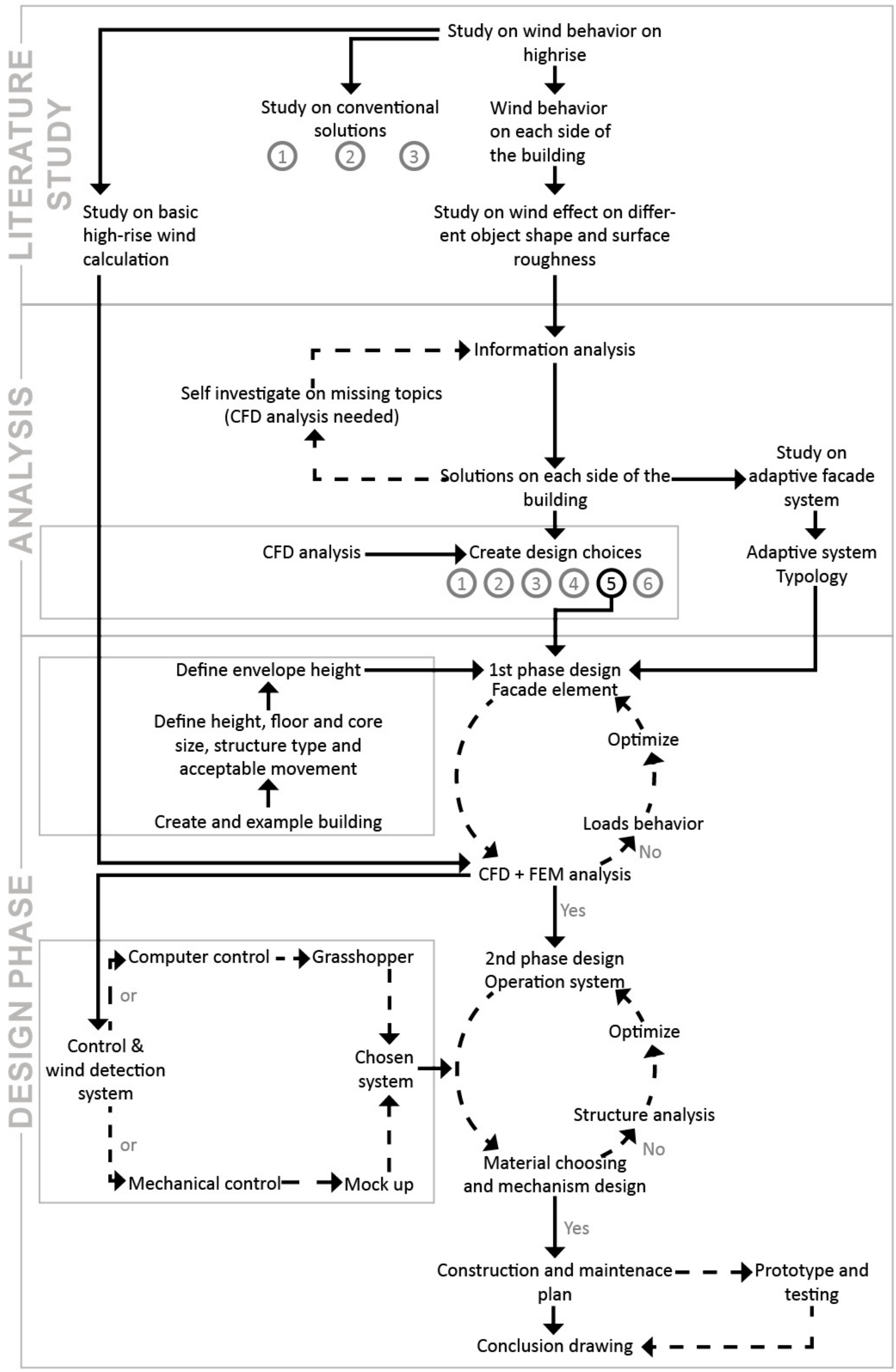

Fig 1.2: Project methodology

Presentation	P1								P2								P3							P4							P5
Course Week	2.1	2.2	2.3	2.4	2.5	2.6	2.7	2.8	2.9	2.10	3.1	3.2	3.3	3.4	3.5	3.6	3.7	3.8	3.9	3.10	4.1	4.2	4.3	4.4	4.5	4.6	4.7	4.8	4.9	4.10	4.11
Literature Study																															
Wind Behaviors																															
Wind Effects																															
Solutions																															
Adaptive systems																															
Technical Requirement																															
Analysis																															
Self Investigate																															
Solutions Applying																															
Design																															
Example Building																															
Façade Design																															
CDF+FEM analysis																															
Command Script Design																															
Selecting Material																															
Drawing																															
Prototype																															
Conclusion																															
Comparison																															
Feasibility																															
Further Research																															

Table 1.1: Project time planning

2

Introduction to Wind Behavior

2.1Basic wind behavior

Wind is the natural phenomenon which occurred by flowing of air. Two basic things about air that need to be considered are that air is like other common fluid elements, it has mass and viscosity. Mass in the air means that in order to move the air, energy is required to create a movement. On the other hands, stopping the moving air will release some energy in the form of force. Viscosity creates friction between two air flow directions and between air and the object surface. Viscosity can also be the cause of an air flow to influence still air to move along with it. Obstacles such as building that stand in the part of the wind; they convert the wind kinetic energy into pressure or friction force to their surface and become *wind load*.

2.1.1 Wind speed

2.1.1.1 Roughness length and relation with height

Wind speed, which influences the pressure to a building surface, has higher velocity by the increasing of the height. Basic explanation is that at the level closer to the earth surface, many obstacles such as terrain, buildings or trees, create friction and slow down the wind speed. According to Euro standard (Eurocode, 1995), there are 5 terrain categories which are 1) coastal area or open sea, 2) flat area with only negligible vegetation, 3) area with low vegetation and isolate obstacles, 4) area with regular cover of vegetation or buildings such as village or suburban terrain or forest, and 5) area which at least 15% of the surface covered with building with average height more than 15 m. The terrain category defines roughness length of the area which is needed in windload calculation. As an approximation, roughness length is value close to one-tenth of the height of surface roughness element ("Roughness length," 2015)

Terrain category		Roughness Length, Zo (m)
0	Sea or coastal area exposed to the open sea	0.003
1	Lakes or flat and horizontal area with negligible vegetation and without obstacles	0.01
2	Area with low vegetation such as grass and isolated obstacles (trees, buildings) with separations of at least 20 obstacle heights	0.05
3	Area with regular cover of vegetation or buildings or with isolated obstacles with separations of maximum 20 obstacle heights (such as villages, suburban terrain, permanent forest)	0.3
4	Area in which at least 15 % of the surface is covered with buildings and their average height exceeds 15 m	1

Table 2.1: Terrain category (Eurocode, 1995)

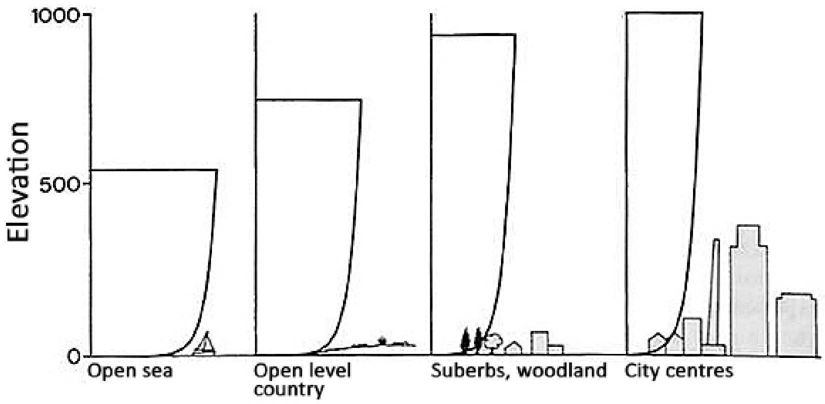

Fig 2.1: Mean wind profile for different terrains (P. Mendis, 2007)

City	Roughness length (Z0) (cm)	Source
Cambridge	74	Dobbins 1977
London	240	Davenport 1965
New York	330	Davenport 1960
Moscow	300	Ivanov and Klinov 1961
Tokyo	170-232	IKondo 1971

Table 2.1: Roughness length in city area (Hansen, 1993)

According to Taranath (Taranath, 2012), over the height of 366 m above ground, surface friction has no effect to the speed of the wind. The movement of the wind speed in this level depends only on seasonal and local wind. The height at this level is called the *atmospheric boundary layer.* It is seem to be that at the higher altitude the wind is more likely to have less turbulent character. It has less fluctuation in its velocity and direction compare to wind that is close to earth surface which is affected by obstacles and being influenced to form eddies, vortexes and change in direction.

It can be concluded that wind in the higher altitude has higher velocity which create higher pressure to the building but it has less chaotic behavior, while wind at low altitude create less load to the building but it is more difficult to predict the direction, speed and type of flow when it approach the building. From Teuffel's research (Dr Patrick TEUFFEL, 2007), he gave the possible assumption that variation of wind direction to the height would take a height of 300 m and an estimate change of 10 degrees. However, a sudden change in wind direction is also possible and happen within a very short period of time, this is commonly observed with the passing of a warm front.

2.1.1.2 Flow behavior in different wind velocity

In theory, the shape of the fluid flow like water or air can be predicted by using calculation of Reynolds number. In different Reynolds number the shape of the fluid after it flow pass by the object is in different shape that will cause the different values in drag force, vortex shedding and separation flow which will be explained later. In the case that the situation has low Reynolds number, it means that the fluid will flow around the object and return to the normal flow right behind the object which cause less effect to the area behind the object. On the other hand, if the value of Reynolds number is high, the flow cannot close itself and leave the "turbulent wake" or "separation area" after it passes the object. The size of the wake has an effect on drag force to the object.

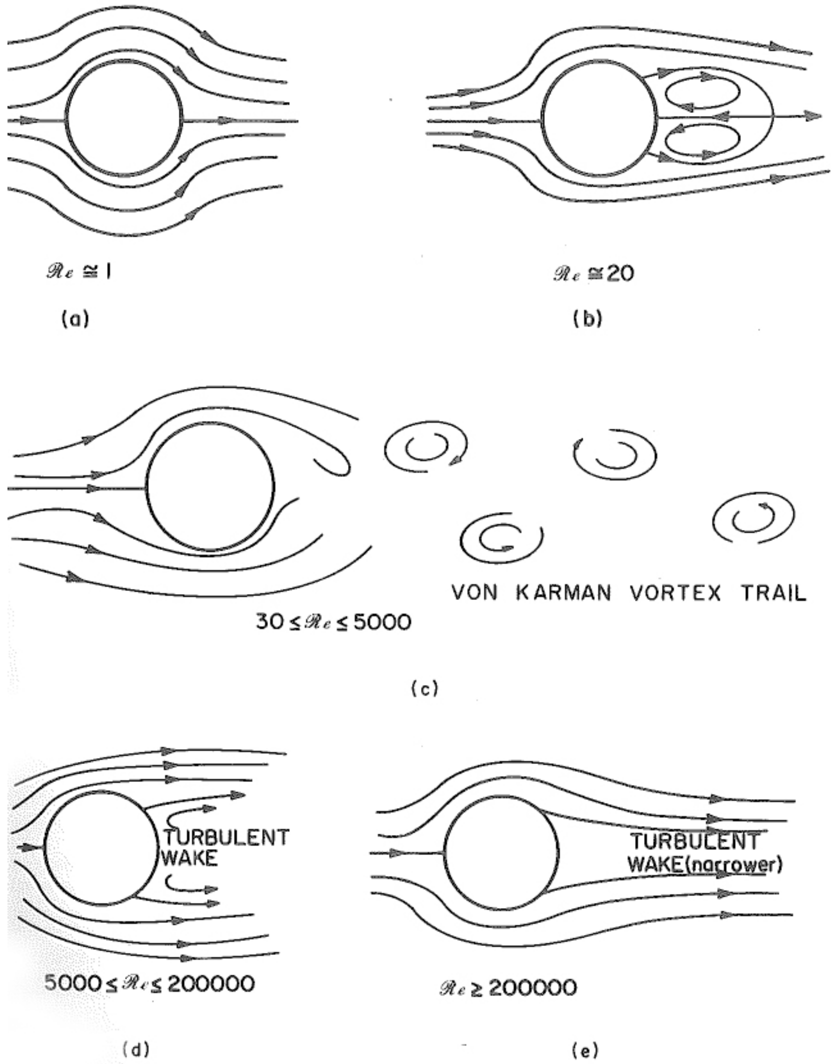

Fig 2.2: Flow past circular cylinder Re = 1. (b) Flow past circular cylinder Re = 20. (c) Flow past circular 30 < Re < 5000. (d) Flow past circular cylinder 5000 < Re < 200,000.(e) Flow past circular cylinder Re = 200,000.(Emil Simiu, 1996)

$$Re = \frac{\rho V L}{\mu} = \frac{VL}{\upsilon}$$

Re : Reynolds number
ρ : Fluid density (kg/m^3)
V : Mean velocity of the object relative to the fluid (m/s)
L : Characteristic linear dimension of the object (m)
μ : Dynamic viscosity of the fluid (Pa.s or $N.s/m^2$ or kg/(m.s))
υ : Kinematic viscosity (m^2/s)

Value of Reynolds number depend on mean velocity of the object relative to the fluid (m/s) and characteristic linear dimension of the object (m) which in case of architecture, the size of the building leads to high Reynolds number ($>10^7$). It might be able to assume that there will always be the turbulent wake after the fluid pass by the building. However, location of separation flow will be different in different wind velocity which will be explained further.

2.1.2 Along and cross-wind load

Effect from the wind load to an object or to a building is a complex phenomenon by its flow effect, flow separation, the formation of vortices and development of the wake. These wind fluctuation create different pressure on the building's surfaces and transfer to the structure of the building. Under the collective of these fluctuation forces, causes the building to vibrate in rectilinear and torsional modes.

2.1.2.1 Experiment on development of wind load to a building

A simple test was conducted to change in location of the wind pressure to the surface. The example object was imported in to **computational fluid dynamics** (CFD) software to make a quick analysis which can be present in a simple graphic. The object is 50x50m width with 400m height is placed in a simulation wind tunnel with wind speed of 33m/s in the perpendicular direction to the object front wall.

The result show that the location of pressure that is occurred by the wind started in two positions, the front wall where the wind approaches and the back wall at the opposite side. The pressure in the front wall was in positive value and increases its value in the early part of the test and then remains steady afterward. The pressure at the back was in negative number which pulls the object along wind direction. However, the location of the negative pressure moved to the side of the object and increases its value.

These effects can be explained that at the moment when the wind approached the object, it created a separation area behind the object that cause drag force from negative pressure to the back wall. However, once the separation area become bigger, there was some turbulence in the area. During that time, the velocity at the leading edge of the side wall became faster. From Bernouli's Principle, the increasing of velocity in fluid flow will simultaneously decrease the fluid pressure. According to the increasing in wind speed, high negative pressure on the side wall was occurred.

The test shows that the back wall negative pressure happens only for a short period of wind, but a long continuous wind creates under-pressure at side wall and causes cross-wind direction loads. The alone-wind load from the analysis is occurred to the object at the beginning of the attack and then reduce it value and is turned in to side wall pressure that cause the cross-wind load. In a long continuous wind the small pressure and vibration at the side of the building can cause a failure in structure, especially in the case that the vibration of the side pressure appear to has the same frequency as the vibration of the building. It can increase the moving length into a critical position that the structure can handle.

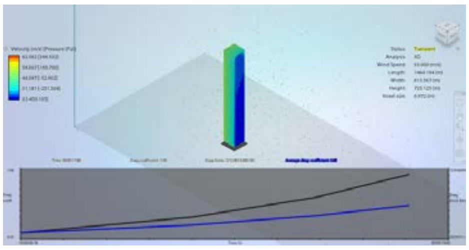

17 second after impact: negative pressure stay at the back of the object.

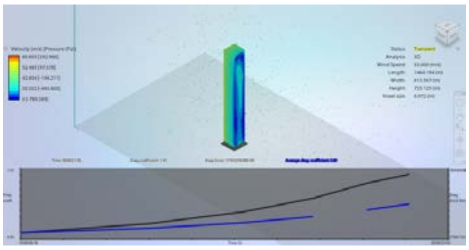

21 second after impact: the negative pressure moved to the edge of the back wall

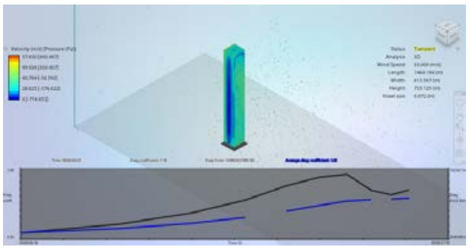

26 second after impact: the negative pressure moved toward the leading edge of the side walls

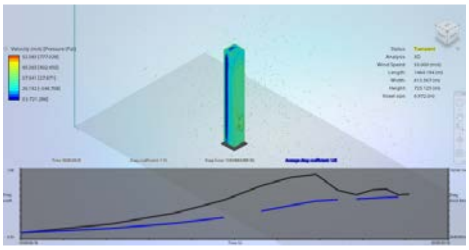

28 second after impact: the negative pressure locate itself at the leading edge

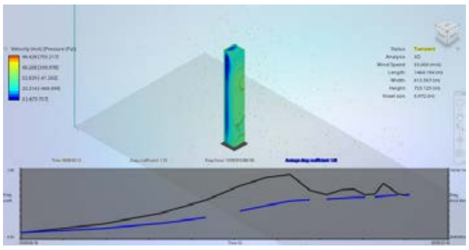

30 second after impact: the negative pressure start to move upward

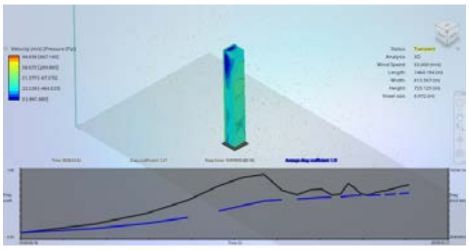

32 second after impact: the negative pressure locate itself at top part of the leading edge

Fig 2.3: Result on location of negative pressure on test object according to wind from the top-left side (Autodesk Flow Design,2015)

2.1.2.2 Vortex shedding

In a low wind speed (22.3-26.8 m/s), the building separates the air flow into two side of the building which is the cause of under-pressure at the leading edge of the side façade. When the vortices are shed symmetrically, it breaks away from the building surface and it creates pull which an impulse is applied in the transverse direction. However, with low velocity, shedding occurs in both side of the building equally which create no vibration to the structure, only along-wind oscillations is experienced by the building.

At higher speed, can happen alternately different in both side of the building (figure 2.4). In this situation, there is a combination of along-wind and cross-wind motions. Moreover, if the transverse impulses that occurs both side of the building create a frequency that is precisely half of the along-wind impulse; it will give rise to vibration in cross-wind direction. This phenomenon is call *vortex shedding* or *Karman vortex* (Taranath, 2012).

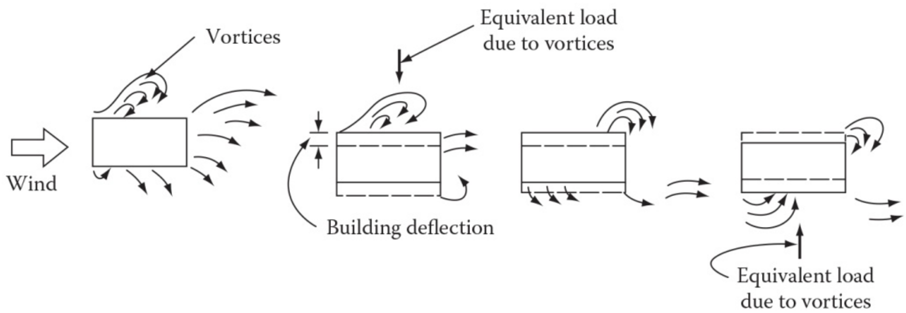

Fig: 2.4 Vortex shedding: Periodic shedding of vertices generates building vibrations transverse to the direction of the wind (Taranath, 2012)

<u>Reducing vortex shedding</u>

There are several solutions to reduce vortex shedding according to Irwin (Irwin, 2009) which relate to how to select building shape.

- Softened corners: the softening should extend about 10% of the building width in from the corner. For example, Taipei 101, the corners were stepped in which result in 25% reduction in base moment.
- Tapering and setback: The building that has varies width along the height confuses the vortices to shed in different frequencies in different height and they become in coherent and reduce the association fluctuating force.
- Varying cross-section shape: the similar effect can be achieving by varying the cross-section shape with height.
- Spoilers: It can be added to outer surface of the building. The spiral Scruton strakes always be used on circular chimneystacks. Also, vertical fins that run along the building height can be acceptable too.
- Porosity or opening: Opening through the building which allows the air to flow from front façade and leave at the back to weaken and disrupt the vortices.

2.1.3 Separation flow and influence in drag force

Drag force is always be referred the resistance of the object to the surrounding flowing fluid which depend on velocity of the fluid. Drag force that occur to the object is separated into two types which are friction drag and form drag (pressure drag) that depend on the shape and direction of the object to the flow.

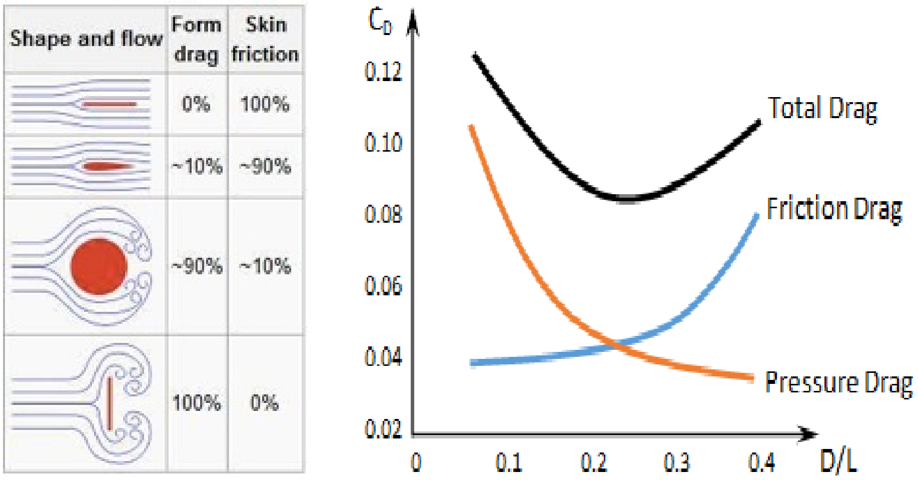

Fig 2.5: Relation between friction drag and form drag that are occurred to different shape of objects (Drag (physics), 2015) (Drag coefficient, 2015).

In aerodynamic design such as airplane designing, resistance to the air is needed to be put to minimum to reduce the energy consumption in driving the object forward. In order to quantify the drag or resistance of an object to the surrounding fluid environment, drag coefficient is a dimensionless quantity that is normally used. Lower the drag coefficient indicates that the object has less aerodynamic drag.

$$Cd = \frac{2Fd}{\rho V^2 A}$$

Cd : Drag coefficient

Fd : Drag force (N) which is by definition the force component in the direction of the flow velocity

ρ : Fluid density (kg/m^3)

V : Mean velocity of the object relative to the fluid (m/s)

A : Reference area

Turbulent wake also relate to drag force which it cause the drag to be bigger if the separation area is big, and on the other hand, smaller wake creates lower drag. For example, air foil shape (airplane wing) is designed to extend the object to have pointy edge at the back to allow the air to flow along the surface without creating turbulence and avoiding the turbulent that can happen between the surface and the laminar flow. In case of other object shape, for example, circular cylinder shape in high velocity flow, the flow will be separate from the surface at widest point of the shape or at the point where the force in the air particle is higher that the force that prevent the flow to create vacuum space. At this location, high under-pressure is occurred. The behavior of the fluid in this area is called separation flow. At this point where the surface flow turns into separation flow, the flow will not turn back to the object and creates the turbulent wake after this point.

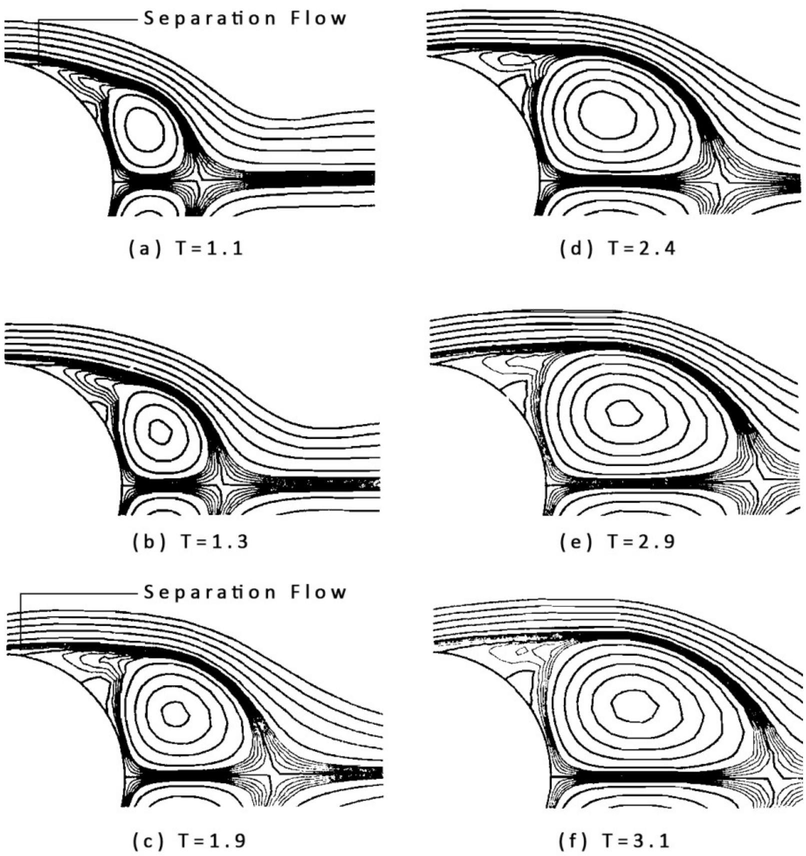

Fig 2.6: Relocation of separation flow according to time (T) (Tetuya KAWAMURA, 1985)

Separation flow and under-pressure area as mentioned before and in 2.1.2.1 their location is changed according to the time that the air reach the object. For 50x50m building, it took approximately 30 second to reach the stabilized position. At this moment, the separation flow is located in the same area. However, from the calculation for Reynolds number, there is possibility that the location of separation flow is different in different wind velocity. In this case it can be that the location of separation flow will be further to the front if the wind velocity is higher.

2.2Influenced by objects to wind effect

There are 3 main loads that are occurred to an object as the flow approach

1. Front wall pressure load: it is caused by direct pressure from the approaching wind. Also there is a high density air that being pressed and unable to move because it is blocked by the flow line around it and shape itself as a dome in front of the wall
2. Side wall suction: it is cause by the shedding of the flow from front wall to side wall which it is the separation flow that create gaps between object surface and the flow. In high wind velocity, it can be the cause of vortex shedding

3. Back wall pull force: when the wind flow pass the object, the flow at one side cannot reach the flow at the other side at once. The movement of two flow line and its viscosity influences the still air at the back of the object to move along and cause suction at the back wall

However, the characteristic of the flow can be modified. It can be achieved by two main methods, by shape of the object or by typology of object surface.

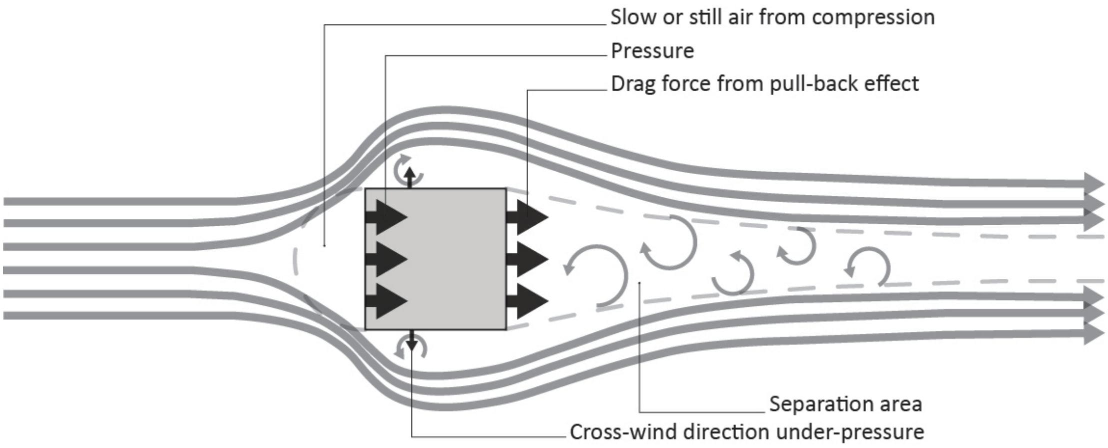

Fig 2.7: Wind characteristic to an object

2.2.1 Object shape

Aerodynamic behavior always is in an important consideration of designing airplanes, cars, ships or even a tall building. Aerodynamic design has the main idea to get rid of problem from vibration and also reduce drag force of an object.

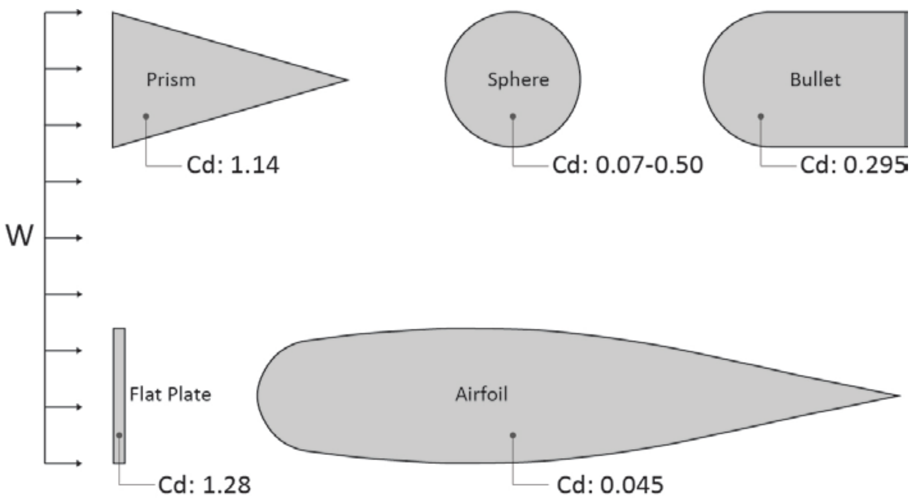

Fig 2.8: Shape effects on drag (2015)

From fig 2.8 shows the different in drag coefficient values in the objects in different shape which were tested in a wind tunnel. Although the frontal areas of these objects are in the same size, the drag coefficient values that are caused by the shape are varies. Streamlined symmetric airfoil gives lowest drag because at the tail of the shape allows the air to flow along the surface and leave only small separation area at the back.

Compare to a flat plate that has the highest drag coefficient because it has flat front and back surface and the shape that creates big separation area which causes pull-force at the back of the object.

The length of the building also perform different result in reduce drag force. In fig 2.9, the drag forces are presented in pressure coefficient which the increasing of building length along the wind can reduce negative pressure at the back façade

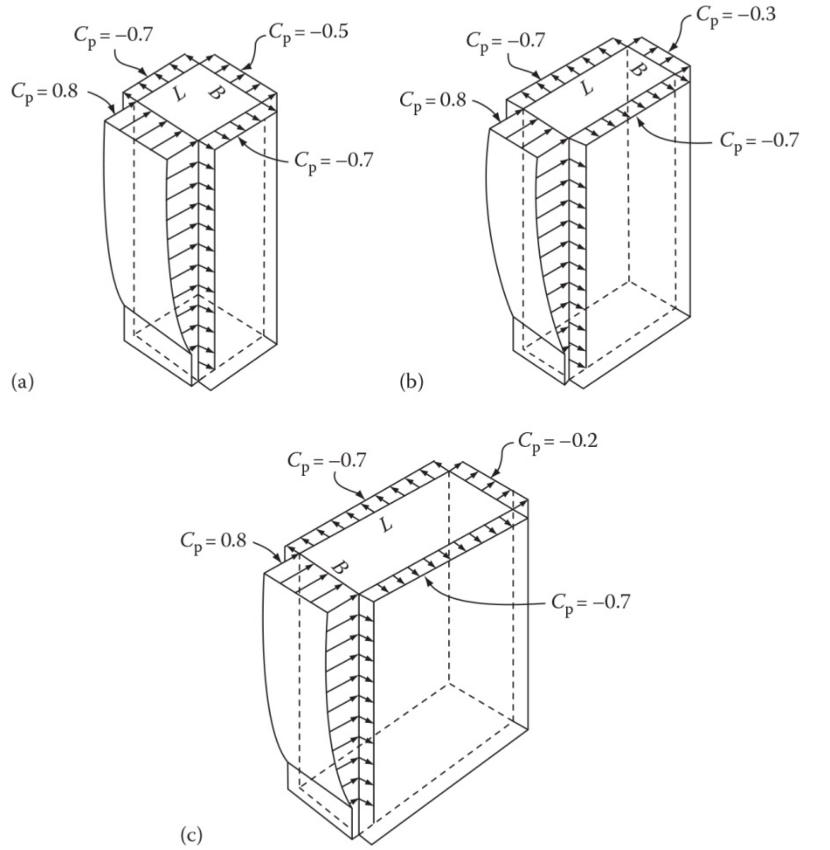

Fig 2.9: External pressure coefficient (Cp) with wind direction from right side of each image.

Plan aspect ratio L/B: (a) 0 < L/B < 1

(b) L/B = 2

(c) L/B > 4

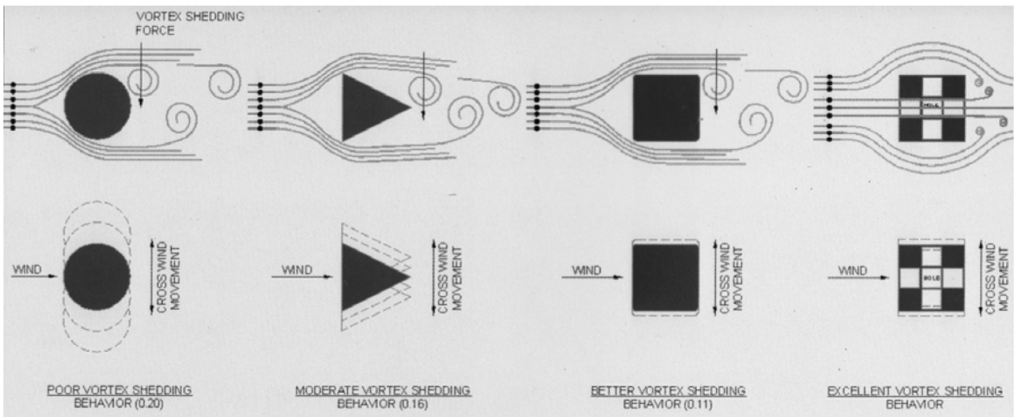

Fig 2.10: Vortex shedding behavior according to building shape (Dr Patrick TEUFFEL, 2007)

Fig 2.10 shows the effect from vortex shedding in different building shape. As mention before, vortex shedding causes vibration to the structure in cross-wind direction. The vortex shedding according to the shape of the object is not related to Irwin (Irwin, 2009) that the object with the curve corner (circular cylinder) creates high vortex shedding. However, the adaptive façade project is located in anonymous areas which are presumed that the direction of the wind is unpredictable. And with this, circular shape building might be the most suitable shape.

2.2.2 Object surface

Aerodynamic and hydrodynamic property of an object depend mostly on its shape, however, there are several research and existing product or object show that surface smoothness and pattern can be used to create specific flow effect that can improve the property. As generally expectation that smooth surface is better in minimize friction from the flow to the surface, which is not completely true in many situation. For example, golf ball dimples was designed to reduce the separation area and create lift while it is spinning or shark skin that can reduce friction drag while it is moving.

2.2.2.1 Relate case study objects

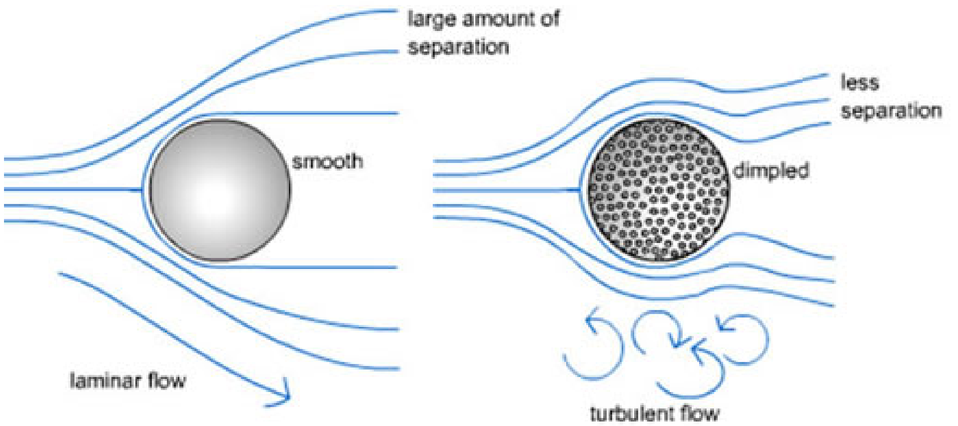

Fig 2.11: Different aerodynamic properties between a ball with smooth surface and surface with dimples (golf ball). Rough surface creates small turbulence close to the surface and draw the flow closer to the back surface of the ball which reduce the separation area and drag coefficient. (image from (Lorenzo Lignarolo, 2011))

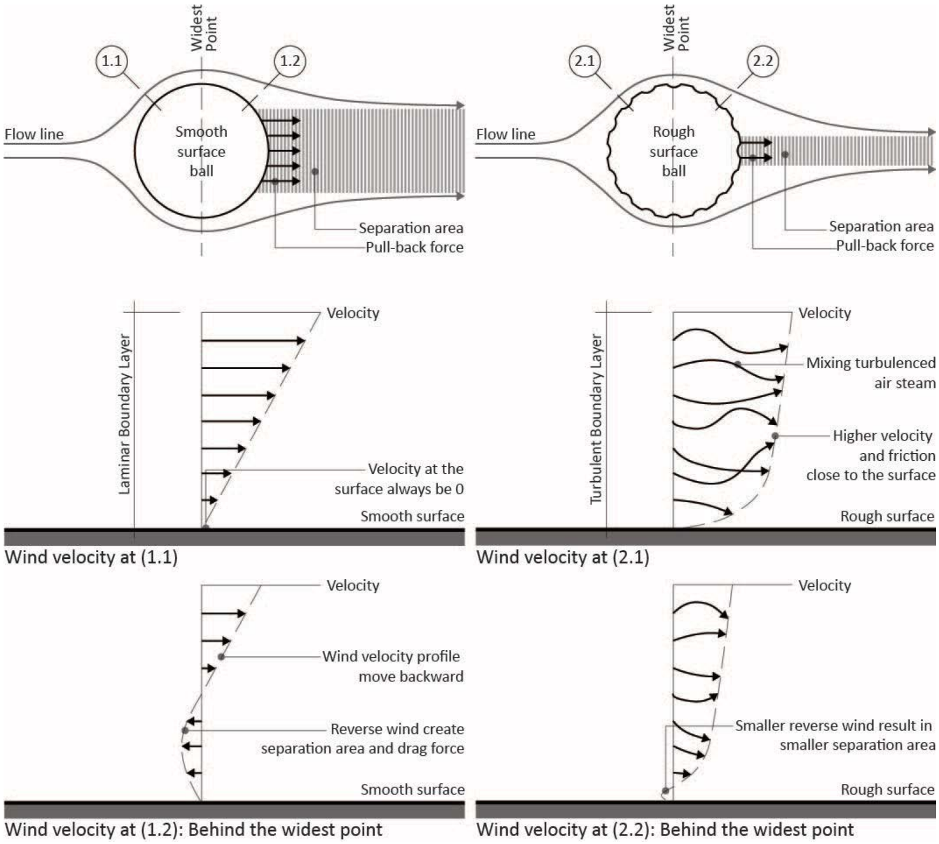

Fig 2.12: Surface air velocity on smooth and rough surface balls which analyze how rough surface can reduce drag force (redraw from(Velo, 2015))

One example is the shark's dermal denticles (skin) which are ribbed surface with longitudinal grooves which improve the efficiency of water flow on their surface. Compare to smooth surface, the groove prevent turbulent vortices or eddies in fast water, and keep the flowing that close to the surface in the comparable speed to the flowing further away from the shark. The reduction of eddy formation is done by the groove are below (Yann, 2015)

1. The grooves reinforce the direction of the flow by channeling it.
2. They speed up the slower water at shark's surface, as the same volume of water going through a narrower channel increases in speed.
3. Conversely, they pull faster water towards the shark's surface so that it mixes with the slower water and reduce the speed differential
4. They divide up the sheet of water flowing over the shark's surface so that any turbulence created result in smaller, rather than larger vortices.

From golf ball surface and shark's skin, there are several design that are developed from the ideas, such as "Fastskin" FSII swimming suit that is developed by Speedo by mimic shark skin to a full body swimming wear. The swimming suit was designed by using computer software to simulate the movement of the swimmer and place the streamline groove in the micro scale to improve the movement in different zone of the body (such as arms and body (Barry Bergdoll, 2007)). Even though, further research shows that the swimming suit is not effective as it was designed to be because the shape and ratio of the ridges and space between them are far different from the real shark skin (Oeffner & Lauder, 2012).But the concept of biomimicry is still interesting enough to be mentioned.

Another "Fastskinz" is the vinyl membrane that is designed to be place on vehicle surfaces as stickers. The special part of the membrane is that it contains small dimples (similar to golf ball) which they generate turbulence when air passes over them. They reduce the air pressure and enable an object to more easily slip through the air. Fastskinz generates a layer of turbulent air that reduces drag coefficient and gas using by 18-25%(Gladwell, 2015).

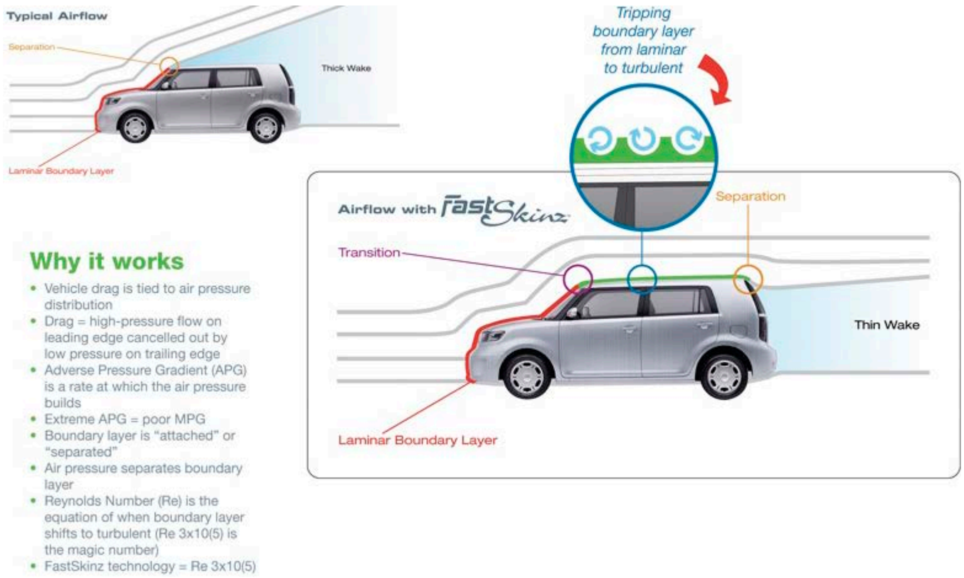

Fig 2.13: Fastskinz wrap for reduce drag coefficient of vehicle and gas usage

2.2.2.2 Experiment on effect of wind load on different surface

Three computer models were set in CFD software to test the different in values of drag coefficient. All of them represent circular shape high-rise building with diameter of 50m but they all have different surface roughness types which are smooth surface, rough surface, and hybrid surface. The rough surface was designed to be vertical stripes along the height of the building. The situation in wind tunnel was set to be the same in all three models, wind speed at 33 m/s. The tests were performed only in 2D analysis.

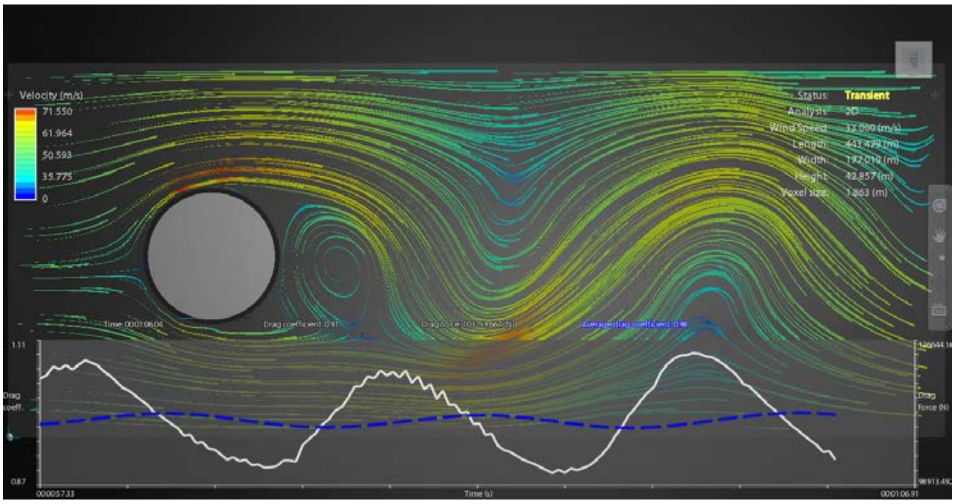

Fig 2.14: Wind analysis for *smooth surface* circular shape building. Drag coefficient is 0.91 (average is 0.98), highest wind velocity is 71.55 m/s and range of pressure is from -2548.53 to 1679.85 pa.

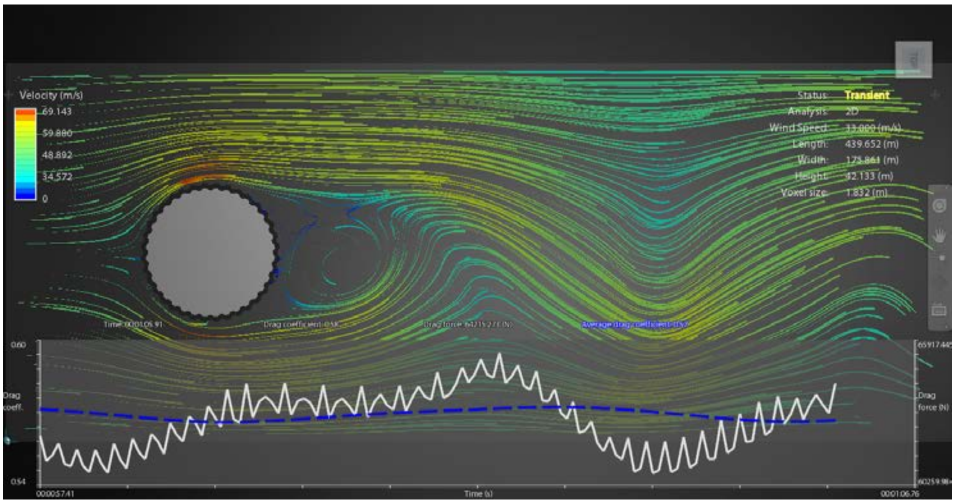

Fig 2.15: Wind analysis for rough surface circular shape building. Drag coefficient is 0.58 (average is 0.57), highest wind velocity is 69.14 m/s and range of pressure is from -2255.56 to 1285.81 pa.

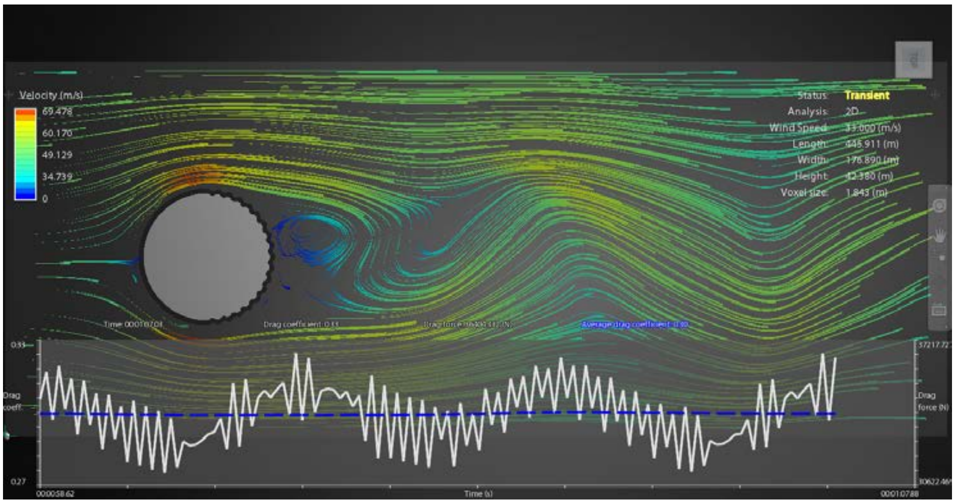

Fig 2.16: Wind analysis for *hybrid surface* circular shape building. Drag coefficient is 0.33 (average is 0.30), highest wind velocity is 69.48 m/s and range of pressure is from -2425.24 to 1166.41 pa.

By comparing the results, it can be clearly seen that the values of drag coefficient are highly different in each model. Drag coefficient in the rough surface model reduce approximately 42% from the smooth surface one, the hybrid surface drag coefficient 48%, and comparison between hybrid surface and smooth surface 69.5% of drag coefficient is reduced.

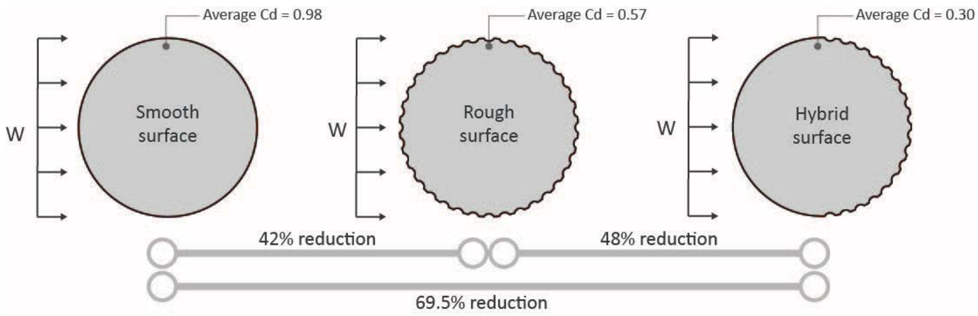

Fig 2.17: Different in drag coefficient in different building surface

The result from smooth and rough surface model can be predicted in the beginning with the separation area reduction of golf ball. However, the hybrid surface model that has front smooth surface and vertical stripes roughness surface at the back can reduce drag coefficient to almost 70% compare to the smooth one is an outstanding result. The prediction of how this phenomenon occurred is that, with smooth front façade, it reduces friction to the surface which results in reducing front façade positive pressure. The laminar flow from front façade after pass the widest point of geometry might be easier to be pulled in close to the rough surface and results in smaller separation area.

2.2.2.3 Surface Roughness

There are several researches that are conducted on different surface roughness (roughness size) to wind load. The interesting one was done by (E. Maruta, 1998), which the test was done in physical wind tunnel on 5 building models. These physical models are different in roughness size and façade pattern. One is the model that was covered by sand paper which has smallest roughness size (0.21 m in full scale), three more are models of building with balconies with different width (0.63, 1.25 and 2.50 m in full scale), and the last one is with balconies with mullion (0.63 m in full scale).

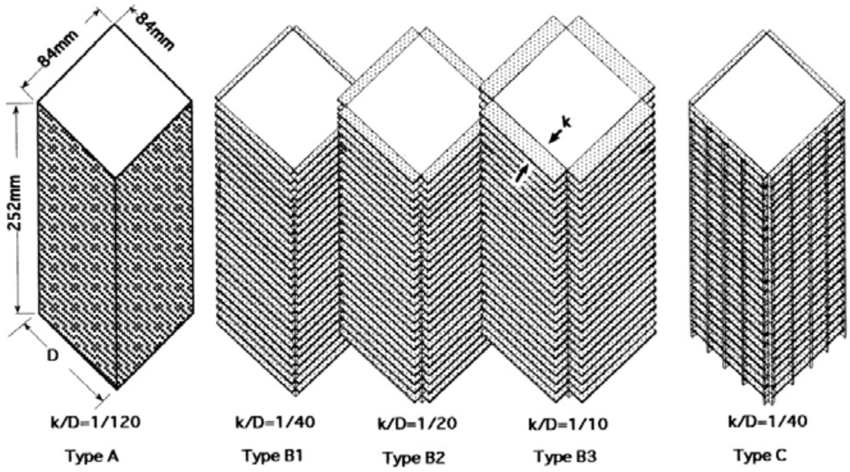

Fig 2.18: Configuration of models and surface roughness (E. Maruta, 1998). k/D is roughness size (balconies width/dept of the building).

The result shows that changing of roughness size has only small effect on front wall (windward face), however, suction forces at the side walls are remarkably reduce by the increasing of roughness size. Compare to roughness length at 0m, the 1.25m (type B2) reduce the under-pressure close to the building upwind edge about 25-30%. Which the result has been concluded that increasing the roughness size can reduce separation bubbles which cause the under-pressure at the leading edge of the side wall and result in reducing the chance of vortex shedding to be occurred.

Another research was conducted by (Lorenzo Lignarolo, 2011)on building surface roughness but vertical pattern. The test was done in CFD software only for at the side façade of the three square buildings, which have different type of façade, smooth surface, horizontal pattern roughness (balconies) and vertical pattern roughness (fins). The result was presented in values of wind velocity at 0.5m away from the surface, which it is possible to notice how much the flow field is affected by the present of the roughness element.

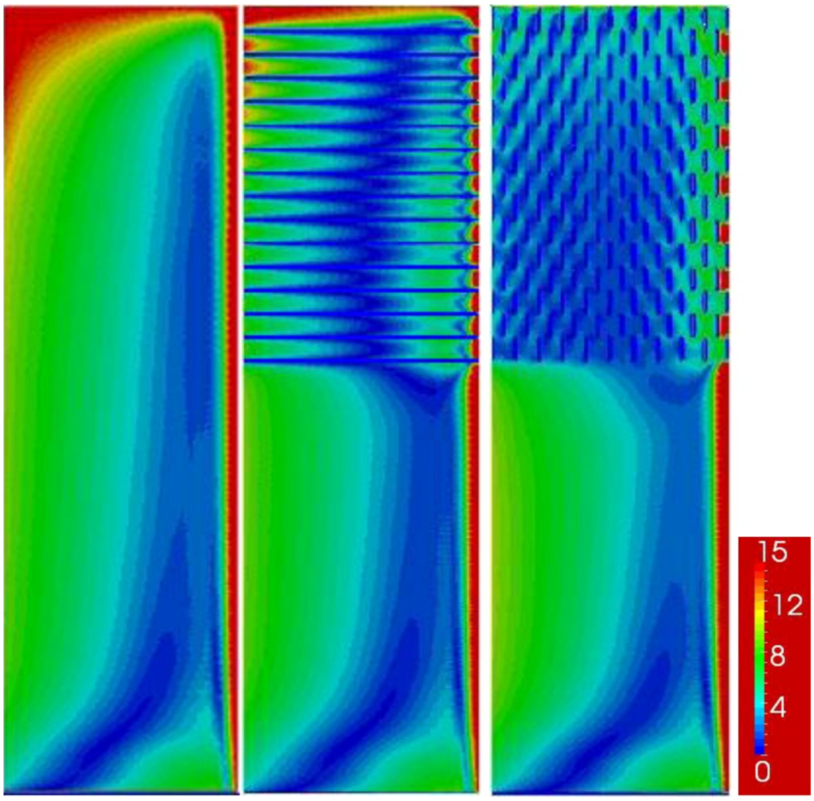

Fig 2.19: Velocity field on the side wall of the high-rise building (case A2, B2 and C2). The wind is coming from the right-hand side. (Lorenzo Lignarolo, 2011)

The result shows that roughness element in vertical direction (case C) provide a larger uniformity of the flow field. It creates high resistance to the wind and lowers the velocity down almost to zero close to surface. At side surface, reduction of wind speed can raise up the pressure from suction force to neutral.

3

Challenges and possible solutions

From previous chapter, it can be indicated that each side of the building handle different type of loads according to the approach direction of the wind. However, there are also solutions to prevent or reduce the effect from each load by using surface shape or its roughness.

3.1 Front façade

Load Types: Positive pressure that is depended on wind direction. In most building shapes, center of the impact area has the highest pressure slowly decease to the edge of the side walls and the roof. The location of the pressure is not change during time but there are also some small changes in value.

Solutions: There is still no possible way to get rid of front pressure. However, shape of the building has some effect in minimize the resistance property from the wind. For example, curve surface is more suitable than the flat one which it can separate the flow better and reduce the pressure in perpendicular direction to the surface into only small area. Circular shape building is also more flexible in reacting to wind load in different direction.

3.2 Side façade

Load Types: Mainly negative pressure which is cause by separation flow, inverted conical vortex and vortex shedding. The location of under-pressure or separation flow moves from the back façade to the side and moves in the opposite direction of the wind. The negative pressure will stop close to the leading edge (in rectangular shape building) and at the point near the widest section (in circular shape building). Also, in any surface that the flow moves parallel to the surface also creates friction drag.

Solutions: If the leading edge can be softened with more than 10% of the building width can reduce the separation bubble and vortices. Roughness on surface can reduce the under-pressure at the façade as well. Different direction of the patterns, horizontal fins and vertical fins give different result but both lead to negative pressure reduction. The horizontal one channelizes the flow which repositioning the under-pressure, and the vertical one stops the flow at the surface, however, it can create big friction and causes the differences in flow velocity between the flow close to the surface and the flow that is away from the surface which result in high friction drag.

3.3 Back facade

Load Types: Pull force according to the separation area. From CFD analysis the negative pressure (suction) start at the center of the back façade and divide into two parts and move to side façade. The along-wind load from pull force happens suddenly at the moment the wind approach the building and the value reduce during times.

Solutions: The solution is to reduce the size of the separation area. The best shape should be like streamlined symmetric airfoil, which has a very long tail at the back to allow the flow to move along the surface and create least separation area possible. The solution in roughness field can be done by method of golf ball by adding specific type of roughness that contains air gaps. It should create enough turbulence to be able to drag down the flow to be close to the surface, In minimizing the problem in this side with surface roughness, circular shape building would be the most suitable one.

4

Mock-up building

In order to be able to study further, a mock-up building was design. On the steps onward, the adaptive façade will be design according to the design of this building. The building itself follow the criteria in scope of study in the first chapter and it was only a rough design which include structure method, safety standard, number of elevators, number of floors, height, rough design for core plan and area usage. Also, it was design to have the most efficiency in used against the strong wind and in applying the adaptive façade.

4.1Building shape selection

There are several criteria of choosing the building shape such as unpredictable wind direction, drag coefficient (along-wind movement), vortex shedding (cross-wind movement) and possibility in applying adaptive façade system to it.

Firstly, different wind direction can create different effect to building surface. For example, in square shape building, small angle wind direction to front façade can has result in different location of front positive pressure location, shape and unequal for side façade under-pressure, and the value of drag coefficient. Circular shape building seems to be the shape that is most logical one to receive different wind direction because it will present the same behavior in all wind direction. Even though, the value of vortex shedding is high but it could be reduce by additional adaptive façade.

Secondly, wind adaptive façade should be one type of system that can be added to the building envelope in any side. Even though, there are different wind effects in each side of the façade, the adaptive external envelope can adapt itself to be no matter front, side or back façade according to wind direction. With square building the effect is quite complex to analyze compare to circular shape building which need to be analyzed only in one situation. And it can be possible that with circular shape the adaptive system can be work as one system and it provide more flexibility in building envelope designing as will be shown in next topic.

4.2 Building schematic design

From scope of study, below is the information that designing of example building should follow.

Building definition: 300+ m height
~50x50 m^2 floor plate
Multi-function used
Width and length ratio = 1 (square or circular) for floor plate shape

However, there are some changes in the design which are height of building and the floor plate size. The final design the building has 400.00 m high and the floor plate is in circular shape with diameter of 48.00 m. Floor to floor height is 4.20 m to be able to fit the module of the façade which will be explain in chapter 6. The building will be used as rental office, apartment and hotel, while the number of elevators was calculated by the number of users per area.

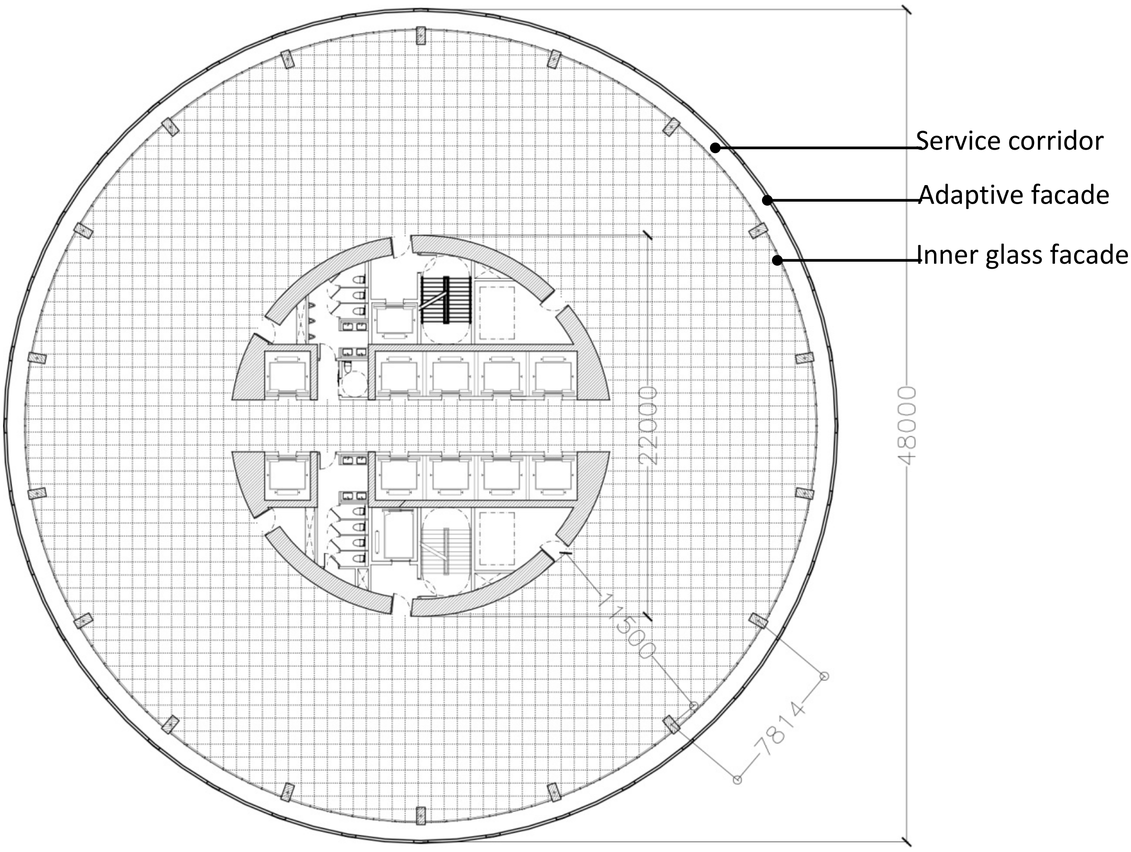

Fig 4.1: Typical plan of the building

Final building definition Floor plate area include core: 1810 m^2
Core area: 380 m^2 (21% of floor area)
Number of floor above ground: 92 floors (400 m)
Floor to floor height: 4.20 m
Number of elevators: 25 units

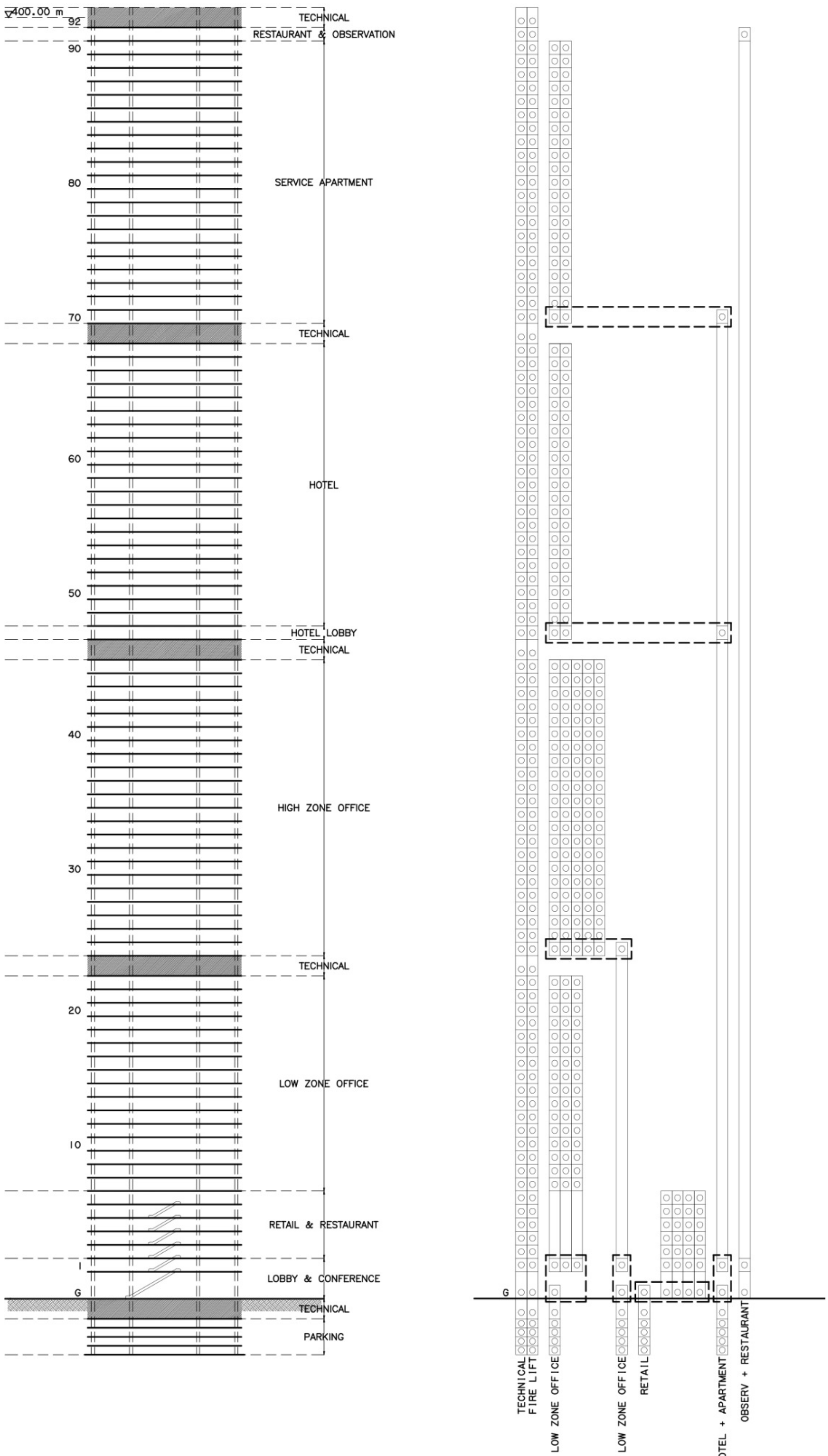

Fig 4.2: (Left) Schematic section of the mock-up building which show the height and functions in each floor. (Right) Number of elevator in each function compare to section.

4.3Structure analysis

For further comparison, wind force was calculated by using standard of EUROCODE (Eurocode, 1995). The calculation was set at highest wind load of typhoon basic wind speed (40m/s). Calculate at flat land with roughness length at very high density urban area (Z0=3m). For detail of calculation see Appendix A.

The calculation result is shown on first 50m above ground which is 972 N/m^2 and 50m from the roof which is 2085 N/m^2. These values will be used in order to calculate bending moment in each part of the building to define the size of the core and columns.

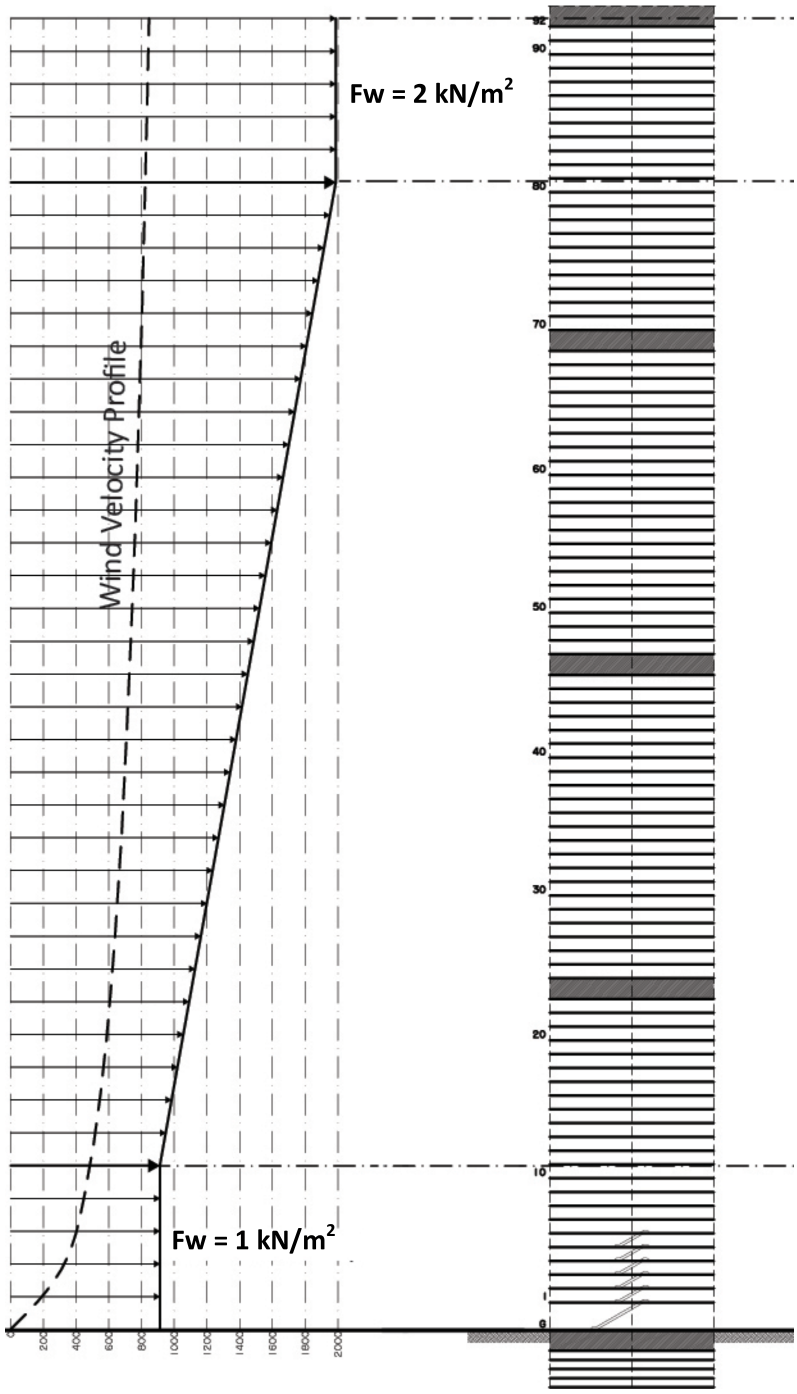

Fig 4.3: wind pressure according to calculation (Eurocode, 1995)

Bending moment of the building can be calculated by comparing the building with 2D beam. The calculation has to be divided in segments and the result for bending moment in figure 4.4. The main purpose of this analysis is to fine out the value and the method of calculation that will be used as compared results in the end of the research and design with adaptive façade, the bending moment was calculated by translating distributed loads to point loads.

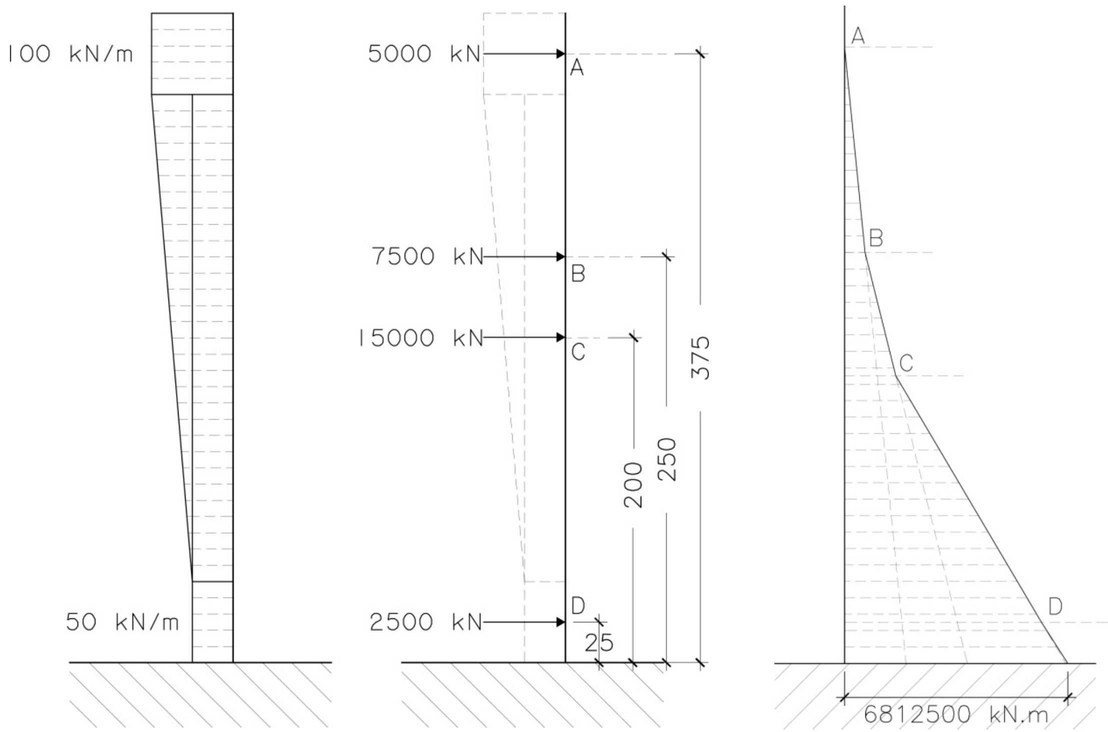

Fig 4.4: Load segments. Surface load was translated into point load as estimation value. The calculation show the combination of all point load as maximum bending moment at the base of the building = 6,812,500 kN.m

In order to prevent failure of structure, bending stress (σ_{m}) at the base of the building needs to be equal or lower than normal stress (σ_{n}) in which is the load of the building as in figure 4.6. From the calculation second moment of area (I) can be used to define the size of the core and thickness of the core wall that can handle the lateral load that cause by the wind. The calculation can be done by using these formulas for σ_{m} and σ_{n}.

$$\sigma_m = \frac{M.Z}{I}$$

σ_{m}: Maximum bending stress or load from the weight of the building (kN)

M: Maximum bending moment (kN.m)

Z: The distance from the middle of the core to the outer surface of the wall (m)

I: Second moment of area. For hollow cylinder can be calculated by $I = \frac{\pi}{64}(D^4 - d^4)$

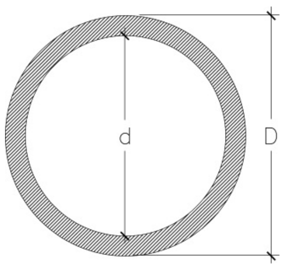

Fig 4.5: Second moment of area for hollow cylinder shape calculation

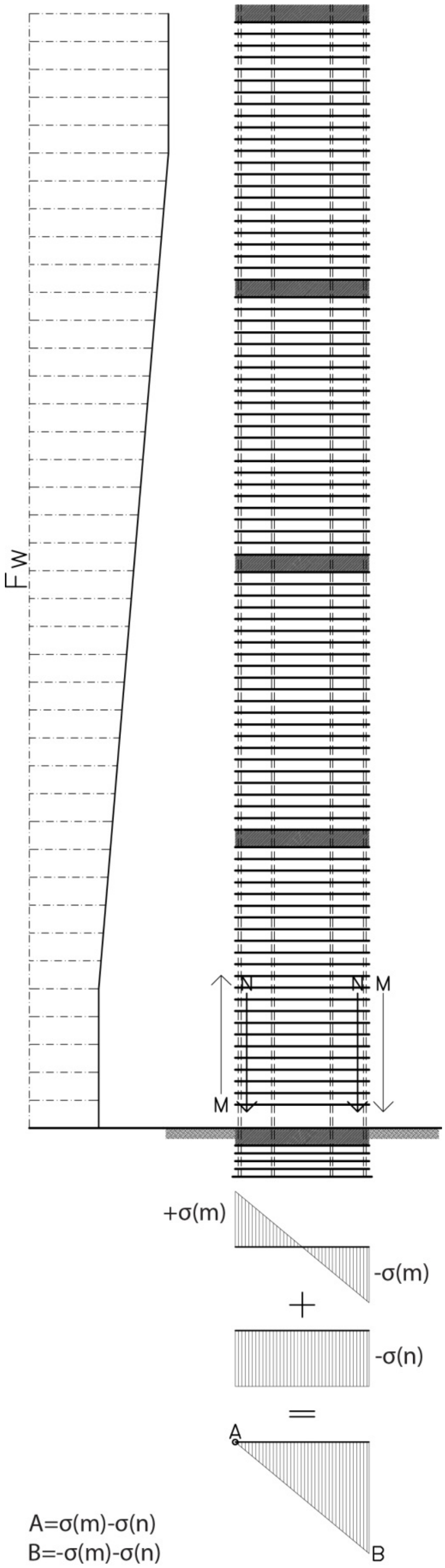

Fig 4.6: Prediction of combine stress in order to stabilized the building. Point A should have value as 0 or lower as the compression without tension.

$\sigma_n = {F_{total}}/{A_{core}}$

σ_n: Normal stress according to the building load (kN/m^2)

F_{total} : Normal force (N)

A_{core} : Cross section area of the core (m^2)

While the criteria is that $\sigma_n \geq \sigma_m$

The calculation in this point is only for estimation which the calculation will focus on the core of the building as the structure that handles windload but not the columns.

The estimation of normal force using the load at $12kN/m^2$ (Appendix B) which has the value of F_{total} = 1987200N.

The calculation for σ_m and σ_n was done by optimizing the radius of inner surface (r_{in}) and the radius of outer surface (r_{out}) of the core. The values were adjusted several times in order to have σ_m- σ_n (point A in figure 4.6) close to zero as much as possible. The values of the radius that would be the result are the most efficient size, with less material as possible.

The result of the calculation for the core that was designed (r_{in}=10) shows that the point where σ_m- σ_n=0 cannot be reached whichever the value of r_{out} was changed. The value is always negative which means that there will be no tension in structure and the structure is stable. Only concern for this case is the size of the core that handles the load of the building.

However, in order to compare the reduction in wind load, the most efficient size needs to be found out. Concerning only for windload, optimization of r_{in} and r_{out}, show the result that the core needs the inner radius = 6.80m and the outer radius = 7.70m (0.90m for the thickness) as the most efficient sizes for handling the wind.

This calculation method will be used in order to compare that reduction of material by using adaptive façade as part of the conclusion of the research.

5

Schematic design choices: First stage design

5.1Possible design choices

After realize wind effect in each building side, several schematic were designed and tested in CFD software to compare the effectiveness of shape and surface roughness in reducing wind effect to the building. At this stage 6 designs were created with different envelope shape and surface but base on a cylinder shape mock-up building. They were compared in term of maximum and minimum surface pressure, peak velocity, drag force (aerodynamic property) and change in location of under-pressure areas (separation flow). Furthermore, some assumption would be made in term of material used, difficulty in construction (technology requirement which relate to construction cost), maintenance, mechanical and energy requirement and user comfort.

The analysis was done in Autodesk Flow Design because it requires only few input data, it has the quick analysis which is depend on the adjustable mesh quality and it is the only software that show the change of the flow through time (other software only show the average value as the result). Seven computer models were made in the same size with 50m for diameter of cylinder shape building. The models are 100m in height because this study tends to investigate only in one segment of the building, exclude the top part of the building. The size of the wind tunnel is also 100m height in order to prevent the flow to go over the model and give inaccurate result.

5.1.1 **Design 00:** Additional smooth surface inadaptable envelope

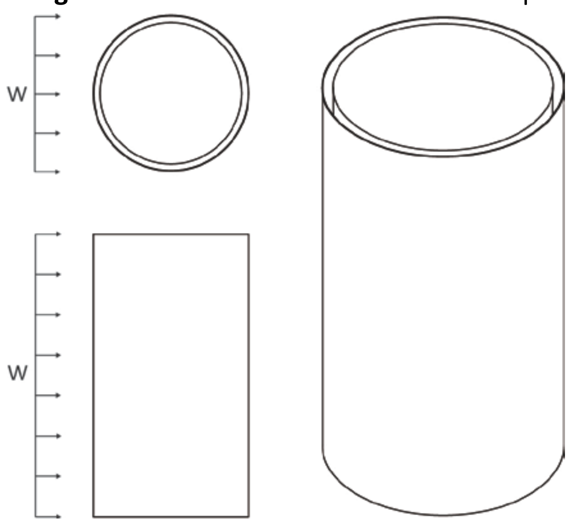

Typical circular cylinder envelope model was made as a normal building façade system for comparing with other designs.

5.1.2 **Design 01:** Shape changing envelope (ellipse shape)

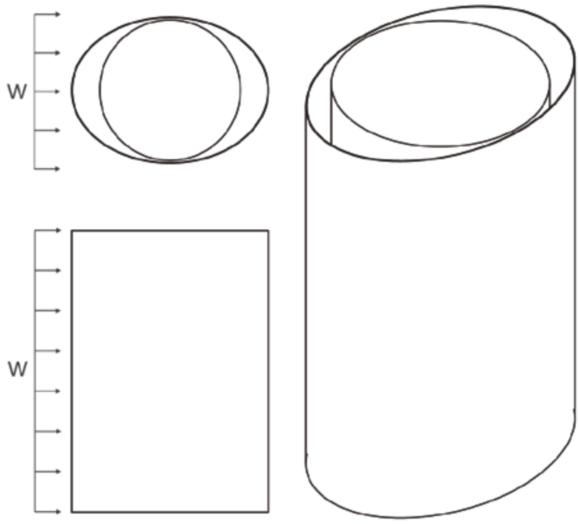

Flexible surface envelope should be able to adjust its shape according to wind direction. The design is similar to EVOLO Tower by (Dr Patrick TEUFFEL, 2007). The design is base on shape changing by reducing wind resistance area and extending the building along wind direction to reduce drag force and separation bubble.

5.1.3 **Design 02:** Rotatable aerodynamic shape envelope (water drop shape)

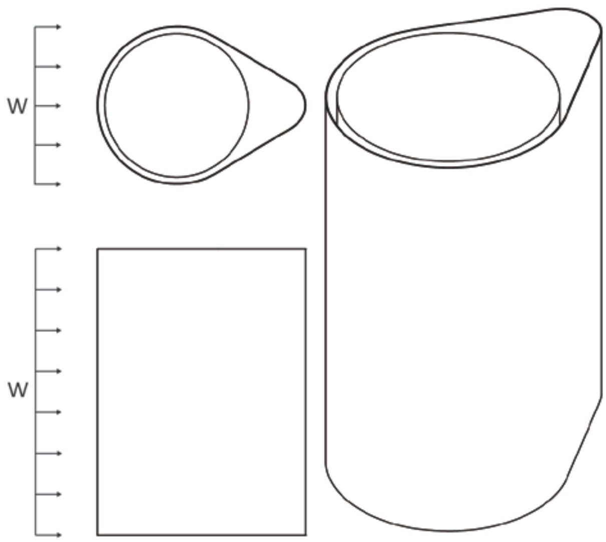

Rotatable envelope with streamline tail was designed to be rotatable by mechanism or by wind force. The streamline shape was designed to reduce turbulent wake and drag force and to make use of wind pressure to turn the tail to the back without energy needed. This concept was used in Wing Tower, Glasgow, UK.

5.1.4 **Design 03:** Adaptable fins outer envelope 1(two directions)

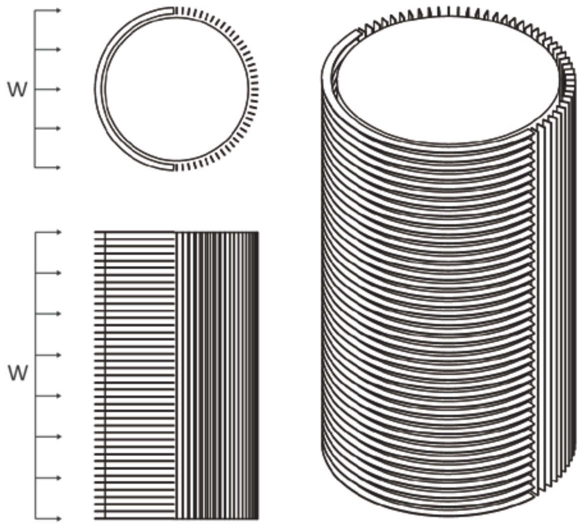

Adaptive fin system was design on surface roughness method. It consists of many small elements. In this case, front façade is included with horizontal fins to channel the flow, prevent vortex and reduce friction drag (shark skin mimicking). Back façade which is placed by vertical fins should reduce the turbulent wake at the back of the building which will cause effect in drag reduction (golf ball mimicking)

5.1.5 **Design 04:** Adaptable fins outer envelope 2 (horizontal direction)

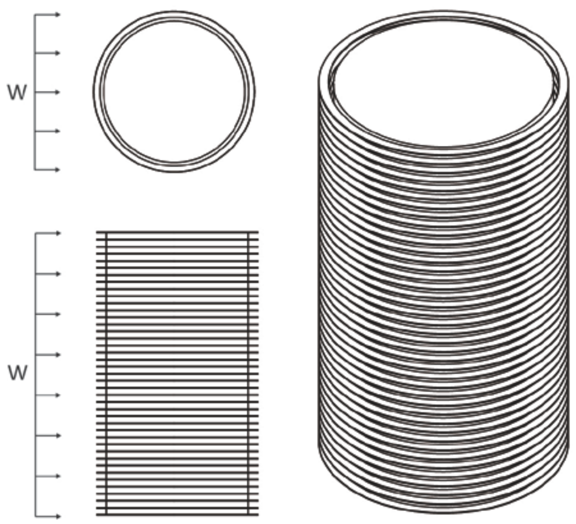

Similar model to "design 03" with only horizontal fins in both front and back façade was made to study the effectiveness of the back vertical fin. This model should show if the adaptable façade is necessary, or not.

5.1.6 **Design 05:** Adaptable surface roughness by using membrane

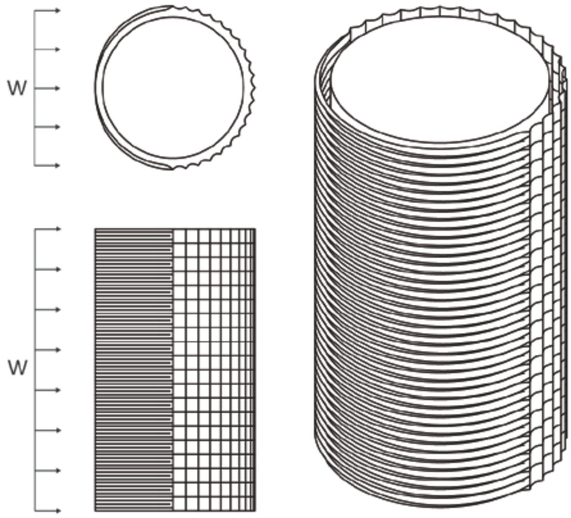

The design was follow "design 03" but the whole surface is covered with membrane that will change the direction of roughness according to wind direction. The membrane surface should be able to create a smoother flow.

5.1.7 **Design 06:** Vertical axis wind turbine envelope

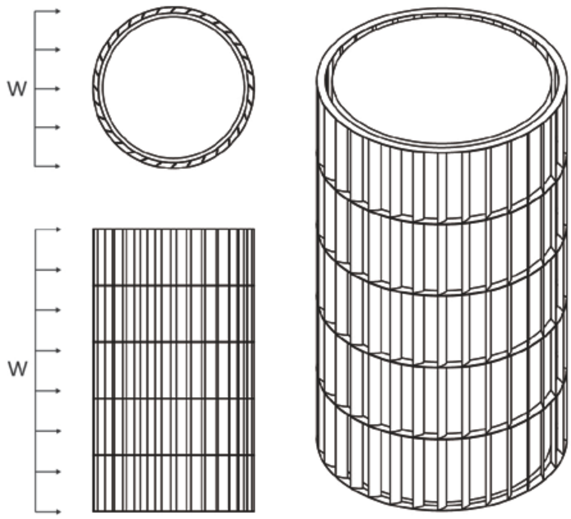

This method was based on transforming energy in the flow to create a useful kinetic energy. The wind will create movement in the turbines which possibly prevent direct pressure to the inner surface and the turbine can be used for electricity production. However, the system was predicted to create torsion to building structure which might be able to reduce the stress in torsion down by different rotational direction in each turbine. Other than that, rotating turbine can create different air pressure between both of side facades and create a push from one side of the building. And it can create vibration which reduces user comfort.

5.2Design choices comparison

Table 5.1 shows the result from CFD analysis in different building envelope. The black triangle in positive and negative peak pressure, highest velocity and drag coefficient columns indicate the development of the values during 16 second. Development of negative pressure is the column that shows the location transition of the area on the surfaces that occur to have under-pressure (negative value). The comparison at the left side of the table defines which system is the most suitable one. The selection will be done from the comparison by exclude “design 00” because it is a normal envelope.

The result shows that design 03 and 04 are the most suitable option. They can reduce drag force more than 90% compare to design 00 which is the normal building envelope. Design 03 and 04 should be the best candidates in the further study.

System	Design	Testing time (00.00 minute)	Possitive peak pressure (pa)	Negative peak pressure (pa)	Highest velocity (m/s)	Drag coefficient	Development of negative pressure	Aerodynamic property	Material cost	Construction difficulty	Maintenance aspect	Mechanical requirement	Energy requirement	User disturbance	Note
			Result						Assumption						
0 Circular building with second skin	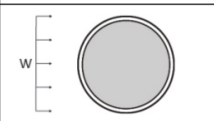	00.04 00.08 00.12 001.6	724.131 795.220 847.218 832.406	-1002.685 -1234.066 -917.309 -799.699	63.427 57.663 50.127 50.357	2.250 1.680 1.830 1.720	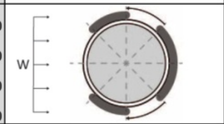	I	IIIIII	IIIIII	IIIIII	IIIIII	IIIII	IIIIII	
1 Shape changing envelope	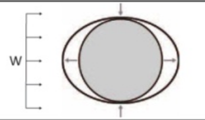	00.04 00.08 00.12 001.6	589.869 704.225 736.986 757.348	-713.649 -899.610 -1251.849 -1208.508	68.578 70.026 70.889 66.257	1.440 1.290 1.060 1.120	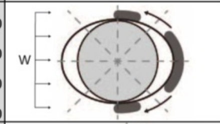	II	IIII	IIII	IIII	IIII	IIII	IIIII	
2 Rotatable aerodynamic shape envelope	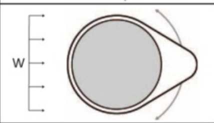	00.04 00.08 00.12 001.6	588.204 665.621 694.376 657.007	-830.256 -949.792 -1098.631 -1507.728	63.731 66.486 53.613 56.498	1.590 1.440 0.930 0.600	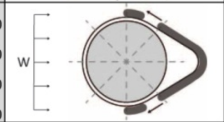	IIIII	I	I	I	I	IIIII	II	- Presume that it is rotated by flow of the wind
3 Adaptable fins outer envelope 1 (two directions)	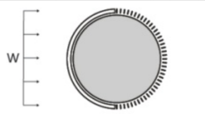	00.04 00.08 00.12 001.6	662.678 790.809 839.304 822.325	-932.782 -1239.290 -888.135 -775.536	65.674 60.053 49.734 50.253	0.190 0.140 0.140 0.130		IIIIIII	IIIII	IIIII	IIIII	IIIII	II	III	
4 Adaptable fins outer envelope 2 (horizontal directions)	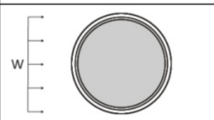	00.04 00.08 00.12 001.6	694.525 879.972 845.762 862.510	-790.782 -1228.723 -1063.581 -941.902	82.919 79.939 69.424 69.382	0.200 0.180 0.140 0.140	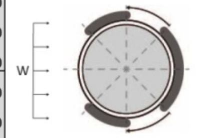	IIIIII	IIIIII	IIIIII	IIIIII	IIIIII	III	IIII	
5 Adaptable surface roughness by using membrane	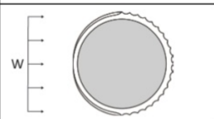	00.04 00.08 00.12 001.6	671.297 804.011 824.068 834.649	-940.604 -1183.865 -1115.886 -903.878	71.098 60.039 49.937 49.643	1.920 1.550 1.400 1.480		III	II	III	III	III	I	IIII	
6 Virtical axis wind turbine envelope	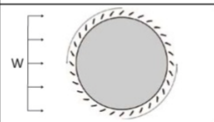	00.04 00.08 00.12 001.6	662.352 790.073 841.876 817.566	-933.667 -1206.572 -943.068 -991.029	65.486 58.593 50.680 50.467	1.280 0.980 1.050 0.950		IIII	III	II	II	II	IIIIII	I	- the analysis has been done without moving components - might be able to produce energy
								more (I) means better aerodynamic property	more (I) means cheaper	more (I) means easy to be built	more (I) means less maintenace	more (I) means less technology	more (I) means low energy needed	more (I) means more comfort	

Table 5.1: Design choices comparison (bigger size can be seen in Appendix C)

*Note that with Autodesk Flow Design cannot be used to analyze dynamic or moving element which in "design 07" case, it was done as normal model without any movement.

5.3 Further research in comparison of chosen design

With the highly and unexpected result of drag reduction, the experiment need to be rechecked again. It shows that design 03 and 04 models have empty space between the building and the fins which is unrealistic. The models were remade to relocate the fins to be placed on the cylinder surface.

The result shows that design 00, 03 and 04 have drag coefficient under 30m/s of wind velocity at 1.13, 0.48 and 0.67 respectively. Design 03 still shows the best performance which reduces 52% of drag force from original façade in design 00.

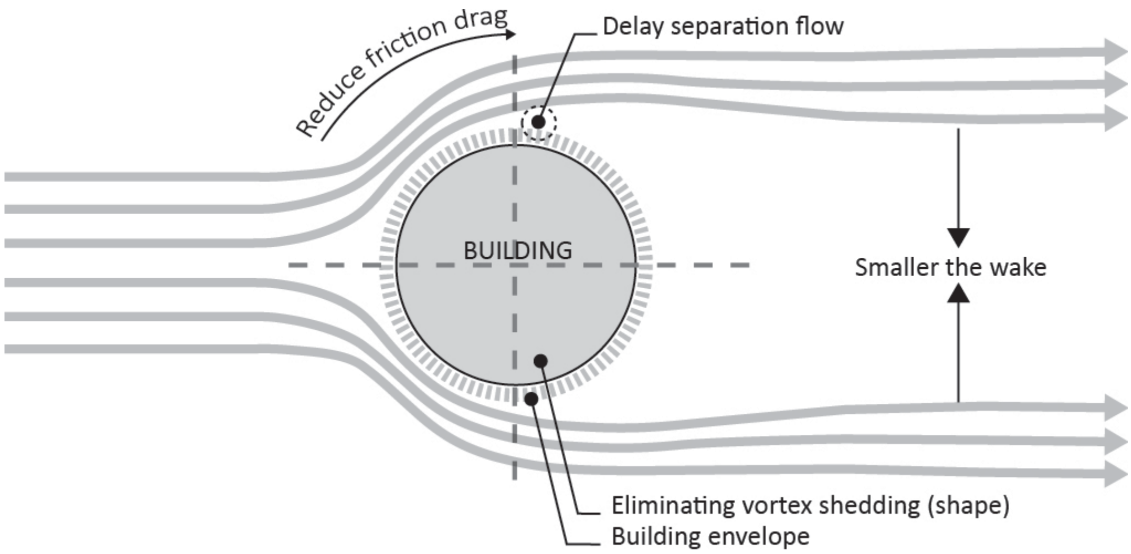

Fig 5.2: Strategy of wind load reduction

The further design and investigation has the main objective to understand and create the situation as in figure 5.2. The vortex shedding is reduced with the shape of the building and horizontal ribs while the design after this point will focus in reducing in friction drag and form drag. Friction drag reduction will be affective on the upwind side of the building while form drag will be reduced by smaller the turbulent wake at the downwind side of the building.

5.3.1 Prediction of flow according to different velocity

According to Reynolds number, wind velocity can create differencial in the flow behavior. The experiment was done again to investigate in effect to drag force in three designs. From wind load calculation, highest typhoon wind velocity which is 43.33m/s at 10m above ground can be 60m/s at 400m above ground.

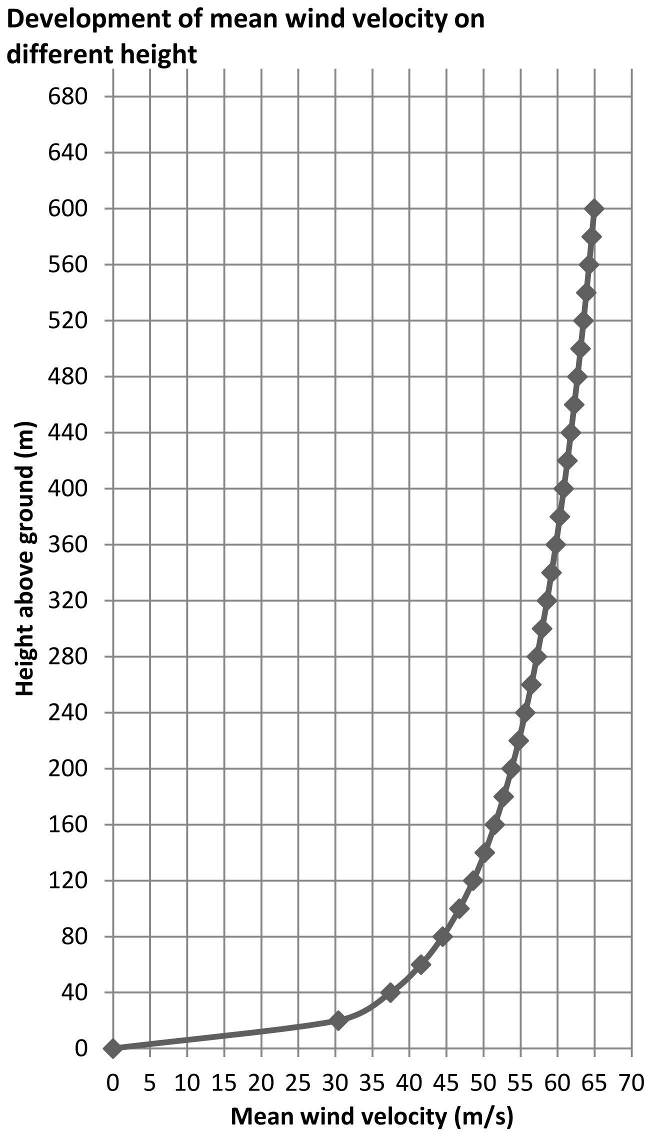

Fig 5.3: Development of mean velocity according to the altitude. Basic wind velocity at 10m above ground is 43.33m/s. Calculation base on EUROCODE (Eurocode, 1995)

The analysis was done in Autodesk Flow Design as before. The experiment was performed with models from design 00, 03 and 04 at every 10m/s of wind velocity from 0m/s to 70m/s. The result is shown in graph in figure 5.5.

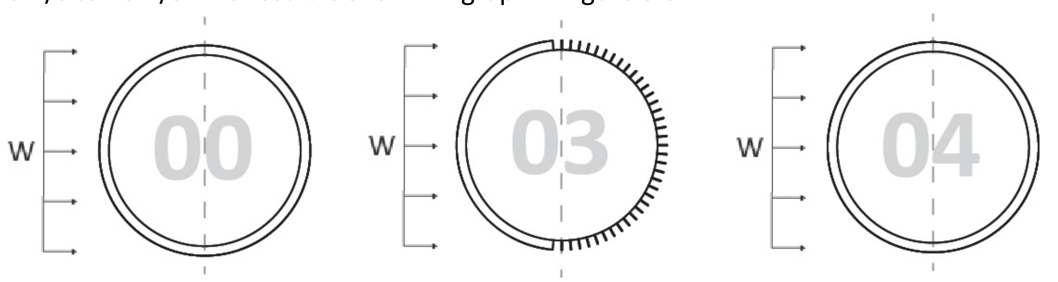

Fig 5.4: Three design that have been used for experiment in different wind velocity

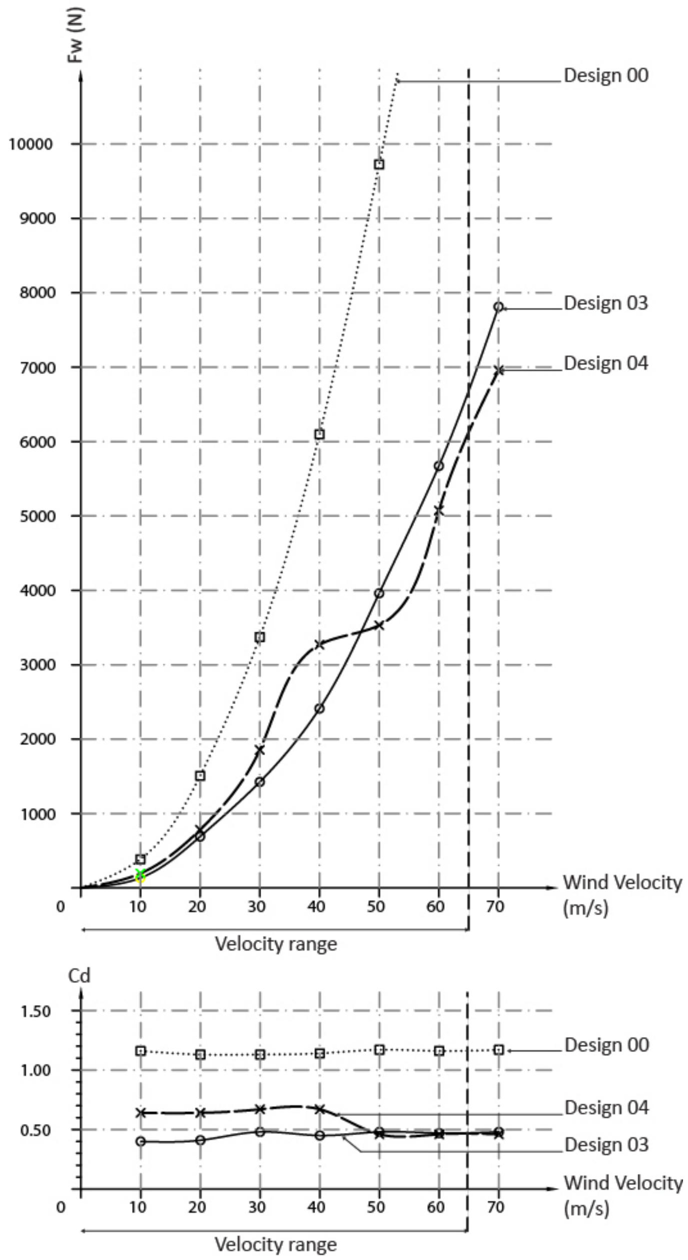

Fig 5.5: Result of drag force (top) and drag coefficient (bottom) that was occurred in three test models in different wind velocity. Horizontal and vertical fins (design 03, 04) can reduce drag force to the object. However, the result from wind speed that is higher than 40m/s start to show the different tendency that the model with only horizontal fins (design 04) performs better.

The result shows unexpected behavior at wind speed that is higher that 40m/s. From visualized image, that was created by the software, does not show any obvious different in the flow. It shows that with higher pressure of the wind, horizontal fins reduce the resistance to the wind more than the other two options. However, a prediction was made in order to make an improvement and perform further investigate. The possible flow behavior could be that, with reference from Reynolds number, the size of the turbulent wake is bigger in higher wind velocity, which means that the separation flow is relocated from the position in low wind velocity (10-40m/s). If the turbulent wake is bigger, it might mean that the separation flow is moved forward against direction of the flow. The result the movement of separation flow can cause the flow to be forced away from the surface than that effect from vertical fin can reach.

At this point, another model that base on design 03 was developed. From figure 5.6, there are couples of additional vertical fins to the front part of the object in order to create effect to the separation flow before it flow away from the object

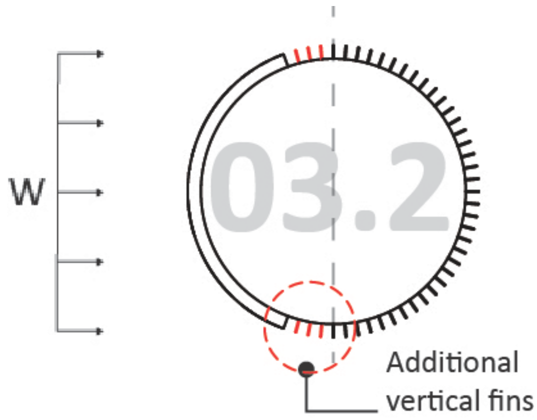

Fig 5.6: Development of design 03 for high velocity wind by adding vertical fins to the object surface before the widest point of the cylinder

The result of design 03.2 in CFD analysis is shown in figure 5.7. Red line on the graph shows the new result from the new model. When the wind speed is higher than 40m/s the drag force is changed and it become lower that design 04. It can be conclude that the location of the most frontal fins depend on wind speed. In low wind speed below 40 m/s, the vertical fins can be located from the widest point of the cylinder to the back and in the high wind speed above 40m/s probably the location of the vertical fins should be in front of the widest point near the location of separation flow.

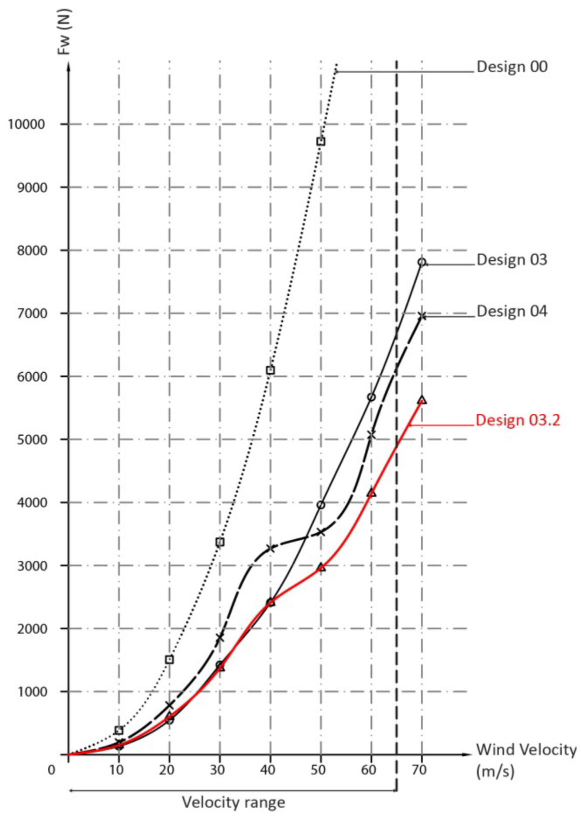

Fig 5.7: Comparison of drag force that is occurred in various wind velocity in design 00, 03, 04 and 03.2. Red line in the graph represents the result from design 03.2 which is the developed version of design 03 for high velocity wind.

However, the values of drag force for the normal flat surface were compared to the wind force calculated by standard calculation (Eurocode, 1995) to prove the accuracy of the software as shown in table 5.2.

CFD result (Autodesk Flow Design, 2015)			NEN-EN 1991-1-4	
Wind speed (m/s)	Drag force (kN) to 50x100m object	Drag force (kN/m^2)	Mean wind velocity (m/s)	Wind force (kN/m^2)
10	384.67	0.08	10	0.05
20	1506.65	0.30	20	0.25
30	3373.18	0.67	30	0.61
40	6096.56	1.22	40	1.18
50	9724.60	1.94	50	1.96
60	13877.32	2.78	60	2.98
70	19084.29	3.82	70	4.25

Table 5.2: Show the comparison of CFD result and standard calculation in drag force and wind force. Note that the values for mean wind velocity were calculated at the roof which is not basic wind velocity at 10m above ground.

The values of drag reduction in each velocity were calculated to define the effectiveness of the façade which shows that the façade with only non-adaptable horizontal ribs (design 04) can reduce drag force from 49-63% while the adaptive façade (design 03 and 03.2) can reduce 60-70% of wind load. In this case, it can be applied only to circular cylinder shape building and also the experiments were done with very simplified model which in the final design the adaptive would be in more complex geometry that can cause drag reduction to be decreased.

Wind velocity (m/s)	Normal surface façade (Desigin 00)	Non-adaptable horizontal ribs façade (Design 04)		Adaptive façade (Design 03 & 03.2)	
	Drag force (kN/m^2)	Drag force (kN/m^2)	Drag reduction (%)	Drag force (kN/m^2)	Drag reduction (%)
10	0.08	0.04	49.28	0.03	60.84
20	0.30	0.16	48.06	0.12	60.01
30	0.67	0.37	44.09	0.27	59.31
40	1.22	0.65	46.38	0.28	60.46
50	1.94	0.71	63.69	0.59	69.56
60	2.78	1.01	63.44	0.83	70.15
70	3.82	1.39	63.54	1.12	70.59

Table 5.3: Drag reduction of non-adaptable horizontal ribs façade (design 04) and adaptive façade (design 03 & 03.2)

5.3.2 Front façade: Fins height and space ratio

Drag force on upwind or front side of the building is mainly from front pressure and frictional force. However, without changing the shape of the building, front pressure might be complicate to be dealt with, which in this case, upwind façade performs as friction drag reduction mainly.

As mentioned before in chapter 2, there are some existing objects in nature also with biomimicry products that has the same method of using horizontal or oriented along the flow rib structures in order to reduce friction drag. For example, shark skin is the most well-known surface that is believed to perform the best in improving hydrodynamic property of shark locomotion, which result in many research to create an understanding of its logic, follow up with some design of the surface in order to create the similar performance as original shark skin.

Friction or viscous drag is caused by the interactions between the fluid and a surface parallel to the flow, as well as the attraction between molecules of the fluid (Dean & Bhushan, 2010). In flat surface, there are possibility that turbulent flow can be happened close to the surface, in which fluid particle move in swirling and cross-stream. The inclusion of cross-flow and non-parallel relative velocities between fluid particles in turbulent flow causes an increasing in momentum transfer. The cross-flow momentum transfer performs the result in drag increasing (Dean & Bhushan, 2010). Ribbed surface similar to shark skin reduce cross-flow turbulent on the surface by forcing the fluid to flow in the same direction.

Riblets are most commonly defined by their h/s ratio (rib height to space between ribs ratio) but the experiment of the shape have varied between each research group. From figure 5.8 that show 3 different riblets shape and the result in drag reduction in each surface. It seems to be that flat blade with h/s=0.6 has the best performance which it is in similar shape with the design 03 and 04 which was mentioned before. However, the experiment from figure 5.8 was conduct with the water as the fluid material which has different viscosity compare to air and the result in both situation could be different.

In order to be able to define the best performance h/s ratio, two models was tested with CFD analysis software. Two ratio was chosen, h/s=0.5 and h/s=1 by the result from Maruta research with the size of balcony compare to size of the building (E. Maruta, 1998), with the criteria that the riblets need to be applied to the mockup building which in this case the ribs should be placed in the same level of floor plate which will not obstruct the vision of the users to outside of the building.

The experiment was done in Autodesk Flow Design with wind speed at 40m/s on cylinder model with diameter of 50m, 100m in height and 2.50m width of the horizontal ribs. The height of the tunnel is at the same height of the model in order to prevent the air to flow over the model. The result shows that the model with h/s ratio equal to 1 perform better with drag coefficient at 0.62 while the model with h/s=0.5 has drag coefficient at 0.97. The model with higher ratio has 36% of drag reduction from model with lower h/s ratio. The model with h/s=1 will be used for further design.

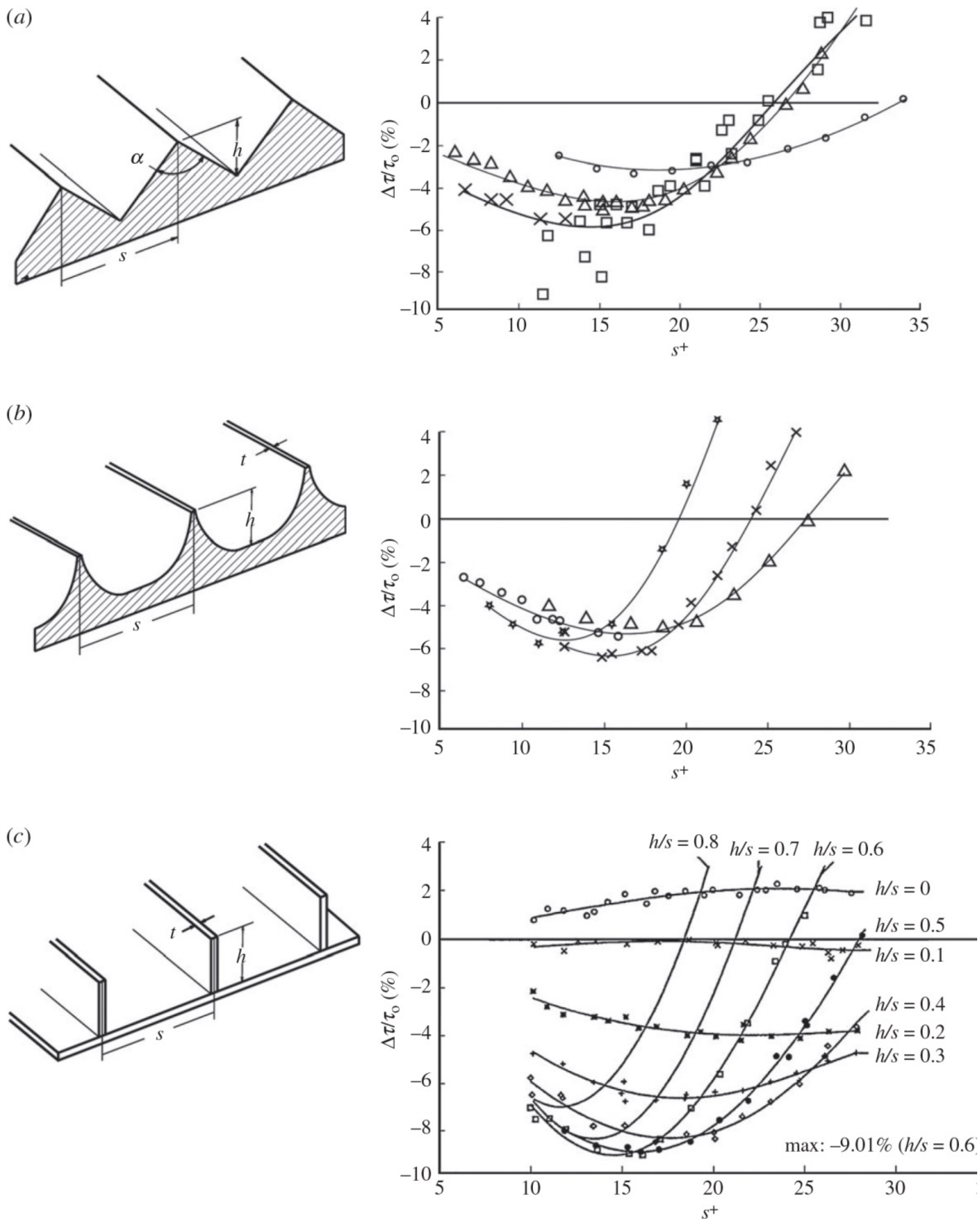

Fig 5.8: Three different surface riblets with the result in drag reduction from the experiment with underwater flow. (s^+) is Reynolds number of the surface. ($\Delta\tau$) is the shear stress reduction and (τ_o) is the shear stress on smooth plate. (Dean & Bhushan, 2010)

5.3.3 Back façade: Delaying of separation flow

In the first place, vertical riblets at the downwind façade was designed by mimicking the method of golf ball to create turbulent in order to pull the flow closer to the surface and reduce the size of separation area or turbulent wake. From the experiment with different velocity shows that downwind vertical riblets affect the performance of drag reduction that it can reduce more of the drag force compare to only horizontal riblets around the building.

From Kawamura (Tetuya KAWAMURA, 1985), they performed an experiment by using CFD software to understand the flow behavior that occur to circular cylinder with surface roughness. From their model, the roughness was on the surface at that point behind the widest point of the cylinder which is the area of separation flow. The result shows that with surface roughness the separation flow was delayed. The roughness created small eddies between vertical riblets and the eddies develop in their size along with pulling the flow back to the surface, result in smaller turbulent wake at the back of the object.

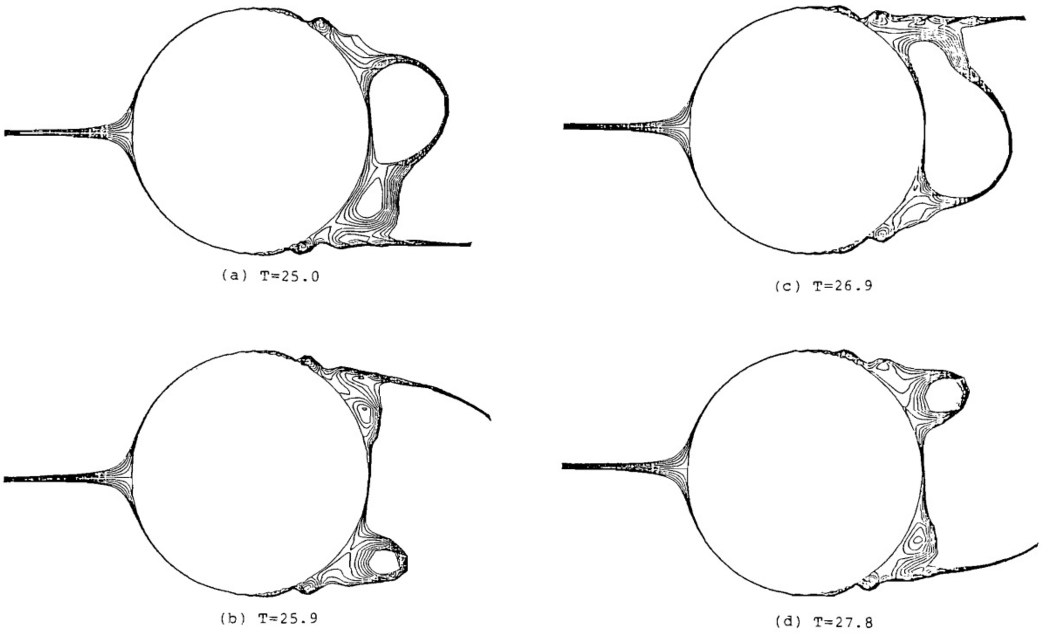

Fig 5.9: Detailed flow patterns near a circular cylinder with surface roughness at Re = 40000 in different time period (Tetuya KAWAMURA, 1985).

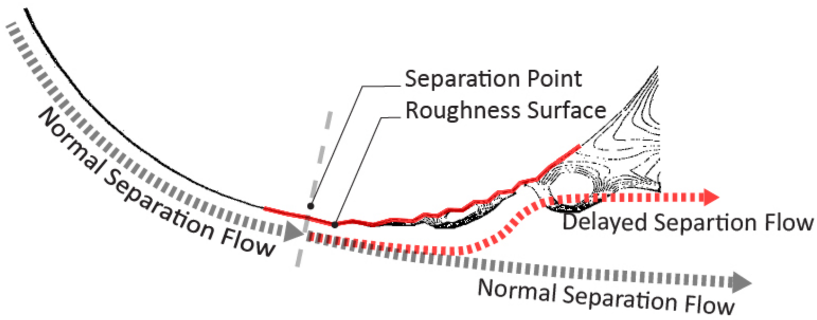

Fig 5.10: Effect of surface roughness to delaying of separation flow. The roughness create small eddies which result in drawing back the separation flow and smaller the turbulent wake and drag force in the end (redraw from (Tetuya KAWAMURA, 1985))

However, there is no available research that define the size or any aspect ratio of the roughness at the back of a circular cylinder in order to create drag reduction. The designing of the adaptive façade at this point, it can be seen that the direction will be the transformation of horizontal ribs to vertical ribs when the wind approach the building. And in order to realize if vertical fins work as mentioned in the research, physical wind tunnel experiments were conducted which will be explained in next topic.

5.3.4 Wind tunnels

The main object in experimental with wind tunnel in this case is to observe the delay of separation flow in the design proposals. In the case that the delay of separation area is occurred, it can be assumed that the turbulent wake is smaller and drag force is reduced. This study will confirm the result in CFD analysis.

There were two physical wind tunnels that were made with the most reasonable budget as possible. Both tunnels are first designed by CFD software (Autodesk Simulation CFD) to confirm the uniform flow that the tunnels would create. And after finishing assembling the tunnels, the flow and wind speed was checked again with smoke generator and anemometer.

There were three testing models, which follow the shape and surface type of design 00, 03 and 04. The intention is to test design 00 and 04 first to define the location of separation flow, and then modify the location of vertical fins in design 03 to match with the flow behavior (the design 03 was pretended to be a building with adaptive façade). The scales of test models are 1:500 with the height of 4cm according to the height of the equipment which will be explained further.

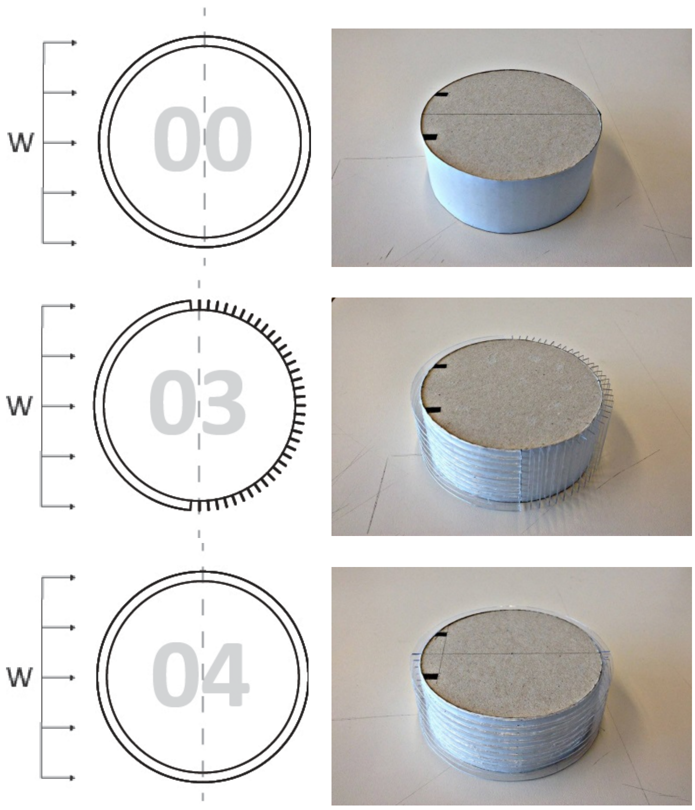

Fig 5.11: Testing objects for wind tunnel experiments. All of them were made by following the design of schematic design model.

5.3.4.1 Wind tunnel 01

By helping from Buckylab course (TU Delft, Bouwkunde, AR1A015), some parts of wind tunnel were provided which are leaf blower as flow generator, wind damper (velocity adjustment valve) and a wind diffuser. Wind diffuser was tested by Bucklab student that it has the best performance in all three of their options with the most uniform flow and wind speed. However it was check again with anemometer, the result show that at the edges of the diffuser has very low wind speed which was only 5-7% compare to the middle area, which mean that the flow was non-uniform.

The cross-section of the tunnel was in the same size with the diffuser which is 58x4cm with the length of 90cm include 20cm of flow straightener. The test objects were placed one by one, 10cm away from straightener. The flow behavior was check in CFD software and smoke tube in the real tunnel. The flow was straight, but the velocity as result from the software and anemometer measured at the end of the tunnel show that there were big fluctuation at the edges of the tunnel. However, with the size of the tunnel compare to model is much bigger, which in the middle part of the tunnel the velocity was quite steady. The whole equipment can be adjust in two different speeds, at high speed the flow velocity was 1.25m/s at the edge to 6.3m/s, and in low speed was 0.30-1.37m/s. Both of them still too high for 1:500 scales which wind velocity in this scale should be approximately 0.12m/s as wind speed of 60m/s in the real scale.

Fig 5.12: Wind tunnel 01. (Left) leaf blower and flow damper, (middle) wind diffuser, (right) wind tunnel

The flow behaviors were captured by video camera as top view. The result was not as expected because of non-uniform and unstable flow that was mentioned before also with a unprepared situation. The velocity was too high that the smoking tool cannot provide the proper visualize result. The result from design 00 and 04 show the result as expected but not for design 03 which is the main idea of this experiment. However, it can be seen that whenever the smoking line was close to the surface of the glass or the floor of the tunnel, it happen to be some delay of separation flow. The rough conclusion was made that because of the surface friction of the glass creates slower velocity close to the surface which perform the result as what predicted.

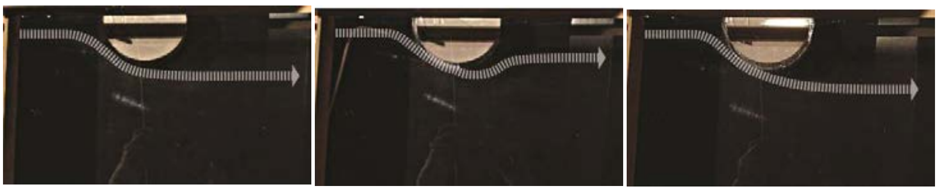

Fig 5.13: Results from wind tunnel with arrows overwrite on the direction of smoke. (Left) design 00, (middle) design 03 with the flow close to the glass surface, (right) design 04.

5.3.4.2 Wind tunnel 02

The second wind tunnel was developed from the first version. The method was changed from blowing the wind to use an air pump to create suction in the tunnel (similar to vacuum cleaner). The tunnel was smaller but still design to be able to work with the same test objects. The cross-section of the tunnel is 30x4cm with 70cm in length. At the end of the tunnel was where the air pump was installed included with velocity adjusting valve. Form CFD software, it shows that the flow in the tunnel is uniform while it will start to change the direction by suction force from air pump approximately 20cm away from the inlet of the air pump. The test objects were placed 5cm from the beginning of the tunnel where the flow still uniform.

The flow velocity was checked at the opening of the tunnel by anemometer in three different adjustments. At high speed the velocity was 1.03-1.05m/s, at the medium speed was 0.56-0.61m/s and at the low speed was 0.13-023m/s. The main experiment was done at the medium speed because at the lowest speed, the velocity is too low and it was lower than the flow from the smoke tube. The flow behaviors were recorded by a video camera shows the flow from top view.

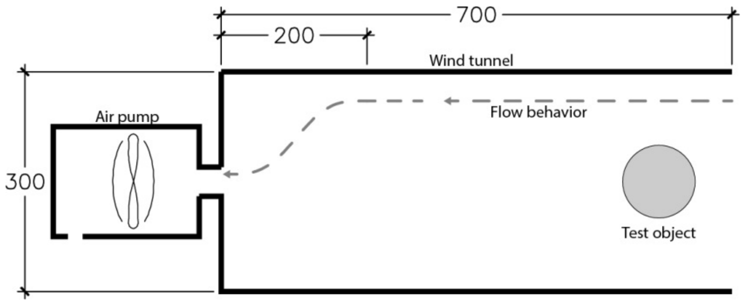

Fig 5.14: flow in the tunnel and location of the test object

For design 00 and 04 the flow behavior perform in the same manner with previous experiment. However, at the medium speed during the test with design 03, the delaying in separation flow was occurred which confirm the effect of the vertical fins to smaller the turbulent wake. Figure 5.14 shows captured images from the record that the flow can be clearly seen.

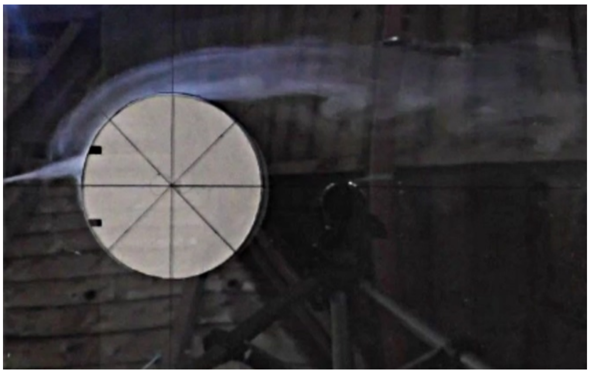

Flow behavior around design 00

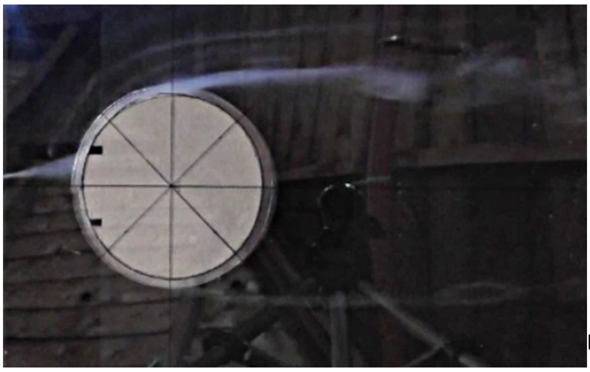

Flow behavior around design 04

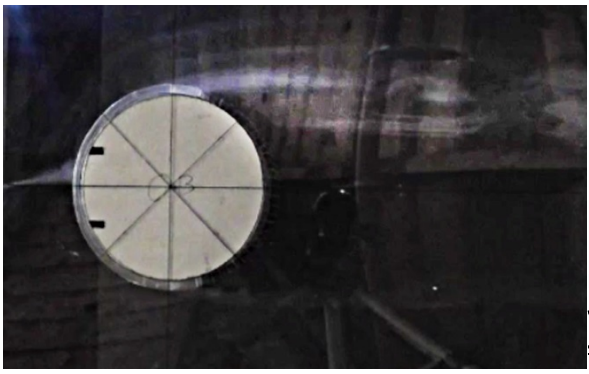

Flow behavior around design 03 which shows the delaying of separation flow

Fig 5.15: Result images from wind tunnel 02 (the wind come from the left)

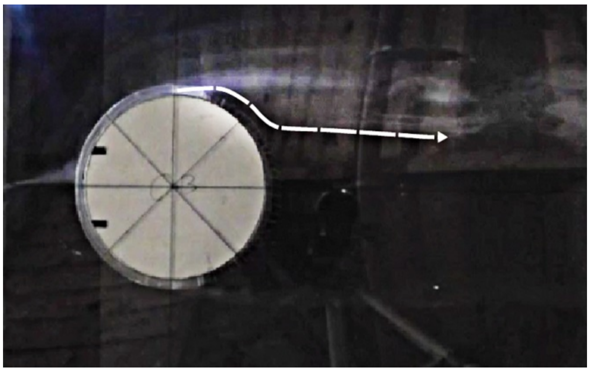

Fig 5.16: Redraw image from design 03 to show the delaying of separation flow and new direction of the flow that occurred because the vertical ribs at the downwind side of the object (the wind come from the left)

5.4Conclusion from first stage design: Schematic plan and surrounding air flow

From the selecting of design schemes and follow-up study, the design objective can be concluded as follow. As the wind approach the building the façade that receive the wind which in this case is called front façade will perform as friction drag reduction by it surface shape of horizontal ribs with h/s ratio equal to one. The shape of circular cylinder building and horizontal riblets surface reduce possibility of the creation of vortex shedding and friction drag force. However, in term of different wind direction, it means that front façade can be any side of the building depends on wind orientation. The horizontal riblets as mentioned before need to be able to transform into vertical riblets at the back of the building whenever the wind approach the building.

The design direction was set as horizontal riblets (fins) in all sides of the building are the basic position. At the moment when the wind approach the building, the upwind frontal façade will remain in the basic position, while the downwind back façade will start to change the shape from the middle part of the back façade relatively to the widest point of the cylinder building and further depend on wind velocity and location of separation flow.

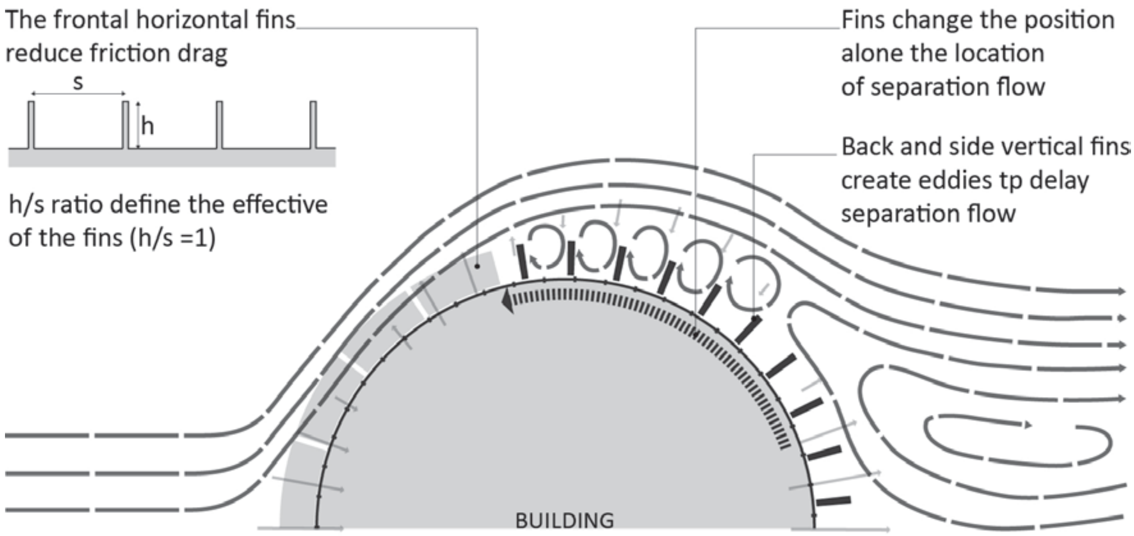

Fig 5.17: Schematic plan of building and wind responded adaptive façade

6

Design development: Second stage design

6.1Operating system method

6.1.1 Adaptive input information

There are three input information for this wind responded adaptive façade which are wind direction, wind velocity and duration after the impact. Information that is received from wind direction will define where upwind-downwind or front-back façade are, and it will command the façade in different type of adaptation (front: horizontal riblets, back: vertical riblets). Wind velocity information can be used for defining the locations of separation. The location of separation flow can be firstly defined from CFD software or physical wind tunnel test in various wind speed. The results from the tests are recorded into a database which will be matched to wind velocity that is detected from the detectors around the building. Time after impact shows in which location the transformation should be. It is also recorded information from CFD and physical tests and being used by matching with situation at the building.

Wind velocity can be detected by anemometer. However, measuring mean wind velocity is not possible in this case, or else, the anemometer has to be installed on the roof top of other surrounding building. The possible suggestion is that the location of anemometer should be around the project building by installing it on the cantilever beam outside the area of the riblets in order to measure the velocity that is away from the surface. If the anemometers are installed around the building, it is possible to be calculated or compared to the database to get the mean wind speed and order the movement in adaptive façade.

The set of anemometer around the building can also be used to define the direction of the wind. For example, when the wind approach the building, anemometer on the front façade will possibly show very low velocity because there is high pressure in the frontal area but only small movement of the air. Anemometer at the back will possibly show low value of velocity or fluctuation of velocity because of turbulent wake. Two of the side façade anemometers will possibly show the high and stable velocity because the concentration of the flow in the area. From the data that receive from the set of velocity measurements, wind direction should able to be computed and the adaptive façade can work according to calculated direction.

From (Dr Patrick TEUFFEL, 2007), wind direction can be 10^{o} different between 300m different in height. The mock up building is 400m height which mean that from the ground floor to the roof top the wind can have only less than 13° different in direction. Moreover that the within the city area with high roughness length, the wind in the level close to the ground has low velocity and possibly highly fluctuated. There is possibility that the set of wind measurement can be in one set on high altitude that has less effect from turbulent of the surrounding building and receive the information mainly from the seasonal wind in the area. The height of the measurement set can be located from wind profile according to roughness length of the area or from physical wind tunnel test.

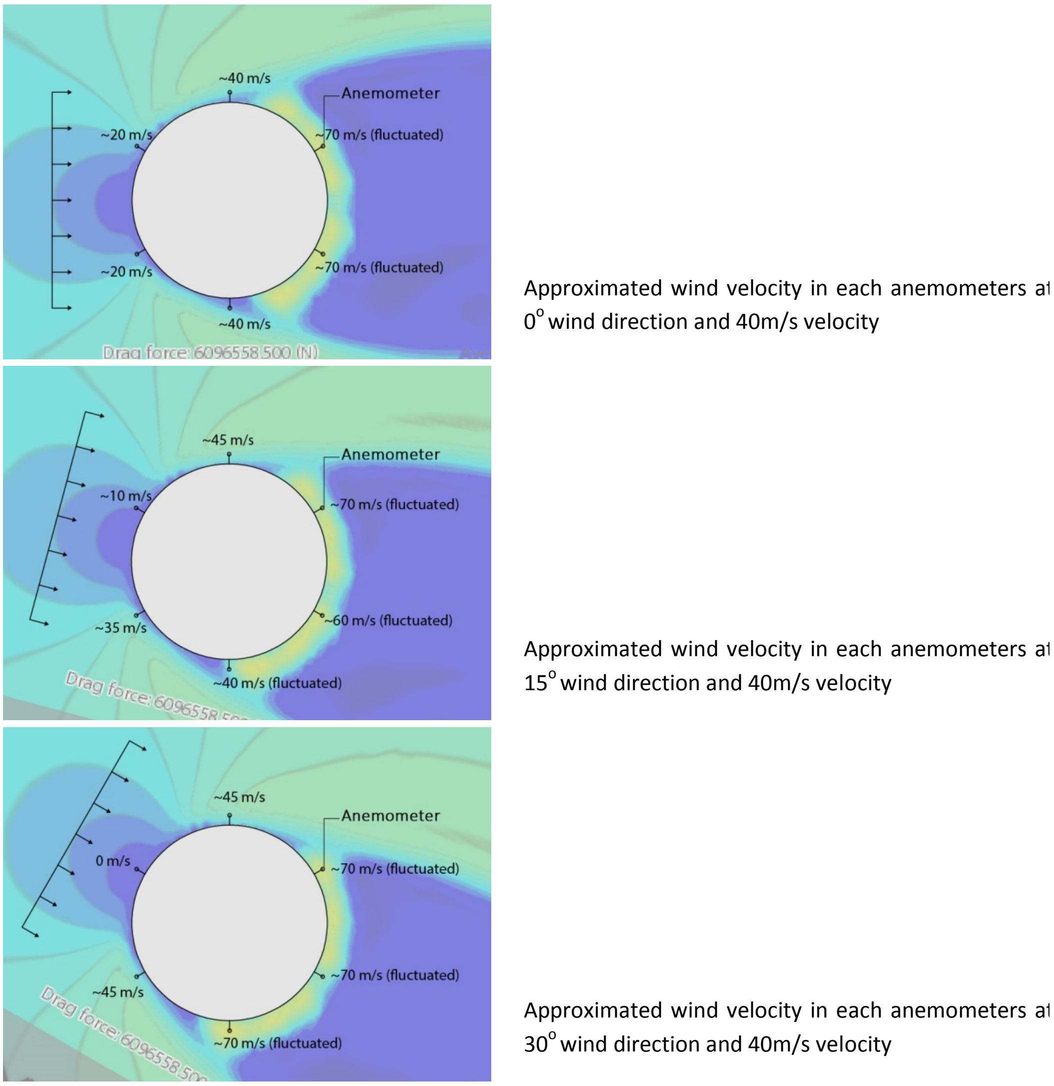

Fig 6.1: Example of wind direction defining by set of anemometers around the building. From the images, mean wind velocity = 40m/s at 0°, 15° and 30° to the building

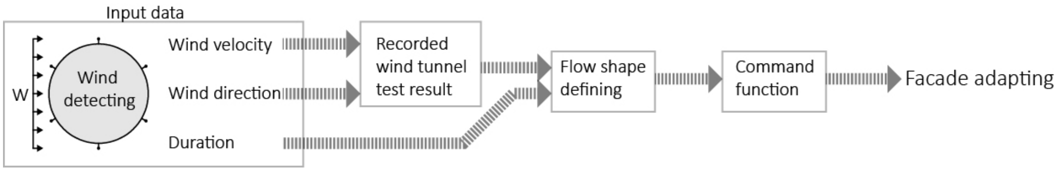

Fig 6.2: Sequence of data translation

6.1.2 Façade adaptive set relate to height

Roughness of earth surface is the objects like buildings or trees create non-uniform wind direction and velocity. Wind speed at low altitude happens to have lower velocity compare to speed in higher altitude. This roughness of earth surface can be defined by roughness length (Z0) which wind velocity in each height can also be calculated by value of this roughness length.

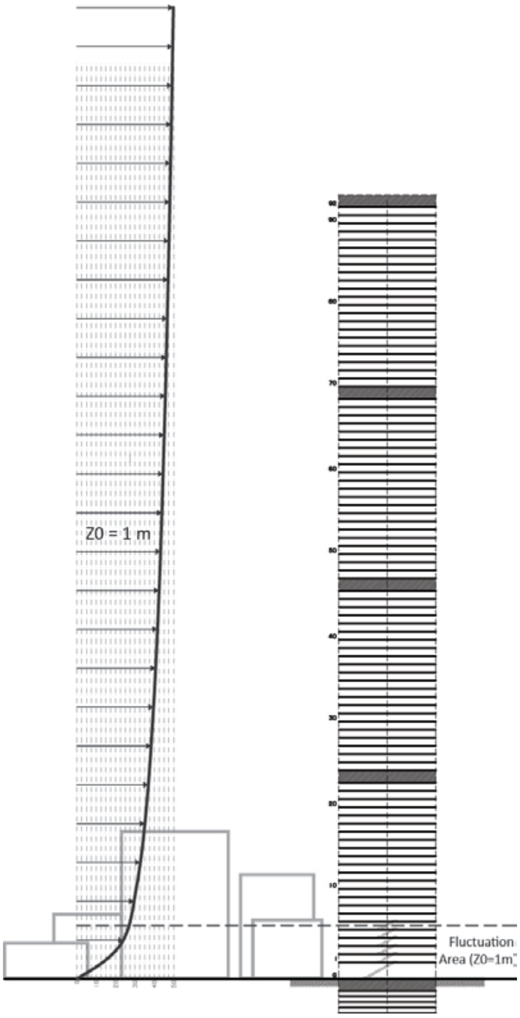

Fig 6.3: wind profile and height of fluctuation area according to roughness length Z0=1

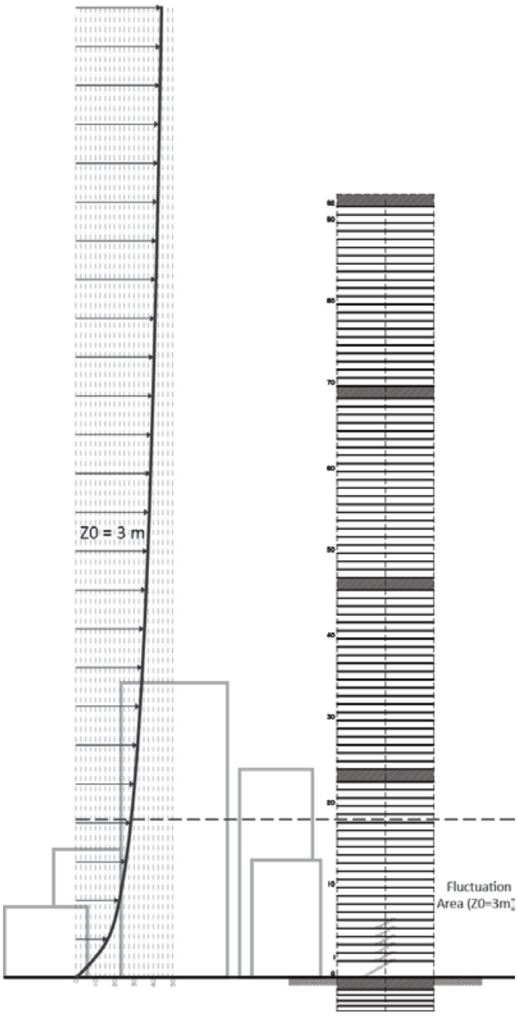

Fig 6.4: wind profile and height of fluctuation area according to roughness length Z0=3

Figure 6.3 and 6.4 show wind profile and fluctuation area according to the surrounding from roughness length Z0=1 and Z0=3 respectively (Eurocode, 1995). These profiles remain the same even in different velocity. Fluctuation area is in the area where air flow has high turbulent according to obstacles around the building and considered to be less effect to the building because it is gust wind with low and unstable velocity, no specific direction and located at the lowest part of the building which cause only small ending stress to building structure. With these reasons, part of the building in this fluctuation area has no require for adaptive façade and can be left open with normal façade. The height of fluctuation area can be defined by the formula below (Mook, 2015).

$$Fluctuation\ height = 20(Z0) - Zd$$

Z0: Roughness length (m)

Zd: Displacement height (m) which can be calculated by $Zd = \overline{H} - \frac{Z0}{k}$ (Emil Simiu, 1996)

$\overline{H}$: General roof top level (m)

K: Kármán constant = 0.4

Note*: Normally, above equations are used to define "effective height" (Z) which is used to calculate mean wind speed in atmospheric surface layer (a.s.l.)

For example, in case that Z0=3, and $\overline{H}$ can possibly be estimated by ten times of roughness length ("Roughness length," 2015) which equal to 30m. The height of fluctuation area for Z0=3 is 82.5m.

Façade adaptive sets

As mentioned in chapter 2 and 6, with different wind speed, the façade will be adapted differently. With varies wind velocity in each height means that the façade will be adapted in each level of height differently. In case that all façade components are independently adapted, the system can be a complex one. By dividing the whole façade in to sets, the system can be simplified. With wind profile that is created by roughness length, the adaptive sets can be defined. For example, in figure 6.5 shows wind profile from roughness length (Z0) = 3m. From the profile, it is possible to create the sets of velocity differences. From the image, red lines are the lines that were projected from intersection points between the profile and wind velocity in every 5m/s. Between each red line can be used to defined sets of adapting façade and all subset in these sets should be adapted in the same moment. This adaptive set is only for suggestion, the wind velocity difference between each sets can be smaller or bigger depend on the test from full scale CFD analysis and wind tunnel test which is in the further development of the project.

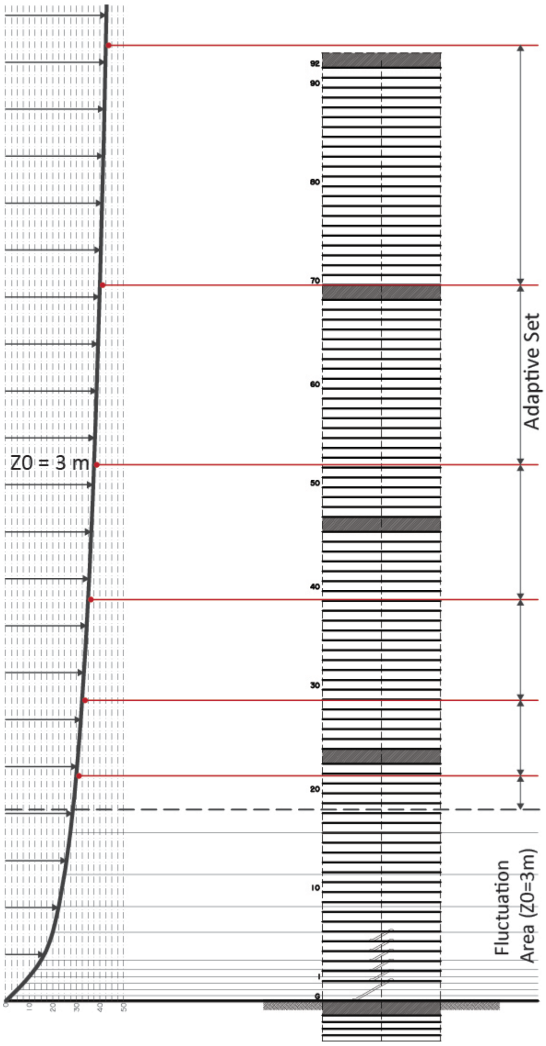

Fig 6.5: Wind profile at Z0=3m and possible adaptive sets that were defined by the profile. Each adaptive set handle the wind ±5m/s in speed different from the set above and below them

6.2 Façade component designing

6.2.1 Façade component design choices

The objective in this part is to fine the solution to create riblets surface around circular cylinder building that is able to be change in their orientations from horizontal to vertical riblets whenever the wind approach the building. The possible solution is to divide the riblets in first stage design into short fins that are placed in the same lines to create overall riblets surface shape. From this point three solutions were created and one was selected weight on h/s ratio =1 (include with CFD analysis) or better aerodynamic property, possibility of being adapted in set, less user disturbance and its attractiveness.

Rotatable fins theme

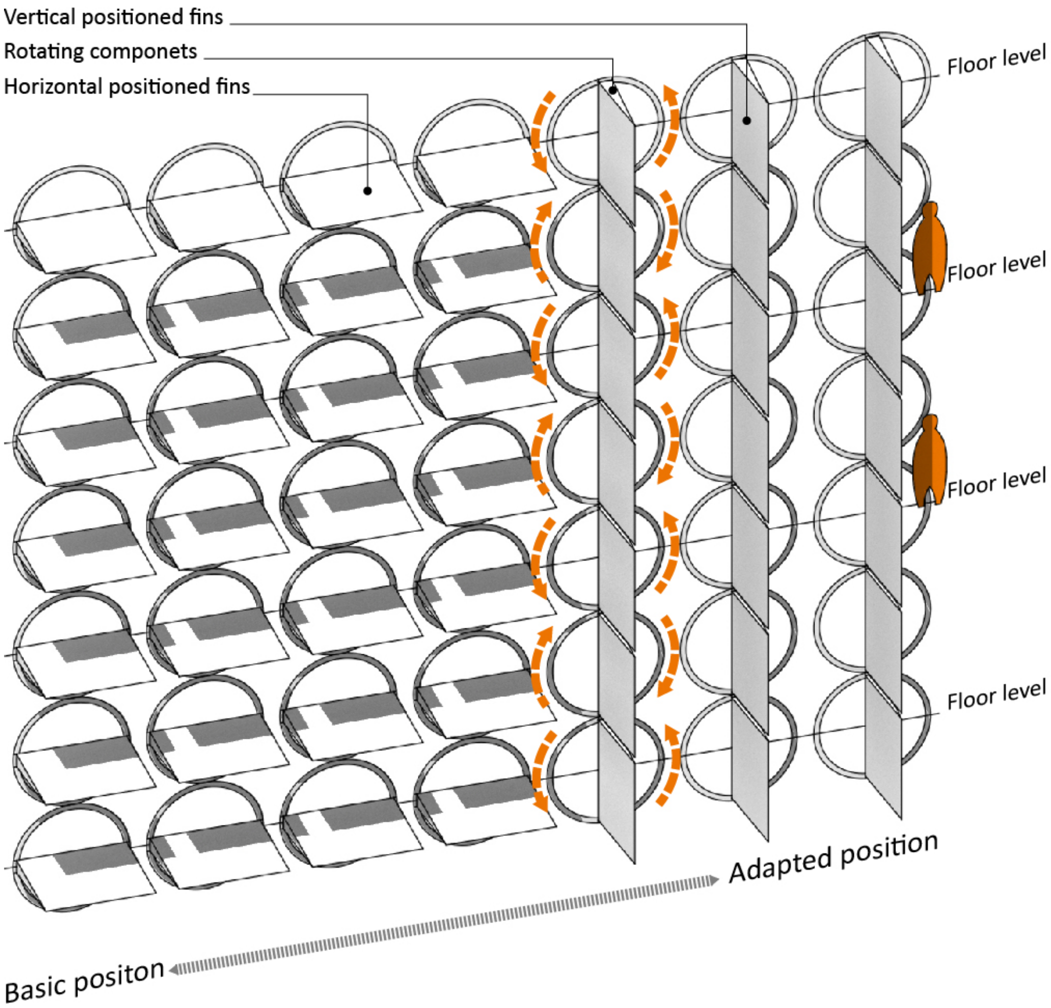

Fig 6.6: Rotatable fins system

Rotatable fins system was the first most basic design option. The set of movement in this system was designed to be in vertical direction with gears that link each façade components in the same set together which is in the end might result in difficulty of maintenance, safety and operating. The alignment of these components is in vertical direction which allows the fins in the same vertical line being rotated in the same time. The benefit of this system is its h/s ratio is optimizable in design process. There is only structure limit in case of cantilevers which means that h/s ratio can be higher than 1. The downside is its combination to façade structure which could be a big obstacle to for the vision from inside the building.

Origami foldable fins with diamond shape frame

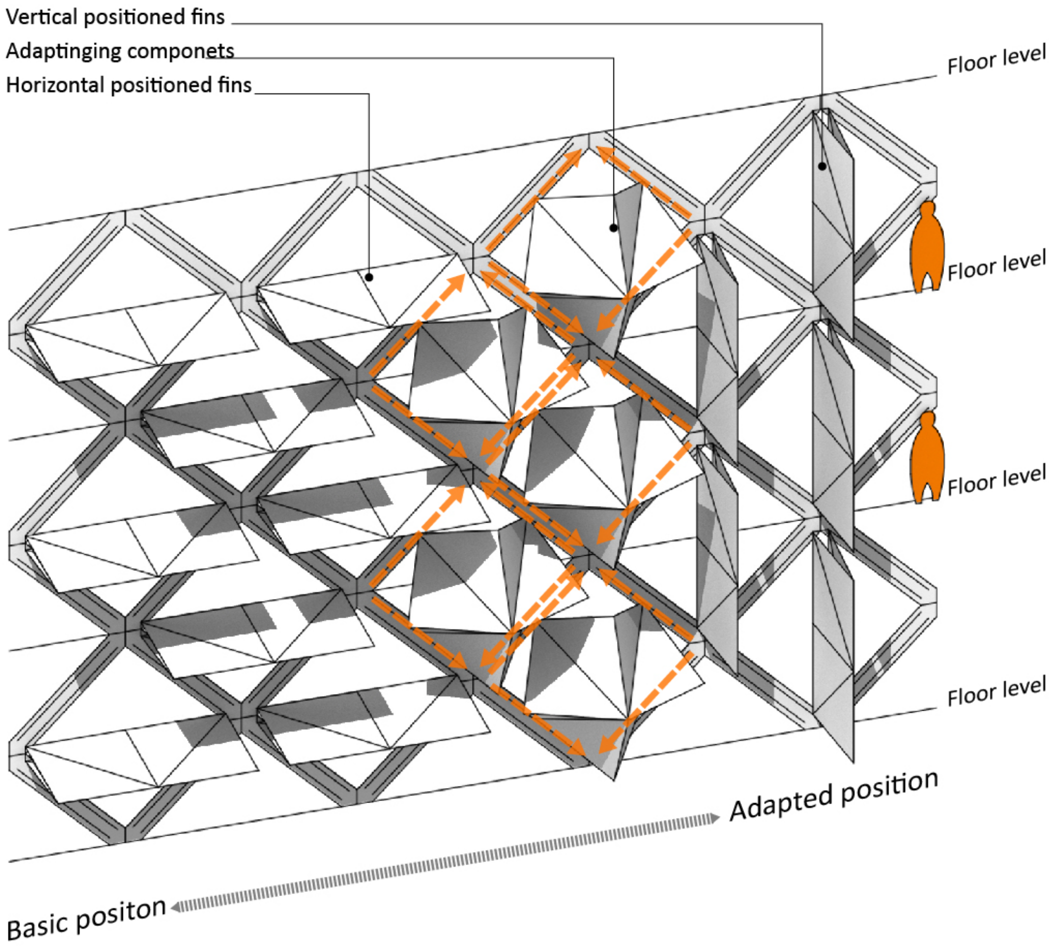

Fig 6.7: Origami foldable fins with diamond shape frame system

Origami foldable fin system is based on origami basic shape. Moving of the connection between the fin and the frame, result in transformation of the fin. One component is consisted four sides of frames which are combined in rhombus shape and an origami fin that is connected to those four edges. Two components of this system share one of the frames. It could be that each component works in the same time with the components next to them in diagonal direction.

This is the selected system for the final design, mainly because of aesthetic reason and combination to façade structure. The moving mechanism will be explained in further topic.

Origami foldable fins with hexagonal frame

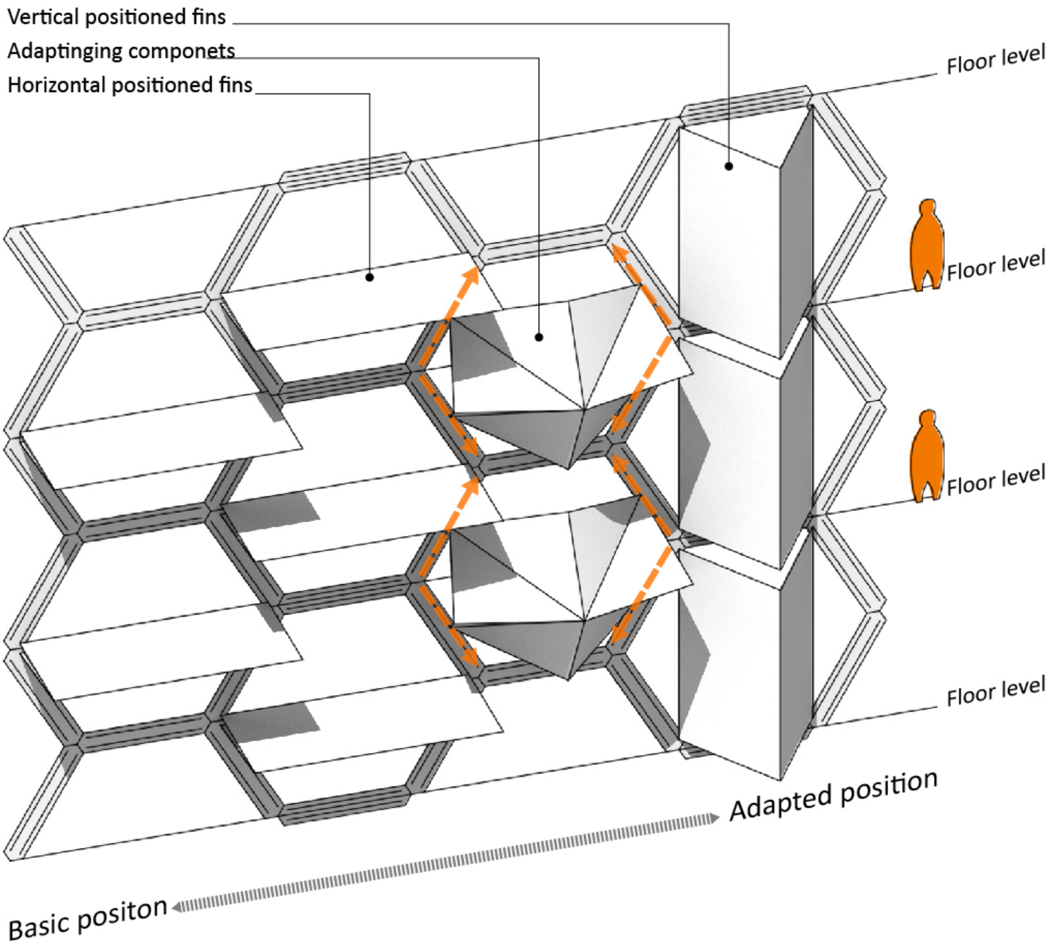

Fig 6.7: Origami foldable fins with hexagonal shape frame system

Origami foldable fin on hexagonal frame was developed base on diamond shape frame. Main objective is to create bigger void on façade for interior vision to outside and to develop the vertical fins part to be able to make smoother flow with less obstruct to the surface flow. In this case, vertical fins can handle more wind load because of the shape and the shape is more similar to research from Kawamura (Tetuya KAWAMURA, 1985) which might create more possibility of creating delaying in separation flow.

This design was test in CFD software, which results in much lower drag reduction compare to the one with diamond shape frame. The problem could possibly come from the frontal horizontal fins that they are not aligned which influence the cross-flow turbulent and create high drag force.

6.2.2 Motion and sequence of movement

A small mock-up model was made to study the movement of the façade. The mock-up show the promise result of possibility in changing shape of the fin by only the movement of the connections between the fin and the frames.

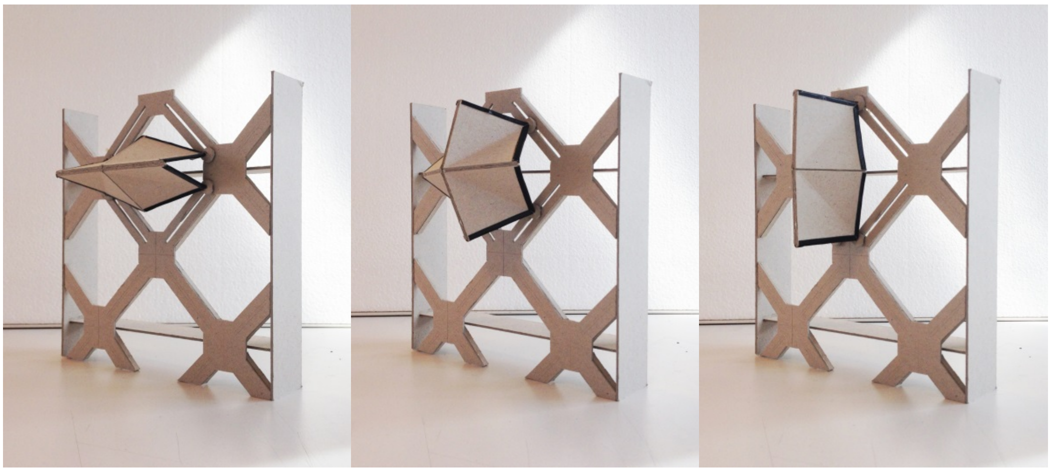

Fig 6.8: Movement study mock-up. (Left) is basic position, (middle) is changing position and (right) is adapted position

Mock-up model from figure 6.8 shows only one component of the façade. However, with the complete façade system, in order to reduce among of mechanism, this component need to corporate its movement to other four components around it (up-left, up-right, down-left and down-right) because they share the same frame. Studying the sequence of movement was done by using computer software (Rhino 5+Grasshopper) and another developed mock-up model.

Figure 6.9 shows schematic of adapting sequencing. The model was done by using Grasshopper plug-in for Rhino. Each module was program to move only half position from the module next to it. The movement also show that the direction of mechanism where the components move in the same moment is not align but in zigzag line. However, it can be noticed that in each frame element, the movement of the connection of two fins that share the same frame still not work in the same way (one connection move but another connection still stay in the same location).

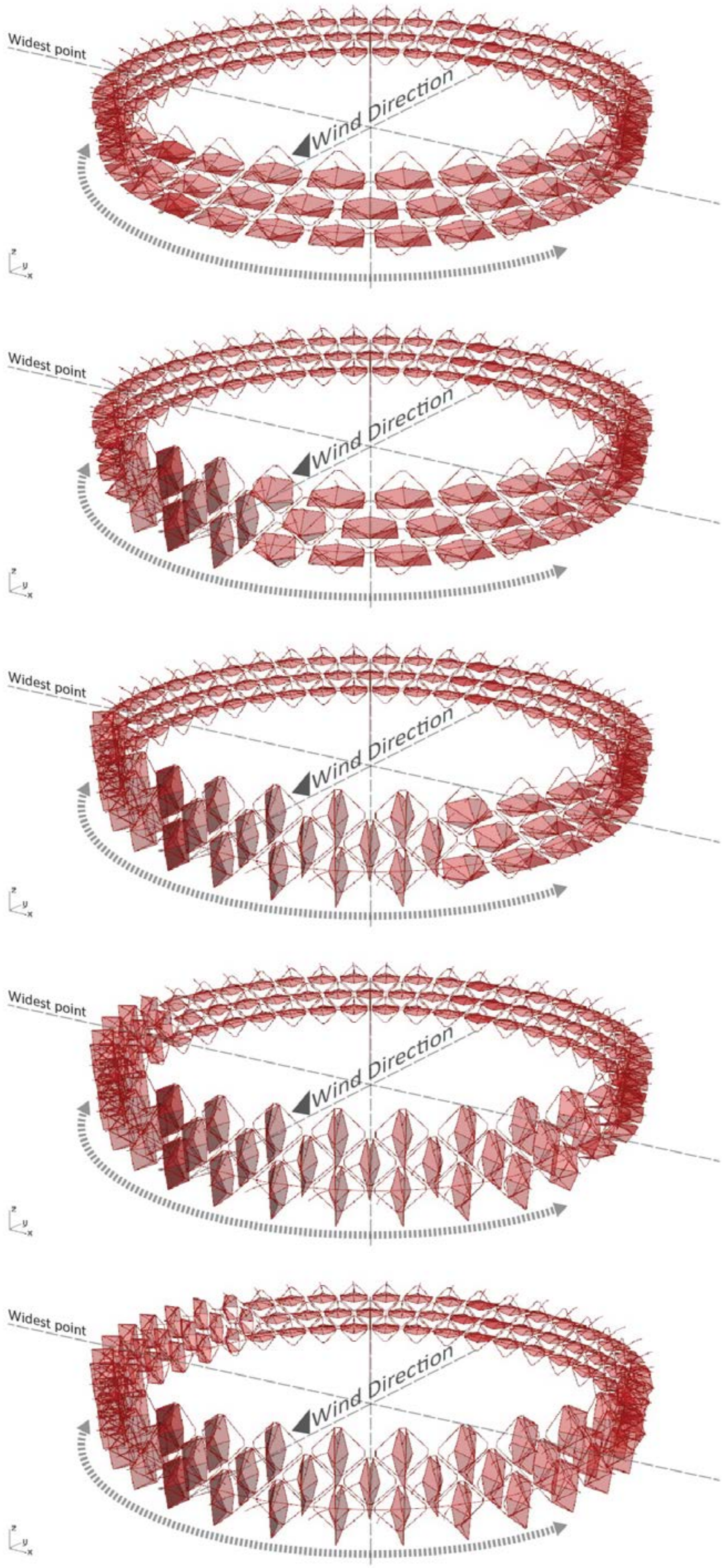
Widest point
Wind Direction
Widest point
Wind Direction
Widest point
Wind Direction
Widest point
Wind Direction
Widest point
Wind Direction

Fig6.9

Further solution was done in order to integrate the movement of the bigger system than the individual component. It can be done by integrating controlling movement inside the frame not at the fin itself. The new combination movement is shown in figure 6.10 and 6.11. The movement of the connection for two fins that share the same frame will move in the opposite direction by only one driver or one motor.

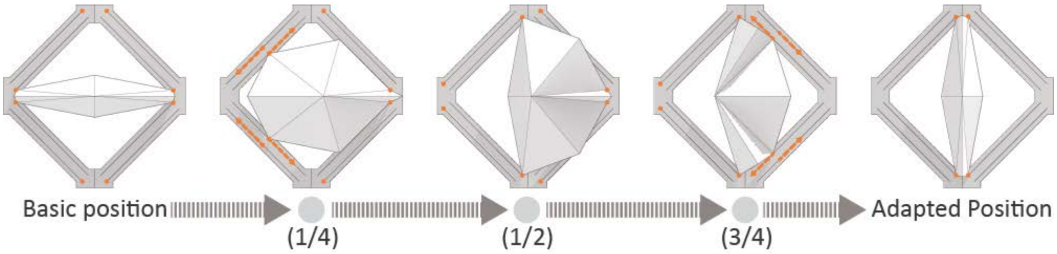

Fig 6.10: Step of adapting. At this design the mechanism in one frame element work in the same time with next façade component that the connections to the fins (orange dots) move in the opposite direction.

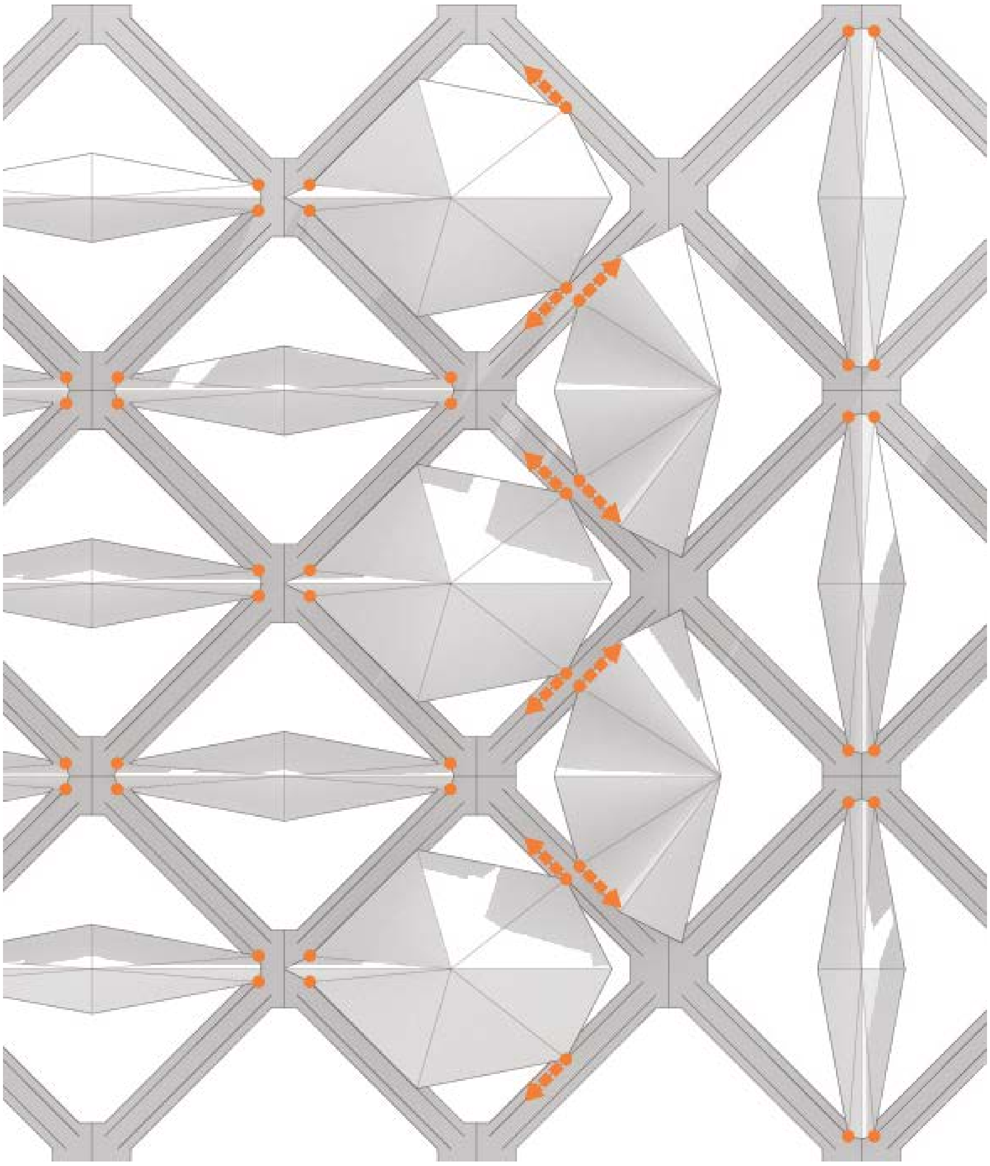

Fig 6.11.1: Fins adaptation during position (1/4) and (3/4). Orange dots are connections between the fin and the frame

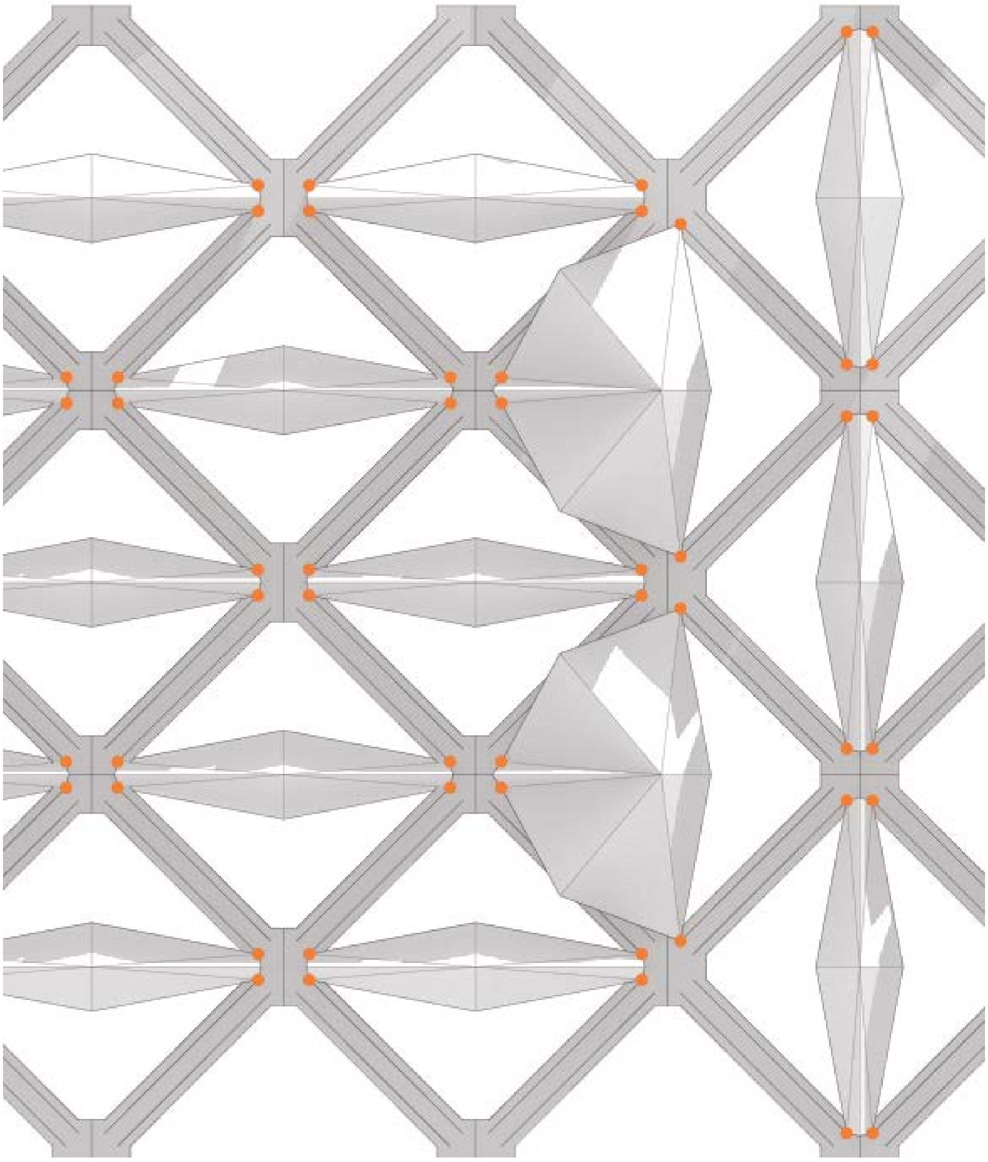

Fig 6.11.2: Fins adaptation during position (1/2) Orange dots are connections between the fins and the frame

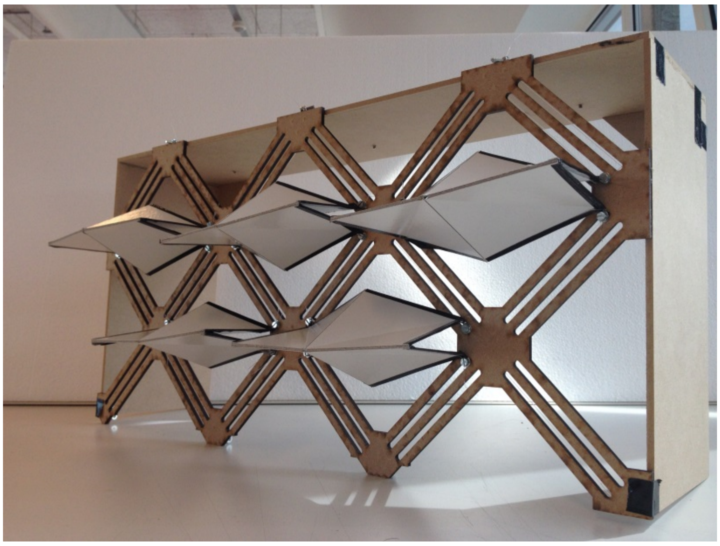

Mock-up with moving mechanism (cable) in basic position

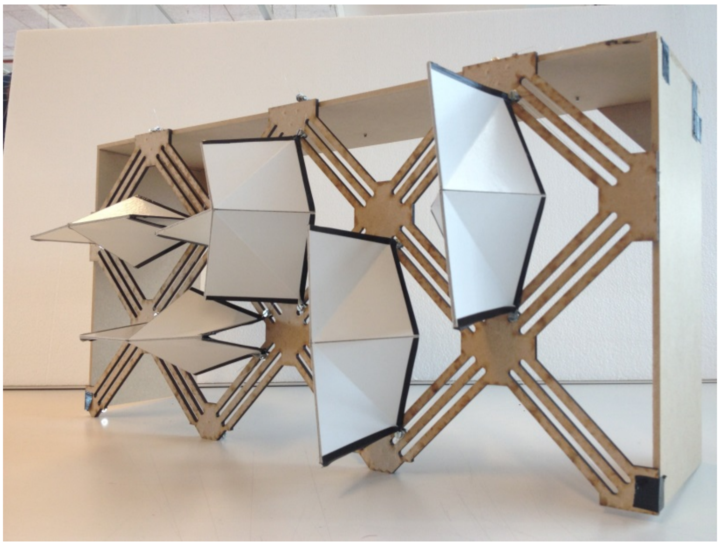

Mock-up with moving mechanism (cable) in changing position

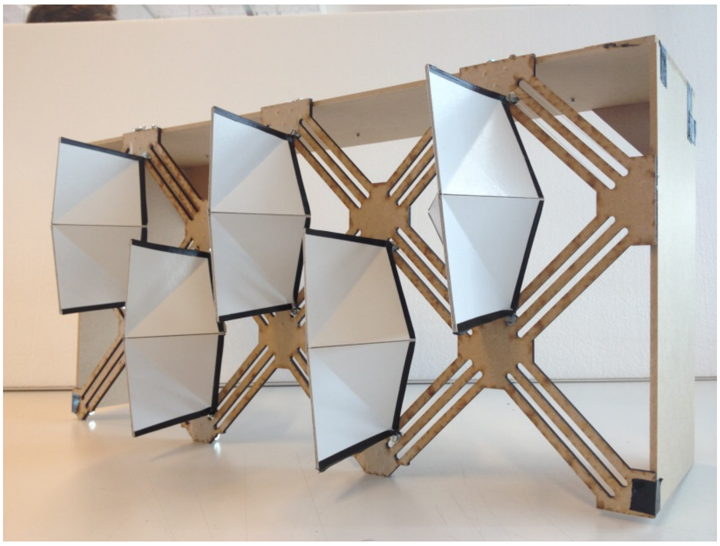

Mock-up with moving mechanism (cable) in adapted position

Fig 6.12: Mock-up model with cable mechanism at the back of the frame in order to control the movement of the fins (scale 1:25)

6.2.3 Defining façade size

The size of façade component was decided by using floor height calculate with floor plate size. Façade structure (frames) needs to be connected to the edge of floor plate which come to the conclusion that the height of the façade is in the same with floor to floor height. The floor plate size define number of façade component in one floor, in this case, there are 36 fins aligned in same level in the middle of the height between floor and another 36 fins in the same level as floor plate as in figure 6.7, with this number the size of the floor plate become 48.00m for diameter.

The final size of the whole component is 4.20x4.20m. Diamond shape frame is consisted of 4 pieces of edges that are identical and being connected to each other at the construction site. The size of the fins will be defined by the size of the moving mechanism which is related to the size and structure behavior of the frame.

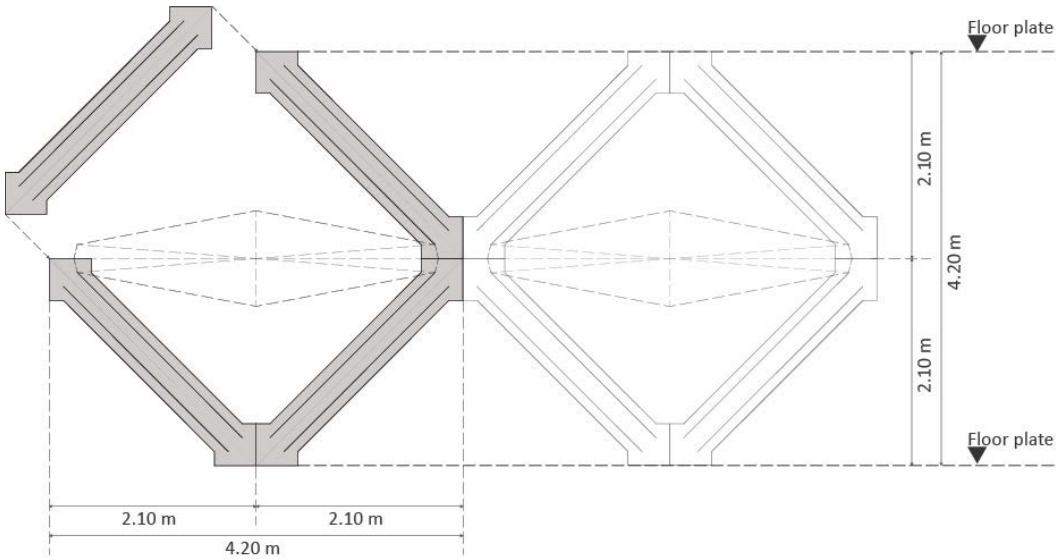

Fig 6.13: Frame components and its dimensions

6.2.4 Schematic system 01: Cable operating

First concept of mechanism is by using cable in order to move the fins supports. The cables are located behind the frames. By wiring the cable in a specific position, two cables in a frame element will move in opposite direction. For one vertical control set, there is a possibility that it needs only one set of motor to control it. Figure 6.14 shows the direction of control set. All the elements that are highlight in orange are in one system, being driven by one set of motor. The arrows in the image show the direction of movement in order to transform from horizontal fins to vertical fins.

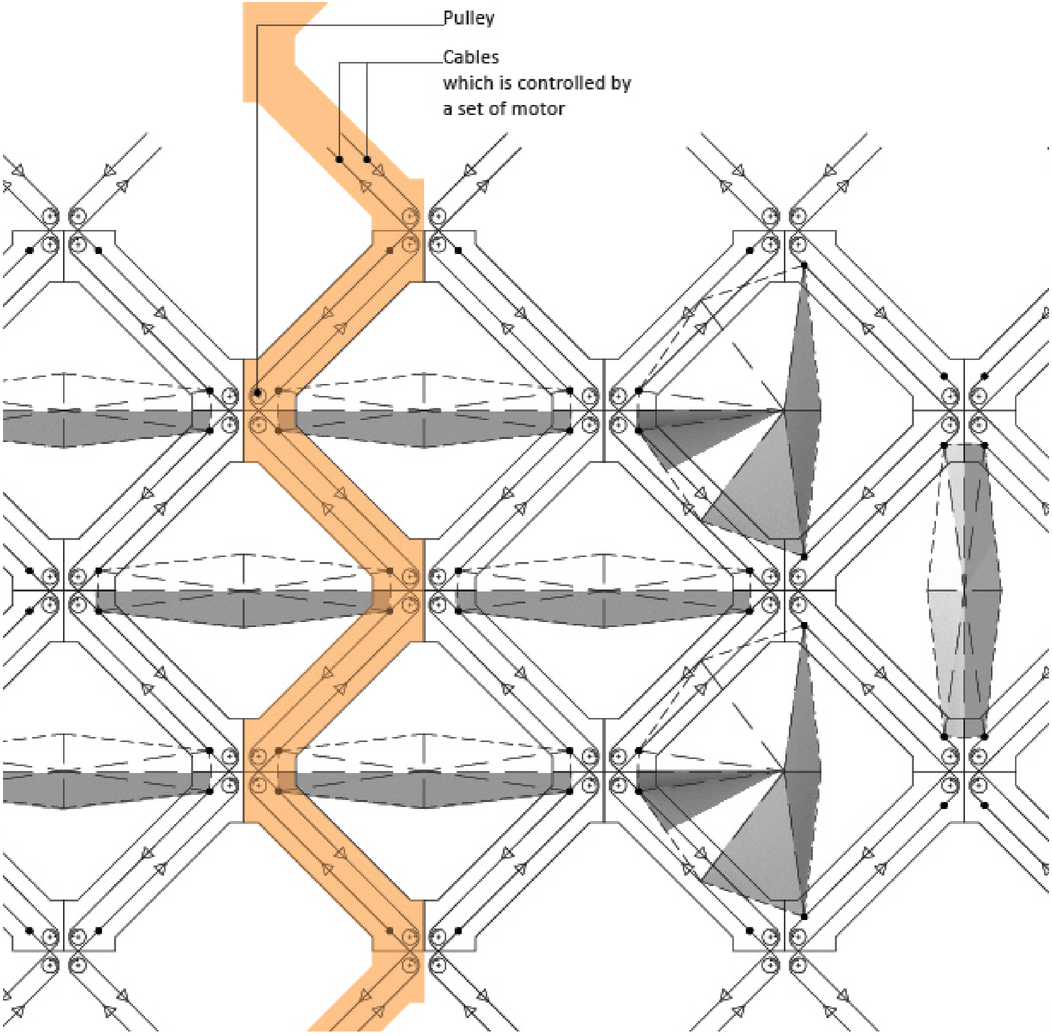

Fig 6.14: Concept of mechanism which cables are the main element of moving mechanism

The benefit of this idea is that one set of motor can maneuver multiple façade elements. However, the cable itself is the weakness part of the mechanism. It requires maintenance and if one part of the cable fails, it will cause the whole vertical line to fail. Another disadvantage was shown when the mock-up model was made (figure 6.12). The first idea of the model was to create more levels and pieces of the façade that would move in the same time by pulling only one cable. But with multiple levels, it requires bigger force to pull the rope. High friction was in the fins supports and at the pulley. While pulling, the ropes try to be straight and create horizontal push to the pulley and increase the friction on the way. The result was that in order for the model to work properly, it can only be possible with one level of the component. In real situation, in order to create proper working system the pulleys are required to have much less friction as possible while the sets of motor has to be very powerful in order to pull the cables from more than twenty stories with very high friction.

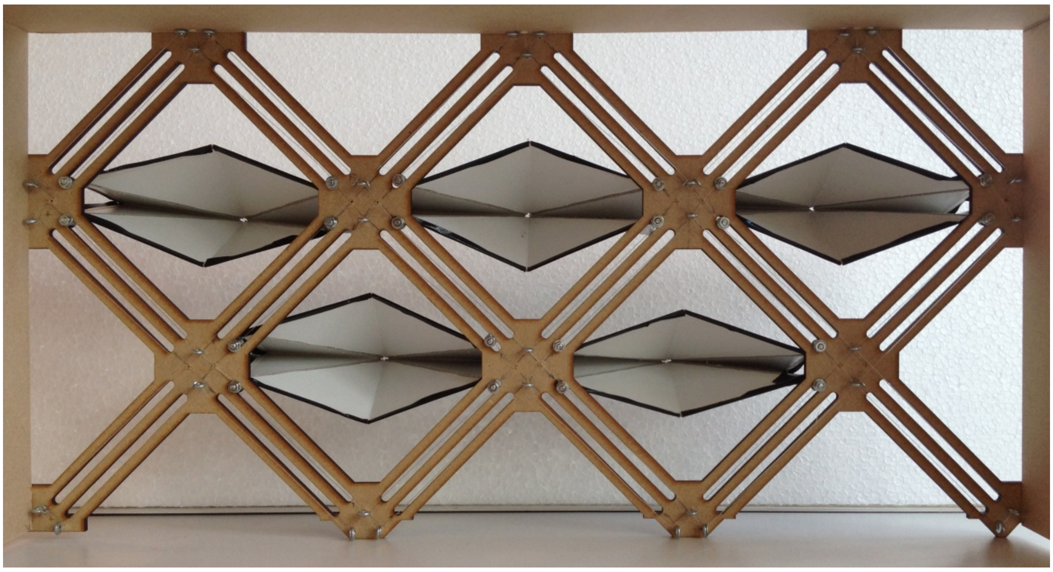

Fig 6.15: Behind the frame of the mock-up for moving mechanism by using cable as the main part.

6.2.5 Schematic system 02: Pneumatic operating

This system is the improvement from the cable system. The principle of movement of the fin supports still similar to the previous design, two supports in the same frame elements move in the opposite direction. However, the movement is control by two pneumatic tubes. The reference system is Linear drive units DGO by Festo which is a rodless cylinder pneumatic drive with magnetic coupling. The chosen unit is the 40mm diameter with 2500m in length. Below is the important data of this pneumatic tube.

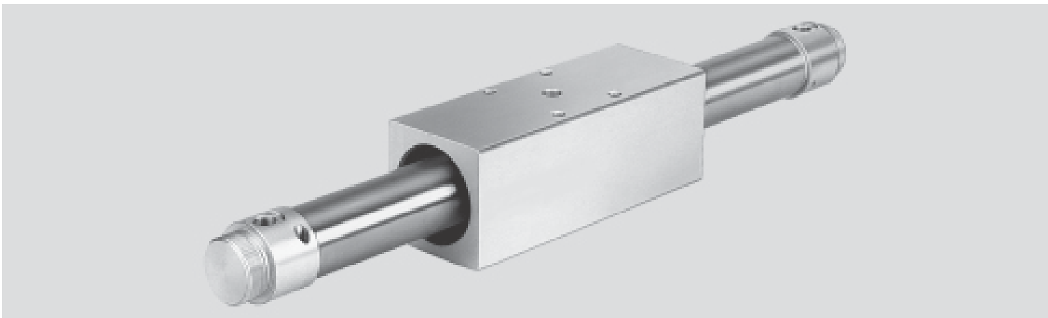

Fig 6.16: Linear drive units DGO by Festo ("Festo: Linear drive units DGO," 2012)

<u>General information for Ø40mm</u>

Driver principle:	Force locking (magnetic) without mechanical connections
Stroke:	10-4000 mm
Operation pressure:	1.3-7 bar
Temperature range:	-20 to +60 c^{o}
Theoretical force at 6 bar:	754 N
Breakaway force of magnetic coupling:	1050 N
Weight at 0mm stroke:	3.92 kg
Additional weight per 10 mm stroke:	0.008 kg
Connection material:	anodized aluminum
Speed:	dependent on the moving mass

Two pneumatic tubes are installed on one frame element and they will be activated by pneumatic switch (direction valve). The direction valve can be activated by small motor or it can be electronic switch that is controlled by main computer. The switch will orient the air from pressurized tube which located under all floor plate to the pneumatic tube for reposition the façade. A set of pressurized tubes can be supported by one air pressure unit which include air pump and pressure tank to control the pressurized level. The diagram of the system is shown in figure 6.17.

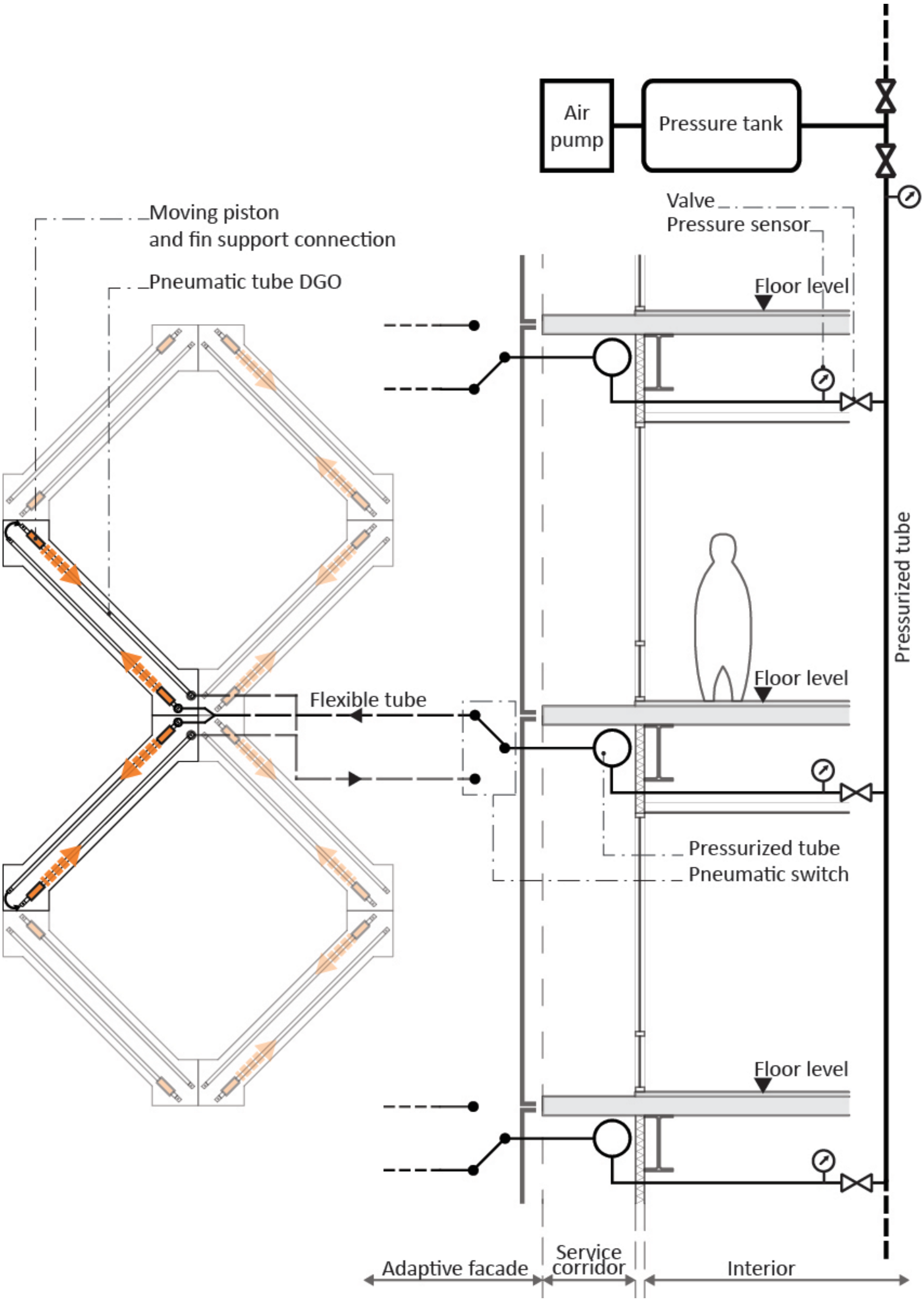

Fig 6.17: Diagram of pneumatic system.

The benefit of this system is that each façade component being activated individually which reduce the effect when one of the systems fails. The pneumatic system requires less maintenance than cable system and gives more accurate movement without high resistance force or friction. The pneumatic tube can be installed to the frame element in the prefabrication process and being brought to the construction site as piece which will be connected to the rest of the system at the site.

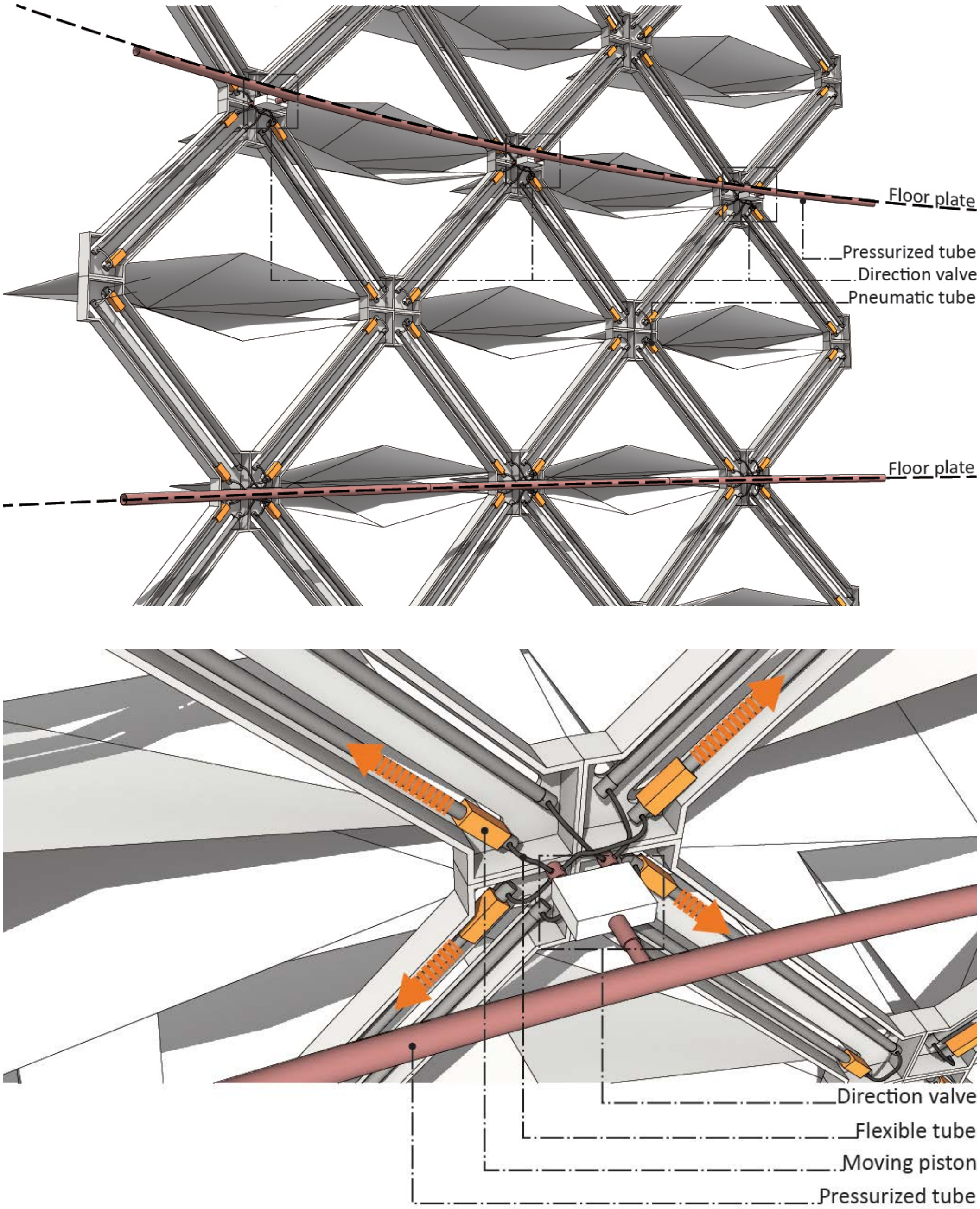

Fig 6.18: Location of direction valve, pressurized pump and pneumatic tube

7

Finalized the design

7.1Detail and material selection

Detail and material of the adaptive façade were considered from case studies and through the material selection process in CES Edupack software. The materials are mainly divided in three types – fin surfaces, connections and fin structures, and façade frames. The selection was concerned with the shape, angle and movement of the fin as well as assembling process.

7.1.1 Geometry study

According to the transformation of the fin, the geometry, folding angle, hinge and connection has to be investigated. In order to measure the value of all connections, 3D computer was made by using Grasshopper and Rhino software. The computer script was written to present the accurate movement into a range of movement which can be selected in any moment of the transformation.

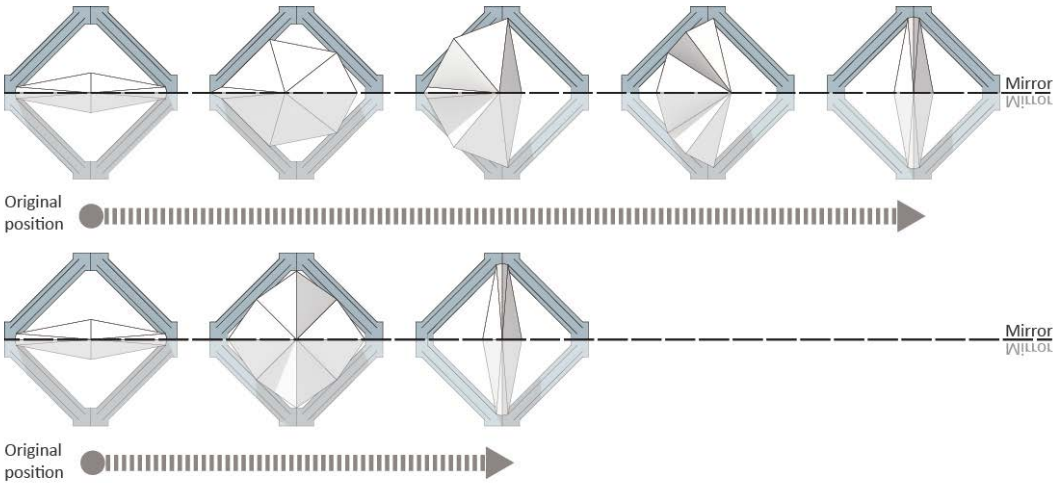

Fig 7.1: Two type of movement. (Top) is the movement of the fin in general. (Bottom) is the movement of the fin that is located directly at the back of the building according to the direction of the wind.

There are two types of fin movement which are the type that two pneumatic tubes are activated, and another type that all four pneumatic tubes are activated in the same time. The second type of movement only occur at the back of the building where the façade start morphing while the rest of the façade components being transformed as the first movement.

The angle of folded corner was measure in this computer model for further detail designing. In this stage, all the folded corners were assumed to be hinge connection and fin surfaces are stiff material which cannot be bent.

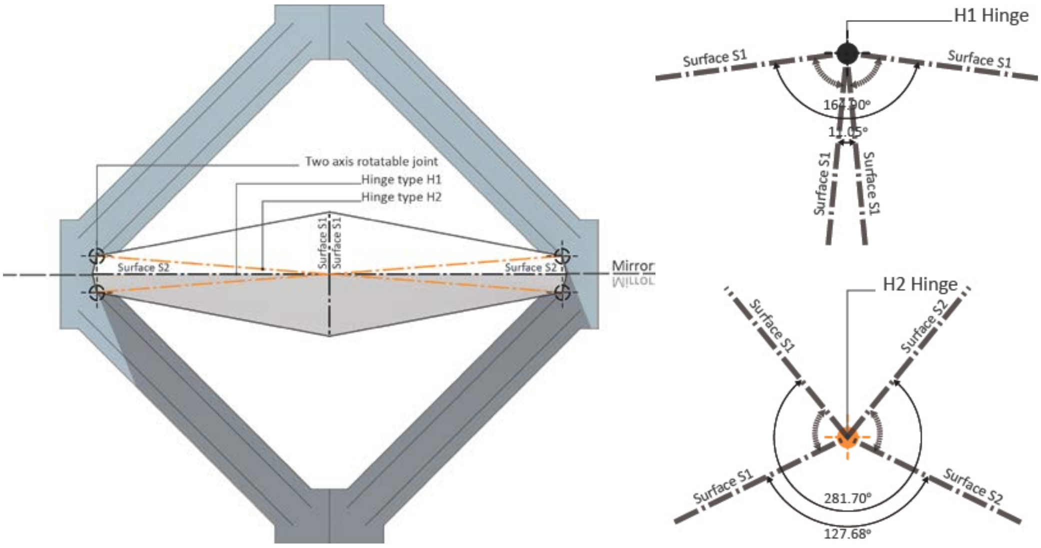

Fig 7.2: Relation between eight surfaces of the fin. The right images show the maximum and minimum angles between each surface.

7.1.2 Material selection

Material selection of the façade was base on the lightness, durability, low maintenance and ability to carry wind load at 2kN/m^2 (0.004 Mpa include safety factor (x2)) without breaking or permanently deformed.

Fin surfaces

There were two options for fin surfaces which are hard material (polycarbonate or aluminum honeycomb sandwich panel), and membrane material (PTFE or ETFE). First material choice was honeycomb flat plate which will be cut in triangle pieces as the pieces of the fin. Each plate can be installed with steel profile or other type of structure inside the plate to increase the strength of the panel. The selection in CES Edupack software was done by using the criteria that the panel has to be function in temperature between -10 to 100 c^o, excellent durability in fresh and salt water with UV, and able to handle 0.004MP of yield strength. The result shows that the lightweight and cheap materials in this case are aluminum honeycombs with the thickness between 25-30mm. However, if the filter is open for the materials that good and excellent in UV, polycarbonate is as well in the range which provide much lighter and less costly, also the transparency.

The second option for the surface is membrane materials. From Al-Bahar as case study, the surface of the adaptive façade of the building was made by PTFE membrane. In the case of Al-Bahar tower, PTFE was selected instead of ETFE because it has better performance in thermal resistance (DuPont™, 2015) which is suitable for the building location. However, ETFE has better mechanical properties, higher tensile strength, less weight and cannot be broken which make ETFE more suitable for the project if it is used in the climate with moderate temperature.

However, in term of structure behavior when the fin receive wind load, there will be high transformation in membrane material. With the foldable geometry, the steel profile need to be small and it has to resist the load in many forms such as wind load, vibration, pull force from the tension of membrane material. If the selected material is honeycomb, the panel will have it stiffness and be able to perform as structure by itself.

The polycarbonate sheet was selected as the final result. The properties of polycarbonate sheet had been investigated through date sheets from product suppliers. With windload at 2kN/m^2 + safety factor on the surface of right-angle triangle with 1.80x1.80m for two sides, the required thickness is 10mm within the permitted maximum deflection (Polygal, 2011).

Connections and fin structures

Connections, joints and fin structures were assume to be same material since the beginning because it is easier in term of connection between each part. The main reason is that there will not be corrosion occurred in the connection of same type of steel, and glue can be used to connect these parts as well.

However, from geometry study most of the component such as hinges and fin structures can be processed by extrusion process with material like steel or glass fiber reinforcement polymer (GFRP), but the connection between pneumatic tube and the fin which is supposes to be a two axis rotatable joint or ball joint can be a complicate geometry and it is more suitable to be made out of steel with casting process. With the same criteria of lightweight, able to receive the load from the surface without permanently deformed, durable to water and UV, the result from CES Edupack presented that aluminum is the most suitable material in this case.

Façade frame

The frame of the adaptive façade works as the protection of the system behind (pneumatic tube etc.) as structure to transfer the load from the fin to floor plate and also the railing of the moving parts. The material has to be hard enough to receive point load from the weight of the fin and can be produced in big amount of number (approximately more than 10000 units).

The material selection was done in CES Edupack. The criteria were that the frames need to be able to handle the load of the fins (presume that the load of the fin will be carried mainly by façade frame, not by pneumatic tube). The load of two panel of the fin which is 10mm thickness with aluminum structure and all hinge and ball joint connections is approximately 204.10N-1062.32N depend on the position of the fin. And the same with other material, it durable against water (salt and fresh), UV radiation, has service temperature from -10 to 100c^o. It requires mass production with economic batch size over 10,000 units approximately. The result for the frame material was selected by the least costly and lightest one which is polyester glass fiber.

7.2Façade structure analysis

There are two main load cases, gravity load and wind load, which are matter to this adaptive façade. Three positions of façade are the main positions that have effect from those two load cases. In this section, one of three positions will be analyzed which the result will be used in detail design.

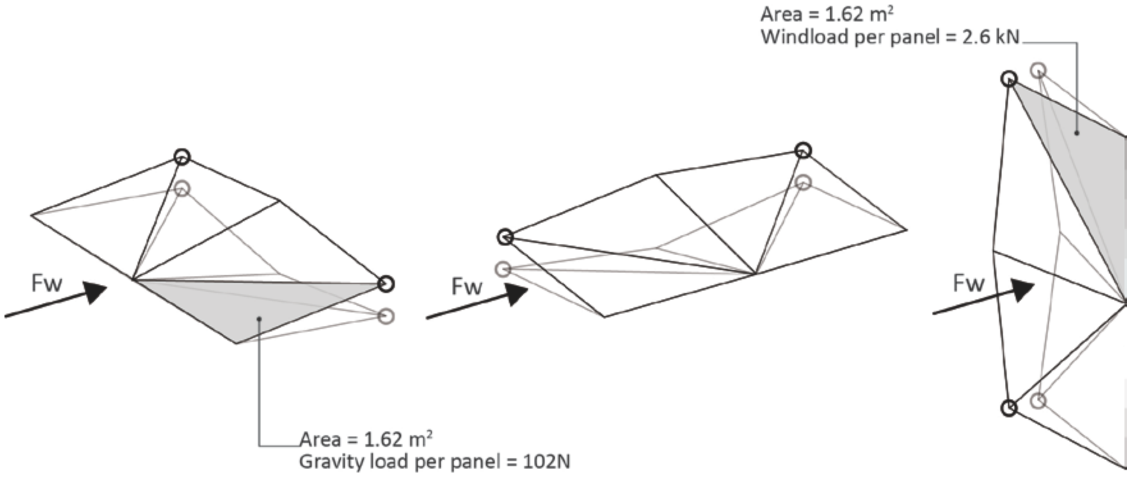

Fig 7.3: Three main façade position and wind direction (Fw), horizontal position at front façade (left), horizontal position at the side of the building (only in the situation with low wind speed) (middle) and the vertical position at the side of the building (right).

From figure 7.3, the gravity load is 9.8N for one mass unit (kg) which was calculated from the volume of materials of the fin (aluminum structure and polycarbonate sheet). Wind load (Fw) is the wind pressure at the top part of the building = 2 kN/m^2, however, according to Eurocode (Eurocode, 1995), the values of force coefficient (external pressure coefficient (C_{pe}))that need to be included into the wind force in each side of surface are in figure 7.4. The component that was selected is the triangle panel of the fin in vertical position (figure 7.3 left) because it receives the biggest load. The main analysis is to understand the roughly structure behavior of the connections and to estimate the size of panel structure, mainly is to be able to make a further design in detail.

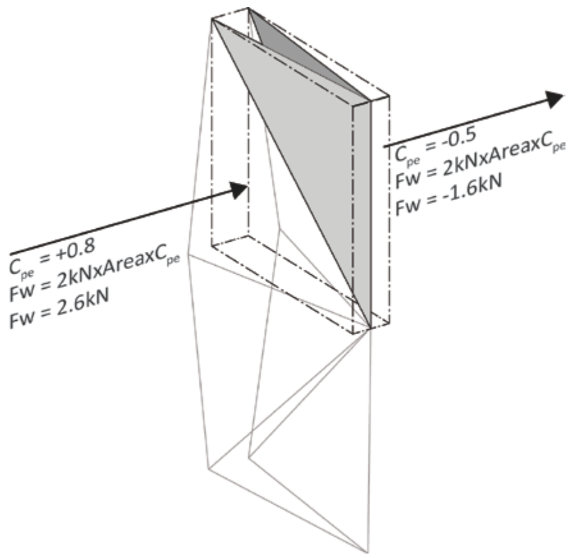

Fig 7.4: External pressure coefficient and the load from wind pressure in each panel with original wind load at top part of the building = 2kN/m^2

<u>Panel structure</u>

The calculation for panel structure which is made of aluminum extrusion will be done base on the front side where the wind approach because it carries higher load (2.6 kN). The surface load from the panel is fully transferred from the panel to the structure in term of linear load along the aluminum beam. In this case, the load was translated as uniform load as a rough estimation. From figure 7.5 shows uniform load at 0.419 to 0.429N/mm. Beam AC from the images is located at the longest edge of the triangle. It needs to carry bigger load and higher value in bending moment and shear stress. In detail designing stage, all the edges should share the same or similar profile shape to avoid the difficulty of connecting them together at the corners of the triangle. From this reason, beam AC will be the main analysis part which it is able to receive maximum load and its result will be applied to the rest of the beams (AB and BC)

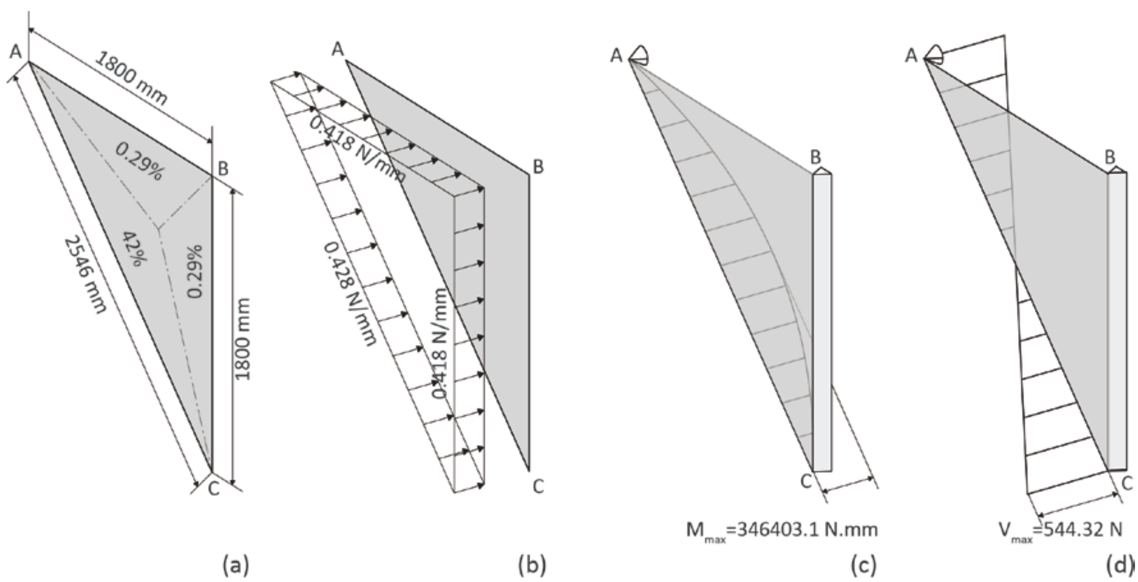

Fig 7.5: (a) is panel size, (b) is the linear uniform load that is occurred to beam AB, AC and BC, (c) is bending moment (M) diagram of beam AC, (d) is shear diagram of beam AC

In order to calculate bending moment and shear stress of beam AC, the support on point A and beam BC are defined as pin support and it needs to be assumed that other panels can receive the load without any displacement occurred. The size of the aluminum beam was calculated by defining the maximum bending stress on the top and bottom of the beam. The size of the beam was optimized until the stress is lower but most similar to the stress that aluminum can handle which is 276Mpa (276N/mm^2).

The aluminum beam was assume to be hollow rectangular profile with the thickness = 3mm with unknown width and height. The calculation was done by the equation below.

$f = \frac{Mc}{I}$ While

f: Bending stress (N/mm^2)
M: Bending moment or maximum bending moment (N.mm)
c: Distance from the center of the beam to the top surface of the beam (height/2) (mm)
I: Moment of inertia which is = I_{gross} - I_{hole}, it can be calculated by

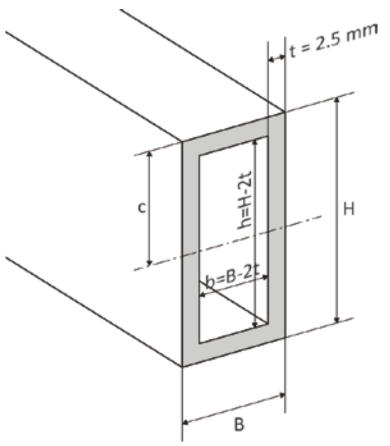

$I = \frac{BH^3}{12} - \frac{bh^3}{12}$ While

B: External width (mm)
H: External height (mm)
b: Internal width = B-2.t
h: Internal height = H-2.t
t: material thickness = 2.5mm

The suitable cross section of the panel structure is 27.5mmx15mm which 3mm as its thickness.

<u>Hinges</u>
The design of transformation of the fin is base on folding origami paper which consists of 8 folded corners. These corners were decided to be rotatable mechanism instead of physically folding material in order to extend the product life. In this stage, the calculation of the size of the hinge will be described.

The hinges have to act as movement mechanism and also are required to handle load both wind and gravity load. There are two types of hinges with different angles as mentioned before, H1 type only carries the load and connect between two panels while H2 type connects two panels with façade frame and one of it carries one fourth of the load from the fin. With higher requirement of performing of H2 hinge, it was selected to be analyzed and defined the size.

Different from panel structure, H2 hinge need to be able to handle along-beam compression and tension depending on direction of the load and position of the façade. The position that was selected is the same vertical position with panel structure calculation because the load is bigger. The calculation begins with defining the value of along-beam compression and tension by calculating for support reaction force (F_{sup}).

Whenever the wind approaches the fin, there will be force that causes the fin to be rotated. Two supports at the front part will handle tension while two at the back will handle compression. The calculation was done at the location of the highest support reaction, only one support. The loads at two panels where the fin receive the win were used as input value because it has the highest value and it creates the biggest reaction force at the support. The method of calculating the load is explained in figure 7.6.

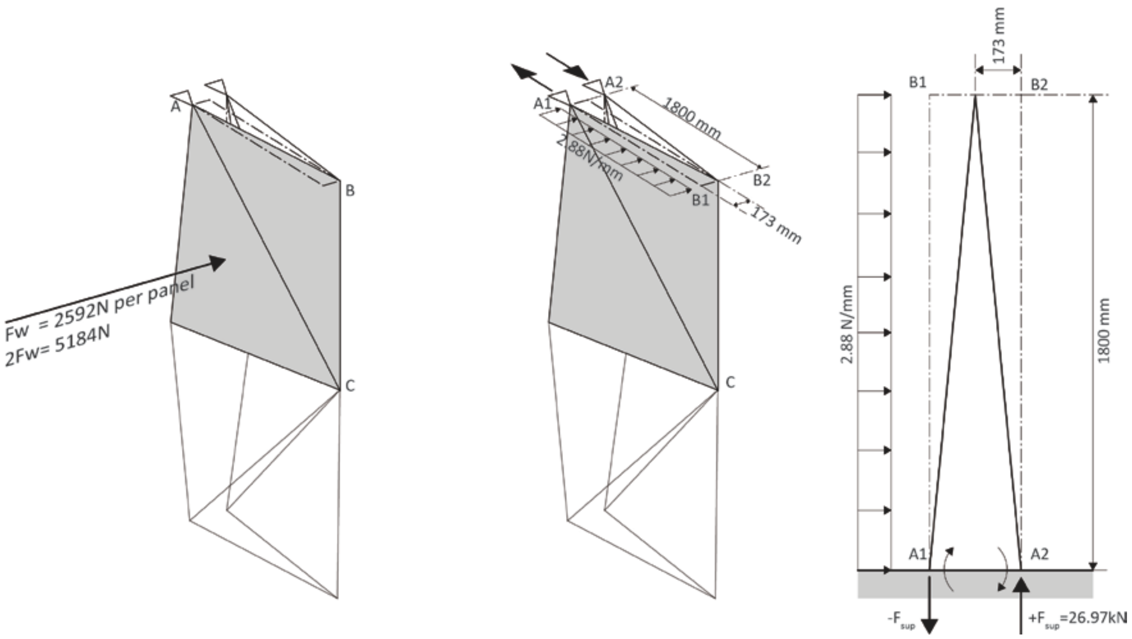

Fig 7.6: Support reaction force (F_{sup}) method of calculation. (Left) two panels that are carried by one supports and total wind load for those panels, (middle) translation of surface load to uniform load, (right) transformation of shape to define F_{sup}.

The F_{sup} was calculated by using defining bending moment (M) (Nmm) at the base which

$$M = \frac{-WL^2}{2}$$

W: The uniform load (N/mm)
L: Length of the fin (mm)

And support reaction with

$$F_{sup} = M/l$$

l: length to the center of the base (mm)

While the load is (W)=2.88N/mm on the (L)=1800mm fin which result in 4665600Nmm bending moment. With the distance between two supports = 346mm (l=173mm) the the support reaction force (F_{sup}) is 26969N.

Presume that the fin is stable and there is no movement in all support, the reaction force was translated to the along-beam compression (F_p)(or tension at the front side of the fin) in the H2 hinge (line AB in figure 7.7). Calculation for size of the hinge, it is necessary to combine the stresses from along-beam compression (normal stress (F_p)) and out of plane load. Out of plane uniform load is the load that cause by the wind and being transfer from the panel to the panel structure and to the hinge which in this case, it was assume that H2 hinge carries two panel and the load become two times of the load that handled by panel structure.

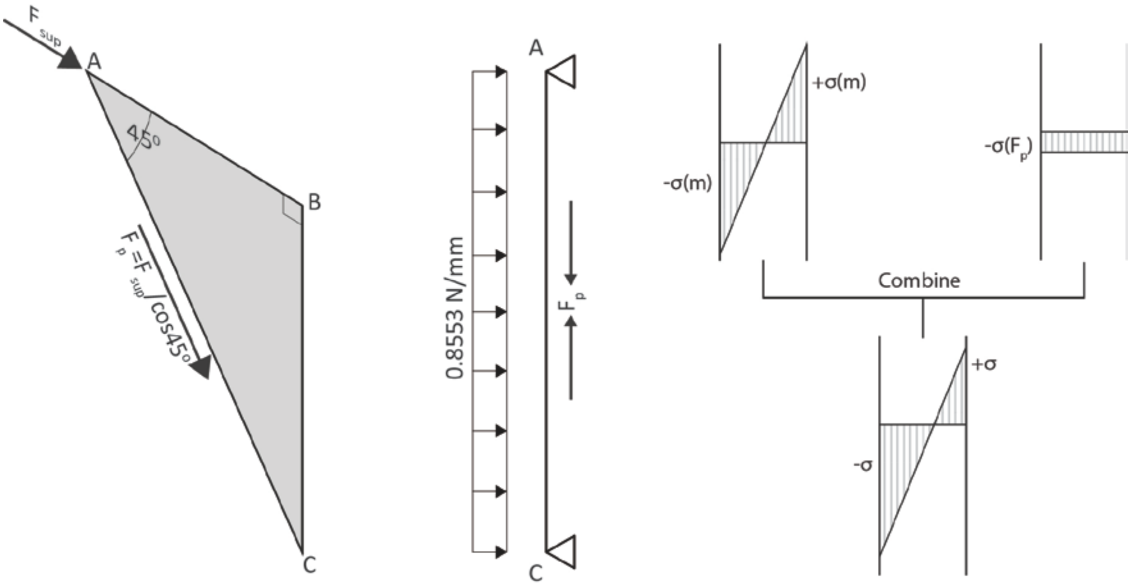

Fig 7.7: (Left) is calculation for compression (Fp) on right-edge of the triangle which is caused by the reaction force. (Middle) is out of plane load from wind and compression in H2 hinge. (Right) is stresses combination of normal stress ((F_p)) with bending stress from wind load ((m)).

The combine stresses should be lower than the compressive strength (386Mpa) and tensile strength (276Mpa) of the aluminum. The calculation was done by optimizing the diameter of the hinge and the thickness of hinge material that it was designed to be a hollow cylinder. The equations that were used for calculating are similar to calculation with mock-up building core.

$$\sigma(F_p) = {}^{F_p}/_{A}$$

$$\sigma(m) = {}^{M.Z}/_{I}$$ While,

(F_p) : normal stress from compression according to reaction force (N/mm^2)
(m) : bending stress from windload of the panels (N/mm^2)
F_p : Compression force (N)
A : Cross section area of the hinge (mm^2)
M : maximum bending moment of the hinge (N.mm) $M_{max} = {}^{-W.L^2}/_{8}$
Z : Radius to the outer surface of the hinge
I : Second moment of area of hollow cylinder $I = \frac{\pi}{64}(D^4 - d^4)$

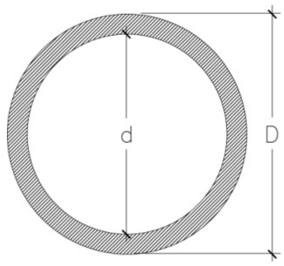

The result shows that the hinge should be 32mm diameter with 6mm of the material thickness.

Pneumatic tube

At this stage of calculation, actually, it was done after the first detail mock-up was made (scale 1:10). The mock-up made as similar as possible to the detail design in this chapter which will be explained later. The model works fine when it was placed on the horizontal position (the façade frame parallel to the ground), however, when the model was lift up to the upright position, the movement of the fin support (two axis rotatable joint) can be done only halfway and it will be stuck. The problem occurs because the fin, similar to cantilever beam, create pull force on the top part. In the model, the force bends the support tube (assume to be pneumatic tube) and cause the moving parts to contact the façade frame and stop the movement.

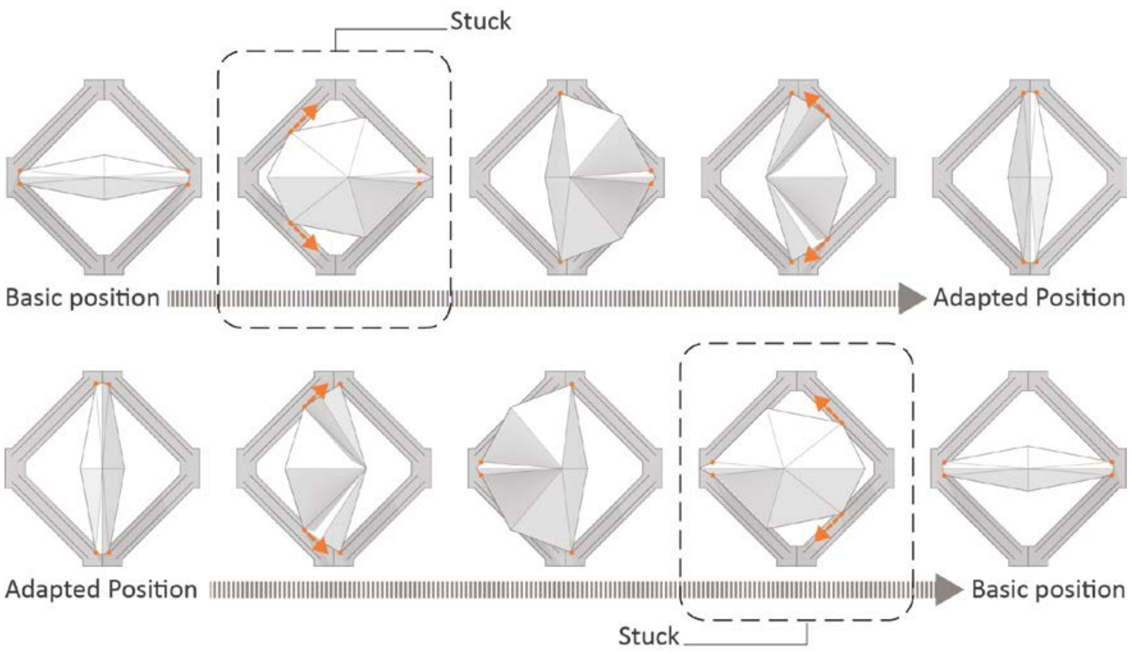

Fig 7.8: The transforming of the fin in two directions and the position with the problem that cause by the force of support reaction.

The investigation goes back to the cross-beam direction load of the Festo pneumatic tube. The maximum lateral load that the tube can handle and still function properly is only 200N, but the force can be very high until 26969N. The suggested solution is to add extra support structure that will be used to handle this load instead of depending only on pneumatic tube.

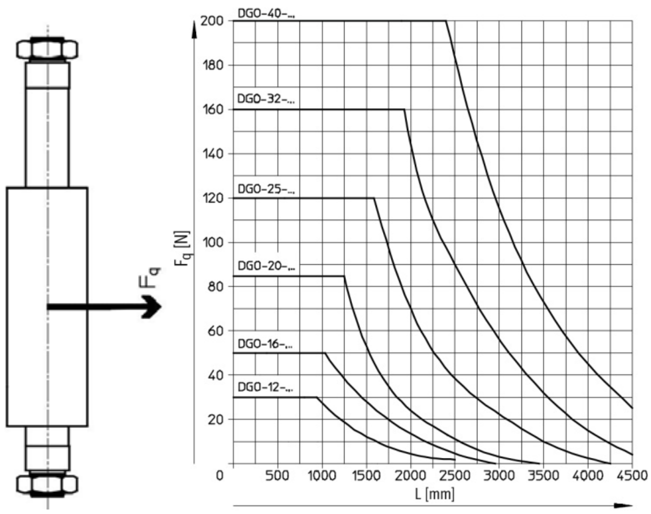

Fig 7.9: Permissible lateral force Fq dependent on stroke length L("Festo: Linear drive units DGO," 2012). In this project the tube is 40mm diameter with 2500mm stroke which can handle the force at maximum 200N

The calculation in this case is quite complicate because it involves with moving mechanism. The lateral load to the tube is different in each transformed position. For gravity load, the highest force is caused by the fin in horizontal position, and for wind load, the highest force is caused the fin in vertical direction. Varies in the size and location of the force create the maximum deflection in the tube differently, both in value and location.

To make sure that the lateral load will be handled only by the extra support but not by the pneumatic tube, the lateral movement joint was designed. In this case, the support beams are allowed to be deflected in perpendicular direction to the pneumatic tube without bending the tube itself. The deflection values were calculated in combination with gravity and wind load in ten different locations along the beam to find the maximum value that will be used for the designing of the moveable joint between pneumatic tube and support beams.

The loads from the gravity and the wind are 102.10N from gravity and 0.00N to 2592.00N from wind depend on the position. One support handles the loads from two panels. The similar method of finding reaction force as hinge calculation was used and the calculation was done in every 10% of movement of the support. The support reaction forces than are caused by gravity load from horizontal to vertical position are 1062.32N to 102.10N and the forces that are caused by wind are 0N to 26968.79N. The detail calculation can be seen from Appendix E.

The calculation for displacement was done in two possible situations. First, the situation where the end-supports of the beam are pin supports, and second where the supports are fixed. The formula are

$v = \frac{Pb(L^2-b^2)^{3/2}}{9\sqrt{3}IEL}$ for beam with pin supports

$v = \frac{126Pb^2a}{3EI(L+2a)}$ for beam with fixed supports.

P: Point load at any point on the beam (N)
a,b: Distance from the load to the support (mm) a≥b
L: Length of the beam (mm)
I: Second moment of area
E: Elastic modulus or Young's modulus of the material (N/mm^2)

The calculation is done in an excel sheet which allow the value to be modified. The objective is to fine the maximum displacement of the beam and optimize the size, shape and material of the beam to make the maximum displacement as small as possible. In this case, the maximum displacement was decided to be less than 5mm, or else, the façade frame will be too thick.

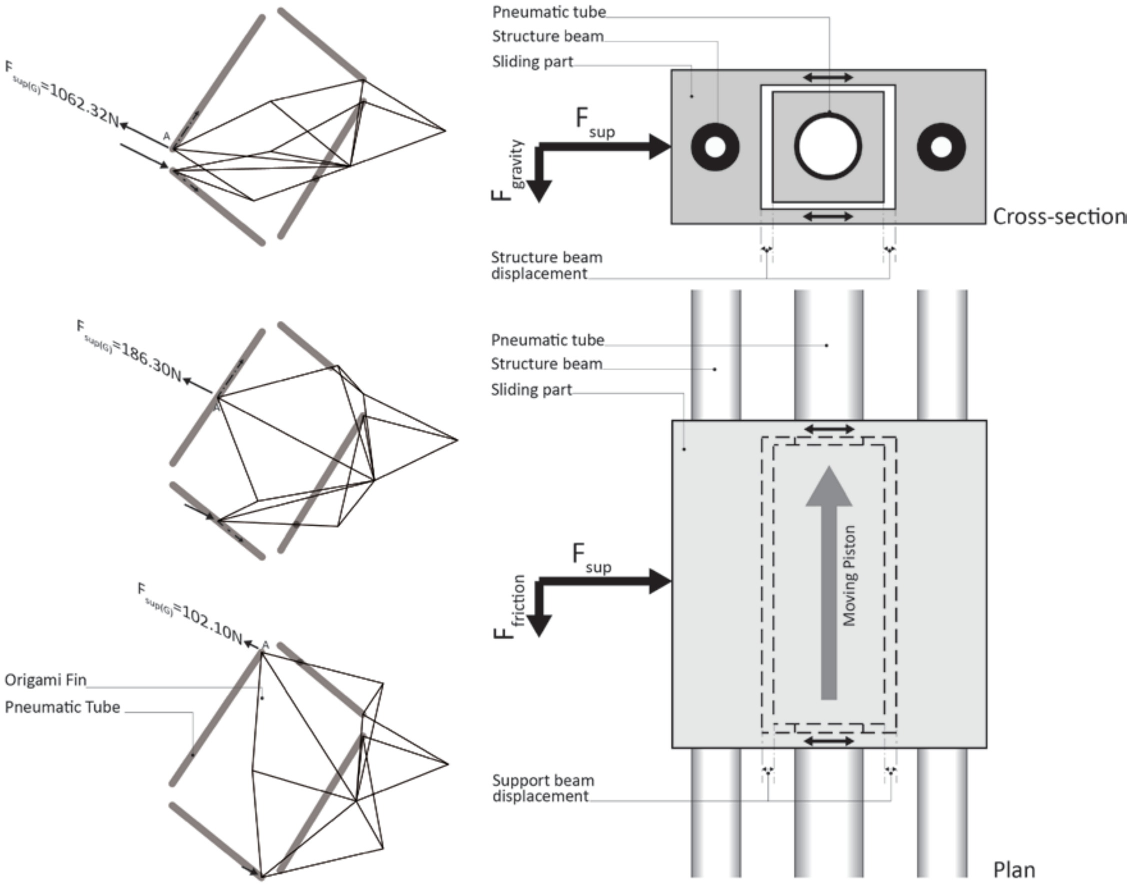

Fig 7.10: Left images are support reaction force in three different locations on pneumatic tube (top: 0% movement, middle: 50% movement, bottom: 100% movement). Right images are schematic design of the detail that allows the structure beam to be deflected without giving the load to the pneumatic tube but still allows the piston to drive the connection.

Second moment of area depends on the cross-section shape of the beam. The comparison was done on hollow cylinder shape, T shape, H shape and hollow rectangular. With the values that can be optimized, the best cross-section shape in term of its effectiveness and material saving is H shape profile. The material is compared between aluminum and stainless steel. To prevent corrosion between different types of steels, aluminum is suitable in this aspect but it creates far too big deflection. The selected material is stainless steel which creates much less deflection. However, in detail designing, there should be pieces of polymer in between the aluminum component and stainless steel component to avoid the corrosion.

The result from the calculation in pin support beam shows the deflection of the beam at maximum = 37.32mm (gravity + maximum windload) which is almost the same size with the diameter of the pneumatic tube. The moveable joint requires gaps in both side of the pneumatic tube, 37.32mm of deflection will require a space of 74.64mm for the bending of the beam which is far too big for the detail. The result from fixed support shows the deflection at 1.92mm with two stainless steel H shape beams at hxd = 40x35mm with the thickness of 5mm.

Overall structure behavior

The overall predicted structure behavior was considered in two position of the fin, the horizontal position with only gravity load applied and the vertical position which being applied with gravity and wind load. Figure 7.8 shows the possible stress that can happened to the fin. The stresses in this case are complicate to be calculated, the predictable here in this place is only to be put into account in the detail design process.

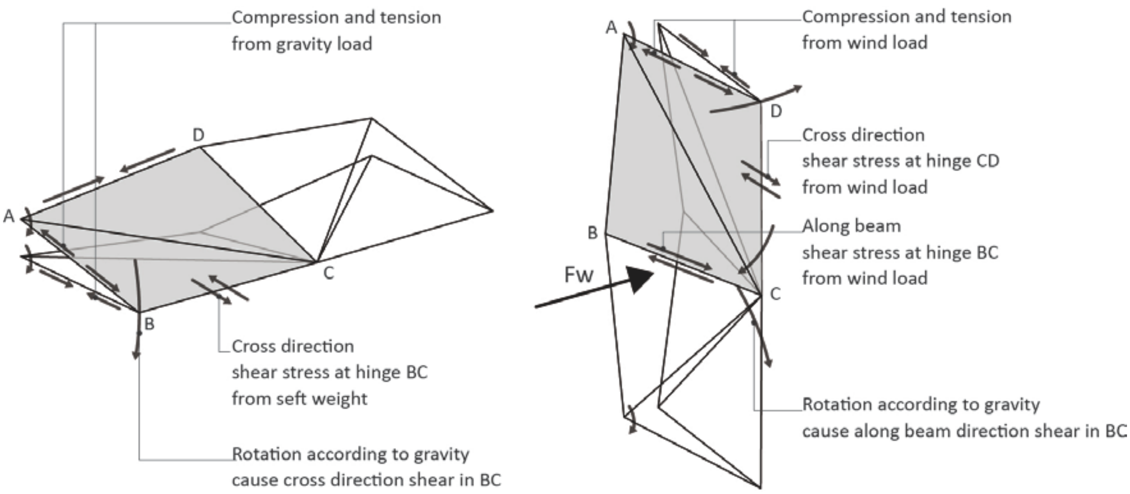

Fig 7.11: Structure behavior that can possibly be occurred in the fin in two different positions. (Left) horizontal position with only gravity load applied. (Right) vertical position with gravity load and wind load applied. H2 hinges (BC and CD) need to be able to handle shear stress in cross beam and along beam direction.

With the thickness of the panels, locations of the folding mechanism or the hinges need to be considered. There can be that the H1 and H2 hinge can be different in design that can be fixed to panel structure (aluminum profile). H1 hinge cover the angle from 11.05^{o} to 164.90^{o} and H2 hinge from 127.68^{o} to 281.70^{o}. The angle at 11.05^{o} in H2 hinge is the most critical angle; it should be the first concern in designing.

The possible solutions for the critical angle were design in two options. From figure 7.12, option B was selected because it require smaller hinge profile which has less weight compare to option A. However, the position of H2 and H1 hinges should be in the same position. From figure 7.13, if H1 and H2 are not in the same surface, the direction of load transferring will not be in plane. And furthermore, with movement, there are possibilities to create torsion in the panel and at the panel structure.

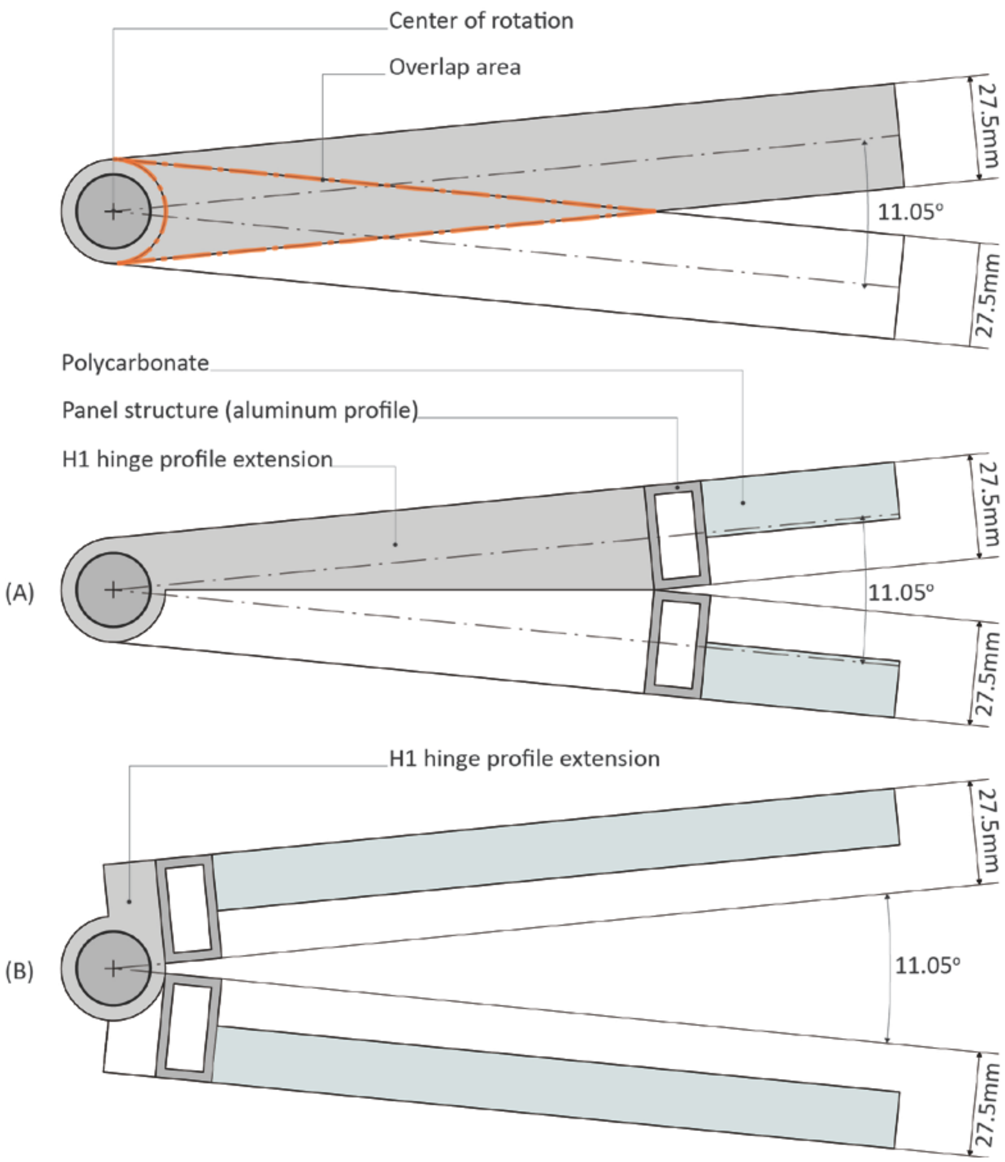

Fig 7.12: H2 hinge design alternative, which show the size of the hinge and the different in distance from the hinge to the panel structure in critical angle.

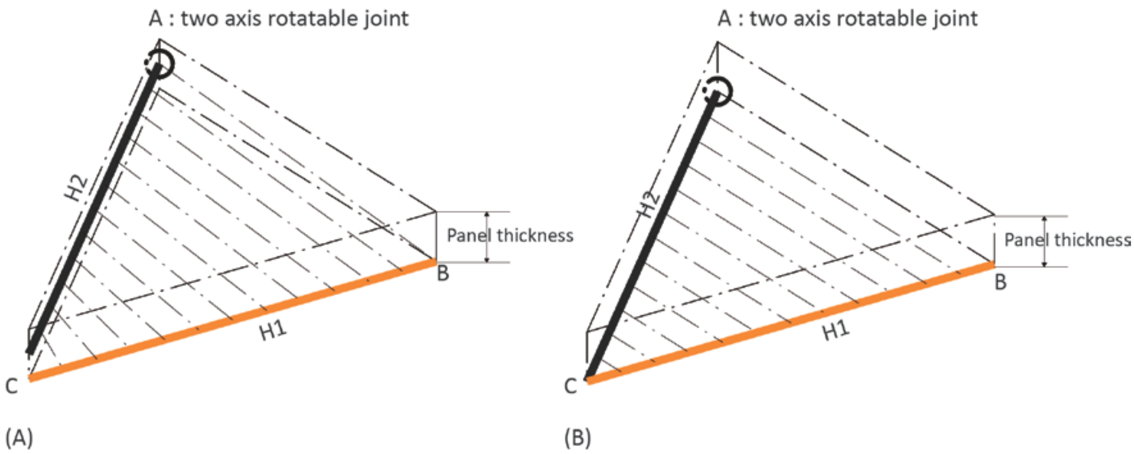

Fig 7.13: Position of H1 and H2 hinges to the panel. Image (A) show the hinges are not in the same surface and it can create torsion and out of plane load. The thickness of the panel is shown to be over size in order to have clearer visualize.

7.3 Detail designing

The whole façade component includes façade frame, pneumatic tube, fin and its connections was made in the full scale 3D computer model in most accurate detail as much as possible which is easier to understand than 2D drawing and it is possible to be rechecked and tested in different positions of the fin. The part of detail designing that relate to assembling process will be explained in further topic. Mainly in this stage, two part of detail will be described which are the hinges and two axis rotatable joint.

H1 and H2 hinges

Designing of the folding corner of the fin was decided to be hinge in the first place to increase the life span of the product, and increase the number of time that the fin can be adapted before the end of life or be broken. The foldable or bendable material was being considered at some point, however, with the movement and changing in tension and compression in the material and outdoor environment, there is high possibility that the material will be broken before its normal end of life

In geometry study topic, it was mentioned that the angle of the folded corner is varies, the angle can be 11.05^{o} up to 281.70^{o}. For H1 hinge type has the most critical angle which is 11.05^{o} and it was considered to be handled by 3D hinge that is normally used for fully swing door (180^{o}). However, the normal 3D hinge is mainly for the door and the hinge is not fully exposes to outdoor environment and the door is mainly close most of the time. Dust or particle can damage the mechanism of the hinge as it is exposed to outdoor for a long period. The simpler hinge was used instead to solve the outdoor issue and also to simplify the whole design.

The design objective is that the structure for the panels (aluminum profile beam) would be in the same profile in all edges but able to be added with hinge profiles which are different between H1 and H2. The design also aims to remove the gaps between the panels as they are folded by using gap closer cap. From previous stage, the thickness of polycarbonate is 10mm that can handle the load of $2kN/m^2$ with displacement lower than permitted and the size of the panel structure which is aluminum hollow rectangular profile with cross section not less than 27.5x25mm and 3mm thickness. Couple of tries were done, which the final details are the images below.

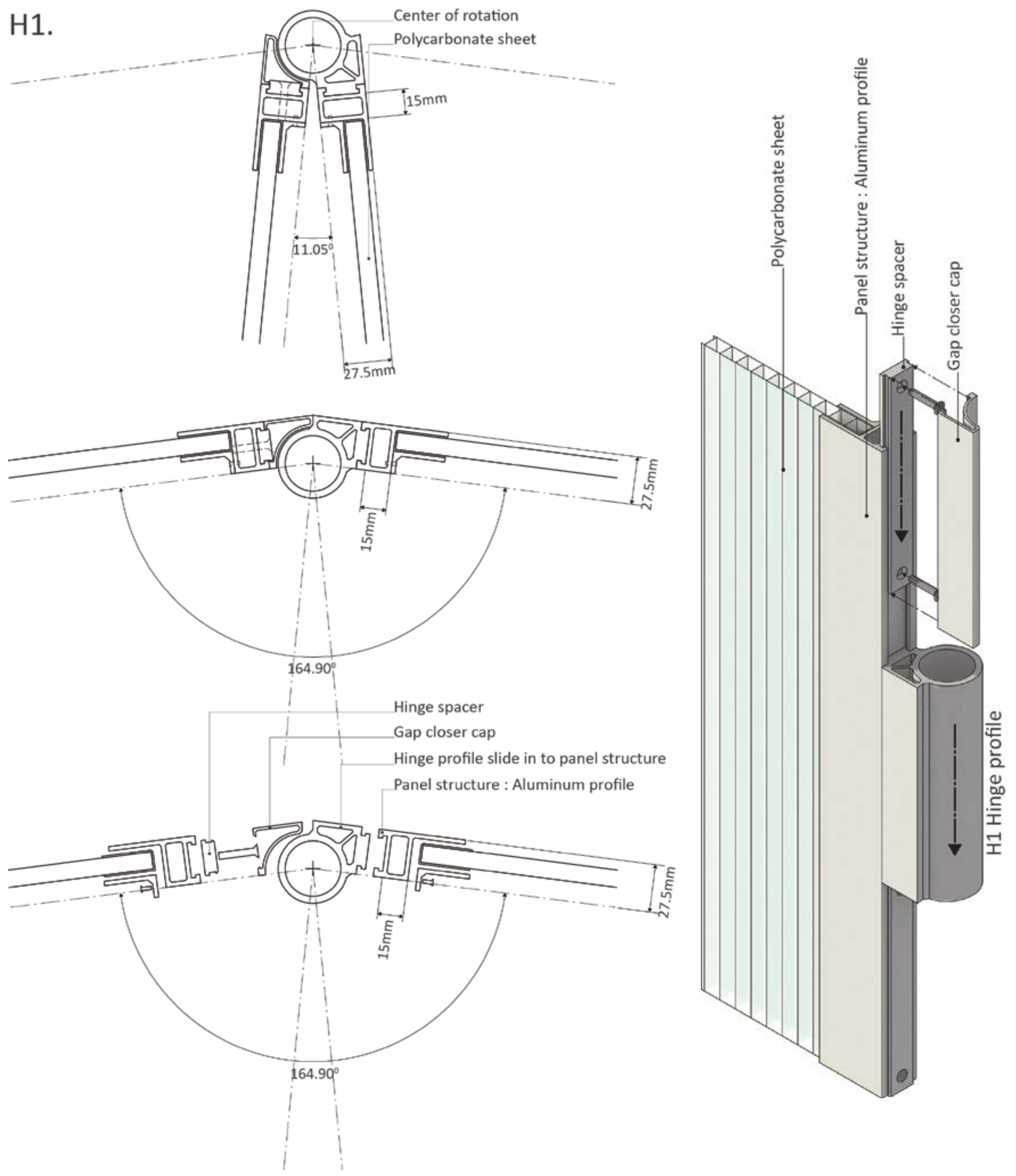

Fig 7.14: (Left) H1 hinge cross section detail and assembling. (Right) H1 hinge assembling process.

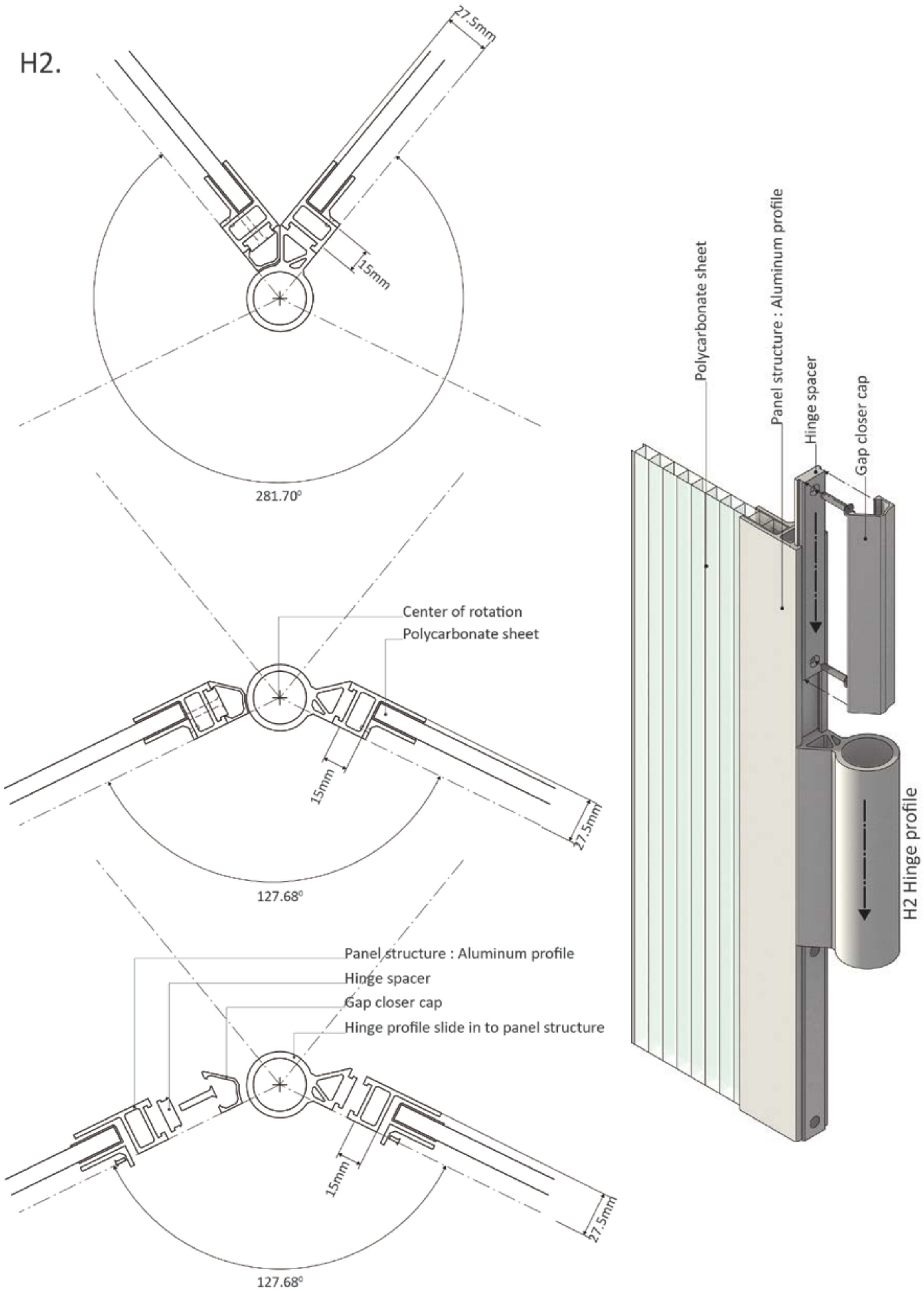

Fig 7.15: (Left) H2 hinge cross section detail and assembling. (Right) H2 hinge assembling process.

Façade frame & Pneumatic tube

As Festo DGO pneumatic drive cannot handle the lateral load to the tube that is exceed than 200N, the extra structure need to be applied to the system. The structure beam, in this case which already described in previous topic, is two additional H beam (40x35x5mm) that will receive the load and being deflected without putting the load to the pneumatic tube (the schematic design can be seen from figure7.10).

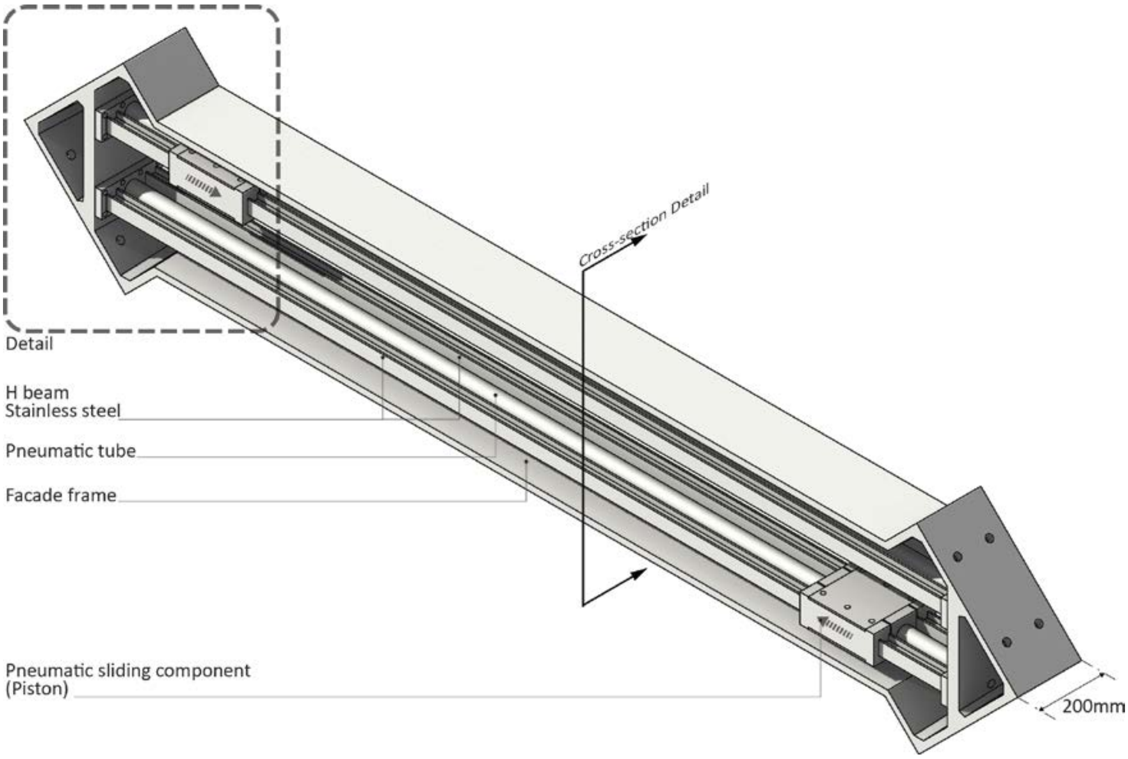

Fig 7.17: Façade frame element that is included the pneumatic drive system and support structure to handle the load of the fin. One module of façade consists of 4 pieces of façade frame.

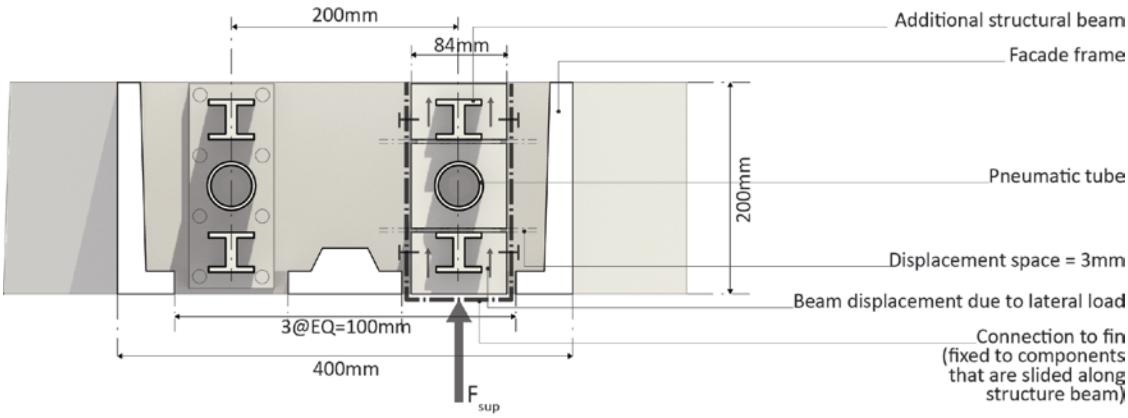

Fig 7.18: Cross-section detail of façade frame. The image shows the position of the pneumatic drive system and the two support beams, the displacement space and connection to the fin.

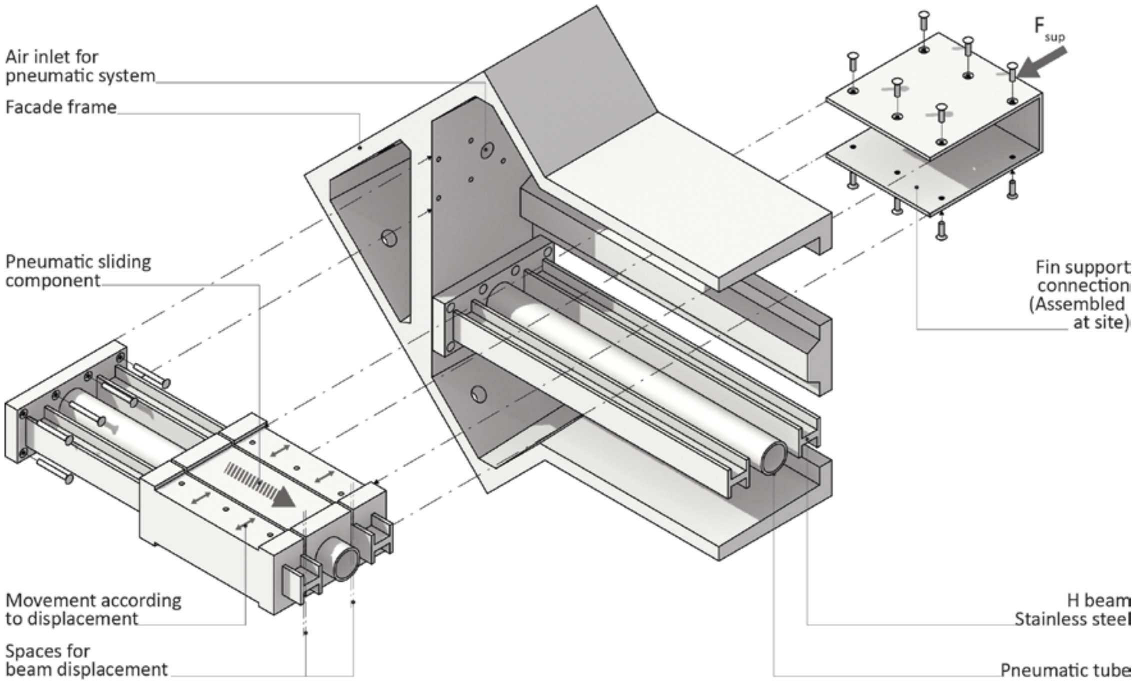

Fig 7.19: Detail and assembling of pneumatic tube + components to the façade frame and connection to the fin.

Two axis rotation joint

One fin element is supported by four connections which work as the joint between the pneumatic tube and the fin. They transfer the movement from pneumatic tube as a driver to the fin movement. From geometry study, this connection should act as a pin support which allows the beam to be free to rotate without translation which the translation will be done by pneumatic tube. This can be possible by using the connection that is rotatable in two axis. First axis is in perpendicular direction to the pneumatic tube and second axis is parallel to the tube which the second axis itself can be rotated along the first one. First design that follows these criteria is in figure 7.20.

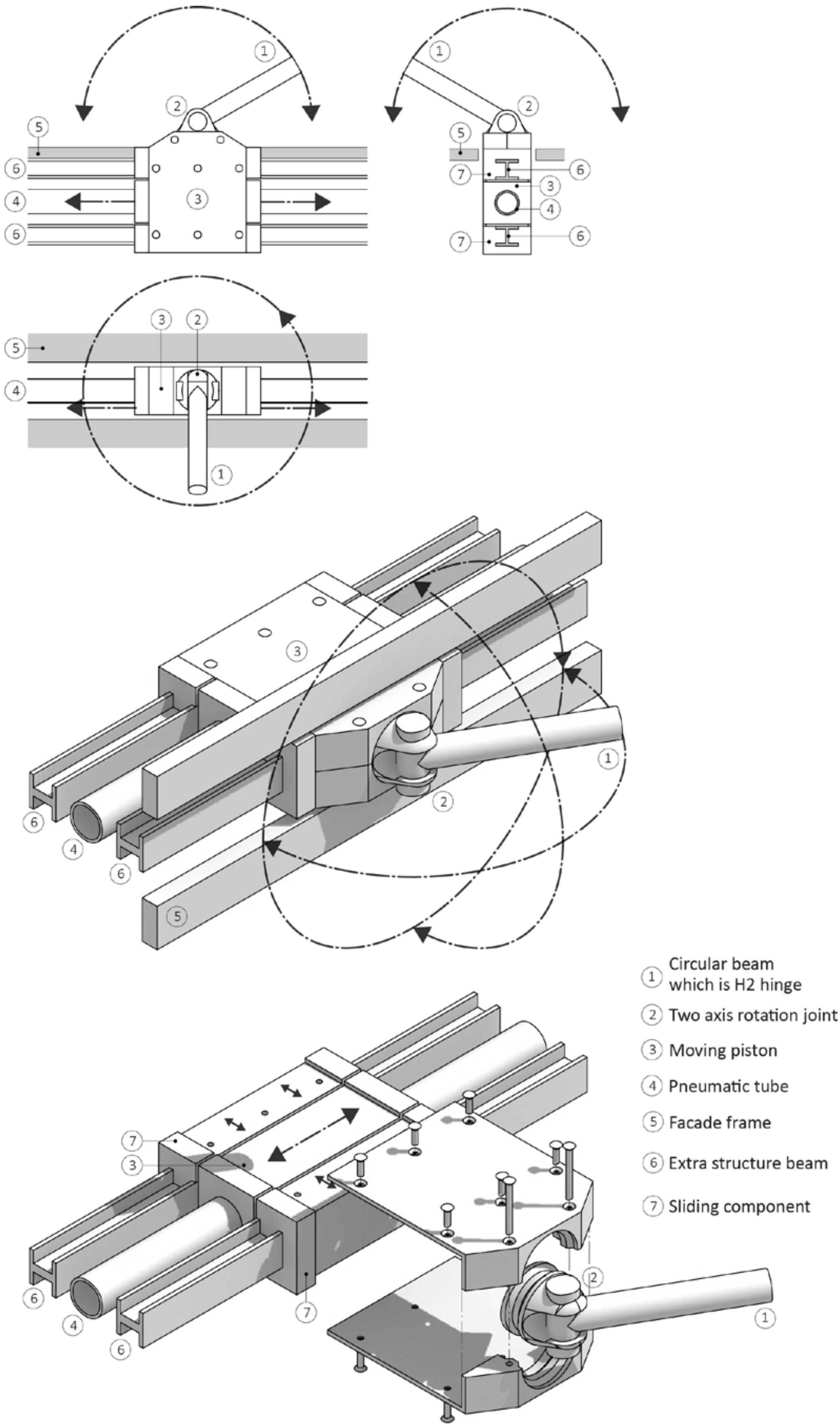

Fig 7.20: First schematic design of two axis rotation joint which allow the circular beam to be rotated and can be directed into any direction.

However, the first two axis rotation joint is quite complex the combination of many moving components. The problem that can occur is the difficulty in maintenance.

The developed design was a ball joint connection which has less mechanism and components. It is more durable and requires less maintenance. However, ball joint cannot create the all-direction rotation like in the first design because ball joint needs some specific angle for the cap to cover the ball without being loose and fall off. In order to proceed with the design, the angle of the movement was studied. The result shows that the rotation on the perpendicular plane to the base is only 13.27° (133.40°-146.67° from the first axis) which means that if the ball joint allow the 360° rotation on the first axis, the second axis needs to rotate only 13.27° and the ball cap will have enough surface to hold itself.

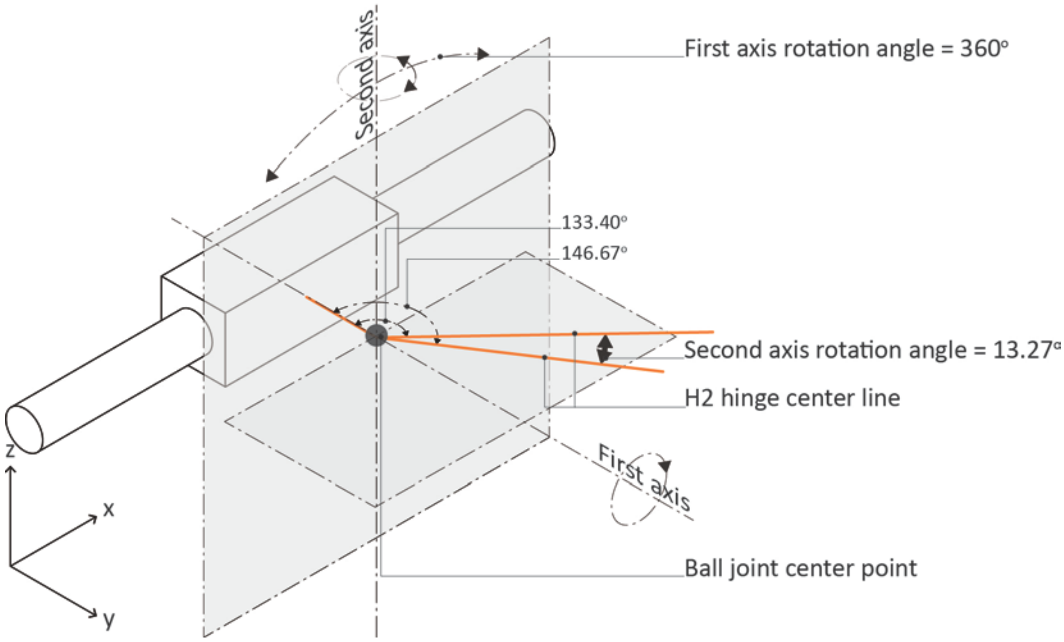

Fig 7.21: Angle of rotation from geometry studies for designing of two axis rotations joint or in this case – ball joint

The final result of ball joint is according to figure 7.23. Its angle of movement was test in the 3D software and the detail was made by 3D physical printing in order to test the ability to hold the structure by ball cap, to test the functional angle, and further, it will be use as part of physical prototype.

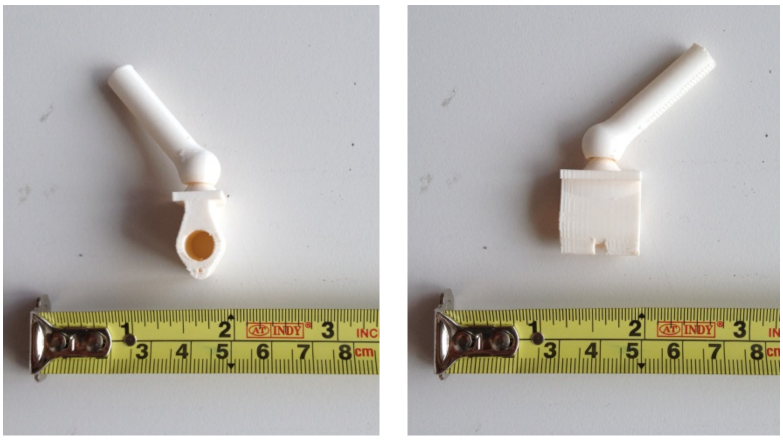

Fig 7.22: 3D printed model of ball joint

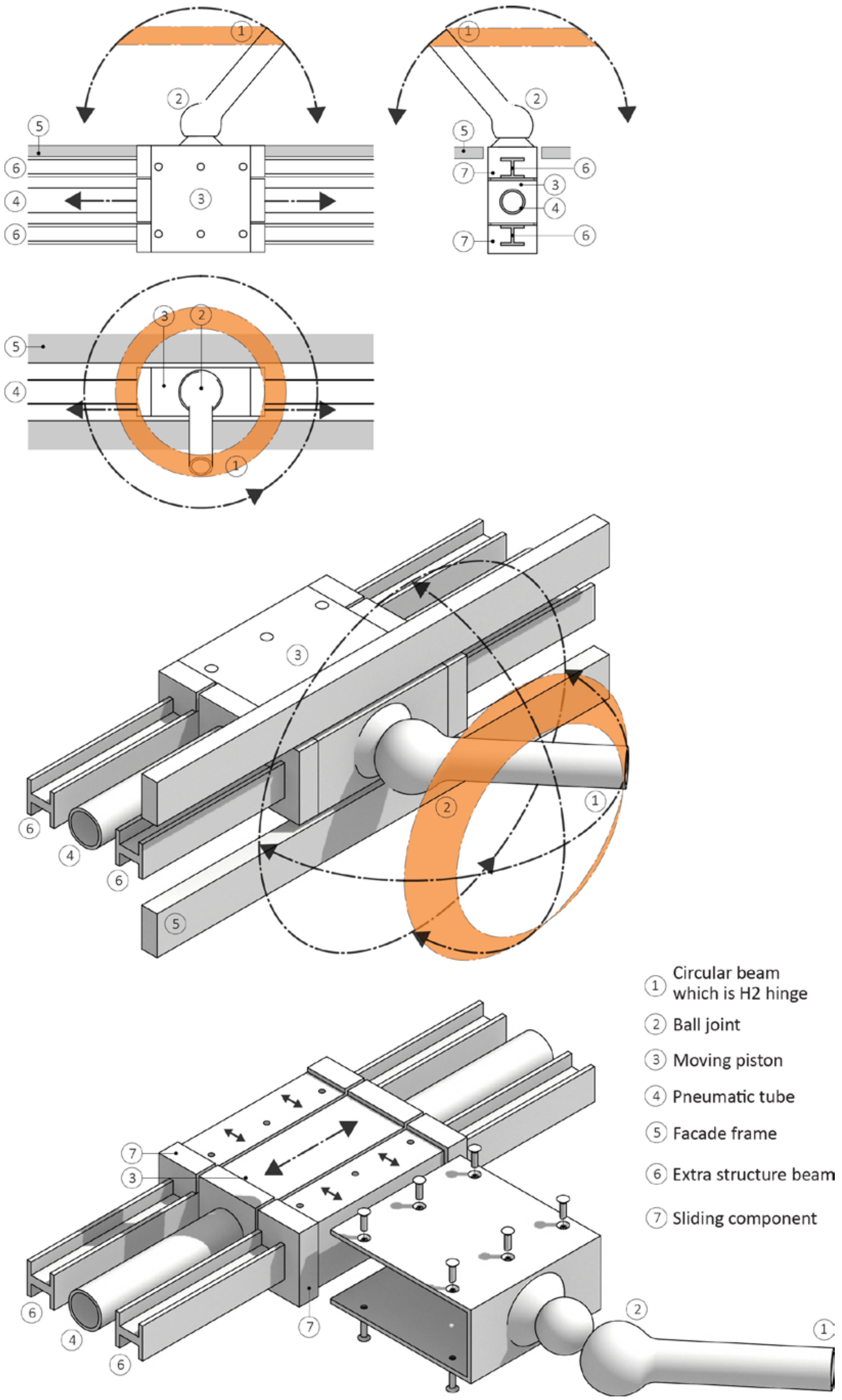

Fig 7.23: Final design of two axis rotation joint or ball joint which allow the circular beam to be rotated and can be directed into any require direction. The orange area is limit of the movement area of the H2 hinge beam.

7.4Façade assembling

The construction of adaptive façade system was design to be as simple as possible. The whole façade system can be divided into two main element, fins and façade frame. Both of the components are brought to the construction site separately and being assembled at the site. With only two pieces of component, it will be a simple assembling process which reduces the construction time, and also, the elements can be replaced during usage.

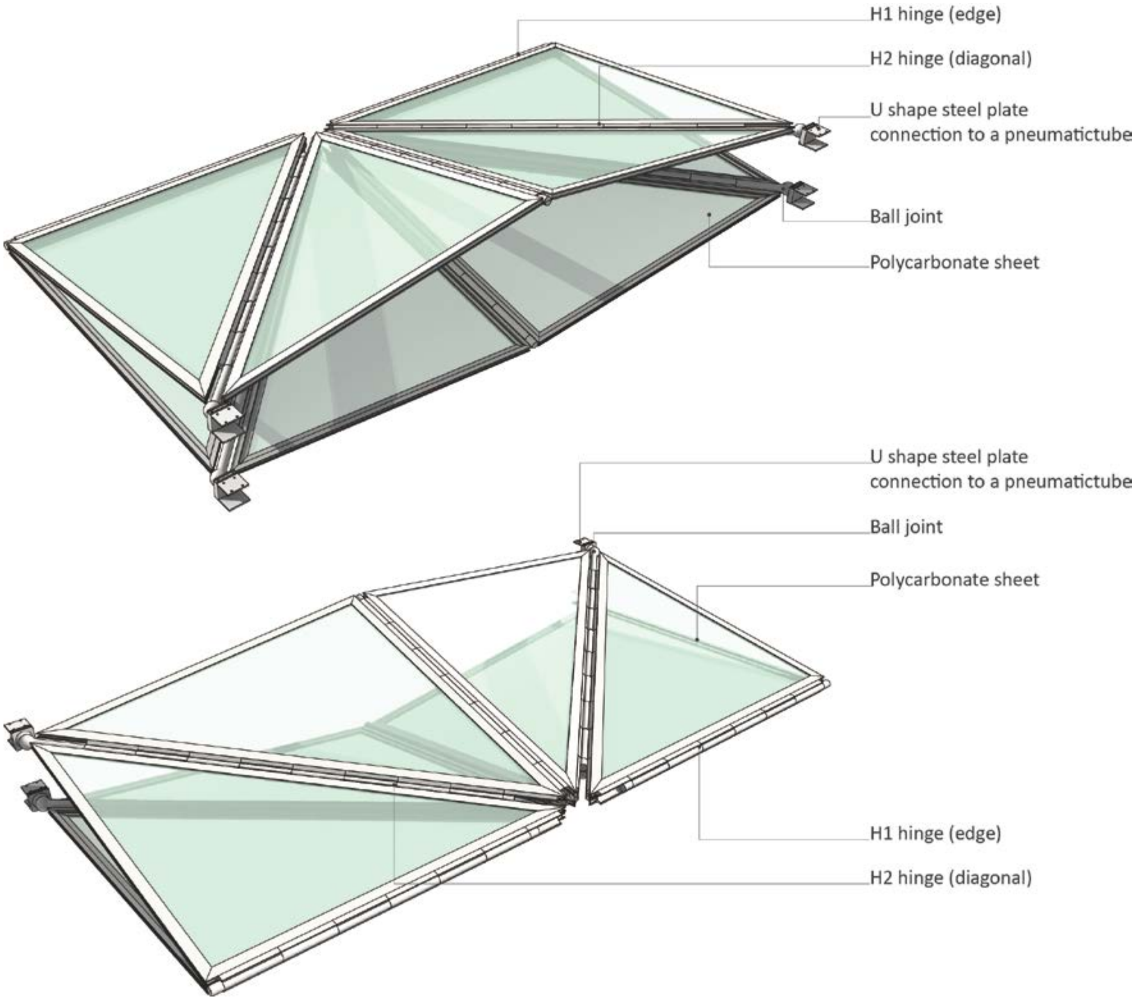

Fig 7.24: Fin component

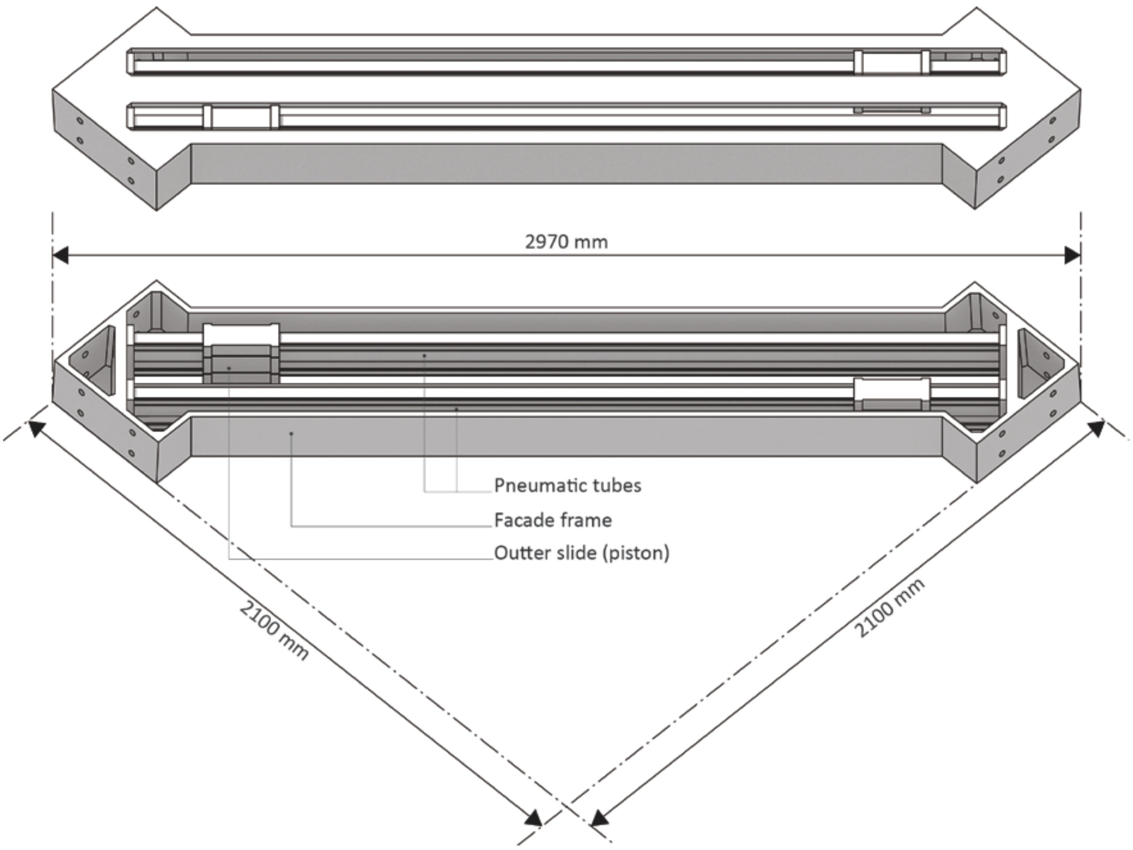

Fig 7.25: Façade frame component with pneumatic tubes

In high-rise construction, it would be more convenient if the façade can be mainly put together from inside without using scaffolders from outside, however, using of crane as a lifting equipment is still needed.

The benefits of assembling two elements of the façade at the site are, firstly, it can reduce the space requirement for transportation (the fin can be place in a flat position and the frame can be placed on the top of each other), and secondly, both elements are not individual operating, the fin connect to four frames while one frame operate two fin in the same time.

In the manufacturing process, the fin, which include ball joint and U shape aluminum plate, will be assembling before transporting or most elements of the fin can be assembling at the site as well, only with precaution and testing. While the frame will be brought to the construction site include pneumatic tubes in one piece. The pneumatic tubes will be connected to the air pressurized system at the site.

However, there are two possible ways of producing and assembling the façade frame. First, the frames are manufactured and transport to the side as individual frame which one frame per one edge of the façade structure as in figure 7.26. In this case, the frame is light, small and easy to be transported but the strength of the façade structure is lower than the second option. Second direction is that the frames are manufactured in pair. One piece of the façade structure consists of two edges as in figure 7.27. With this alternative, the façade structure has higher strength but it require more space for transportation.

The step of construction start from assembling pieces of façade frame together into one complete frame which it will be lift up to its location and being fixed to floor plates or the façade frame can be brought up piece by piece and assembled on its level as well. The fins can be placed and lift up later with a crane and being fixed to the pneumatic tubes from inside the building by only one or two construction workers.

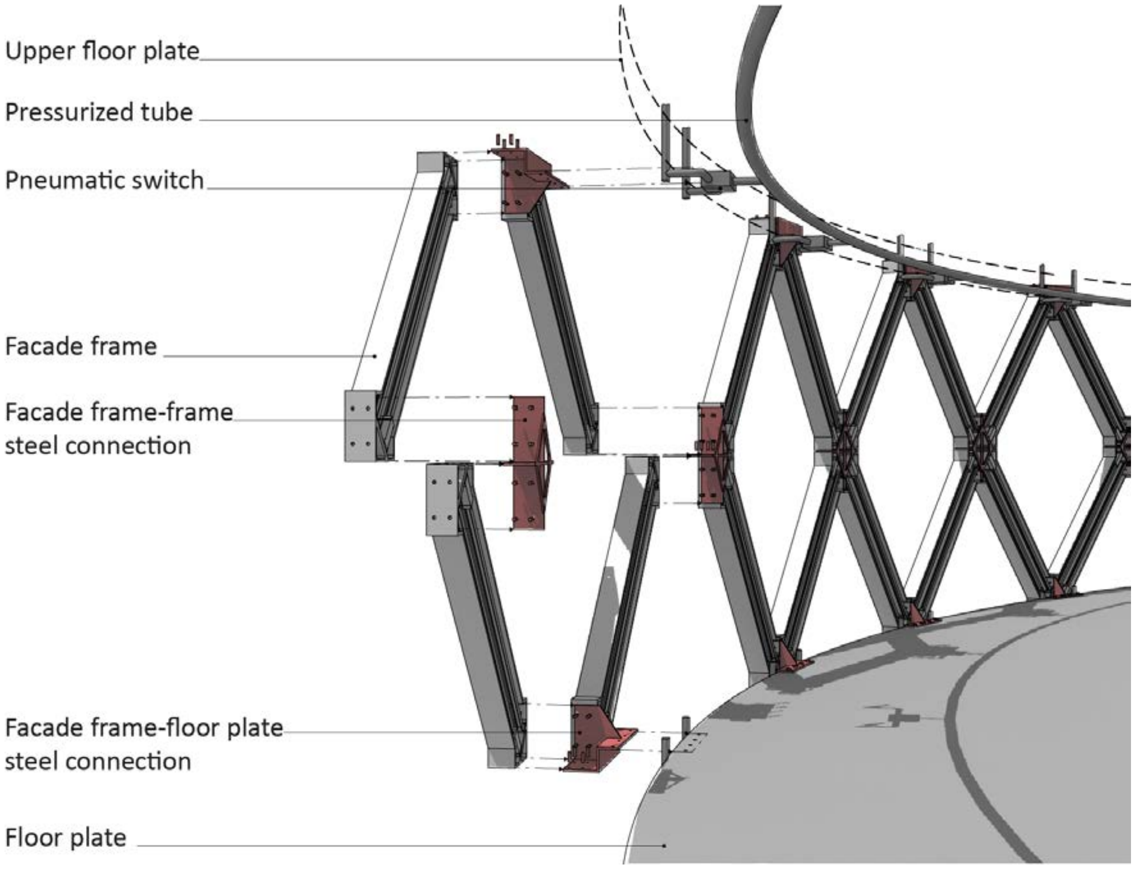

Fig 7.26: First option of façade frame assembling. The connections between the frame to frame and frame to floor plate are done with steel connections.

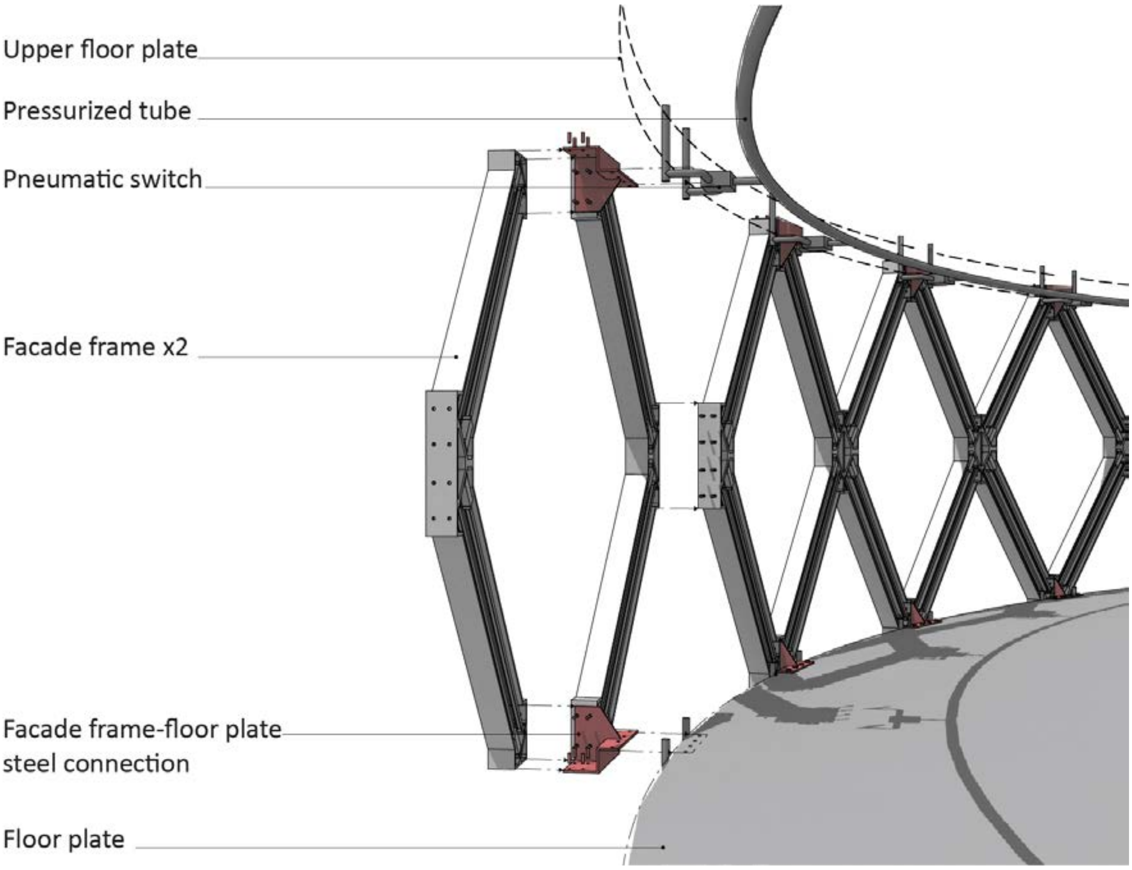

Fig 7.27: Second option of façade frame assembling. The connections between the frame to frame and frame to floor plate are done with steel connections.

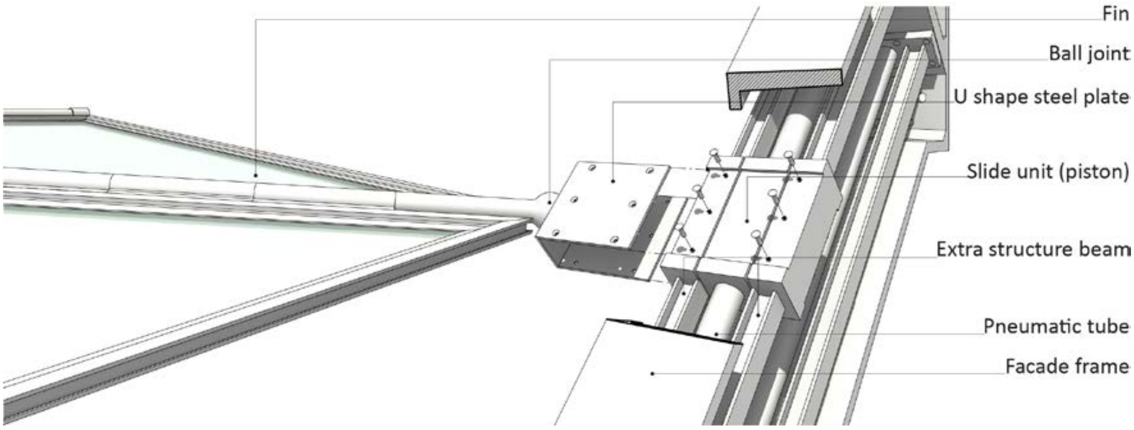

Fig 7.28: Assembling of fin to pneumatic tube. The fins need to be installed from outside the building by lifting crane. However, the fastening process has to be done from inside, the service corridor provides the access to those area inside.

7.5Mock-up

As mentioned before, the mock-up model of the adaptive façade was made. The purpose is to test the effectiveness of the details and to define the problem that is unexpected in the first place. Then, the model was made with the details that are similar to the design as much as possible. However, with the limit in budget, size and material some parts were modified but the concept of the movement in all pieces still remain the same.

As in pneumatic tube topic in 7.2, the mock-up models were done two times. The first one shows the problem of extreme lateral load to the pneumatic tube which caused the mock-up to be function partly. The designed detail was made by adding two extra beams, however, in the mock-up, those loads are transfer to the façade frame directly by redesigning the ball joint.

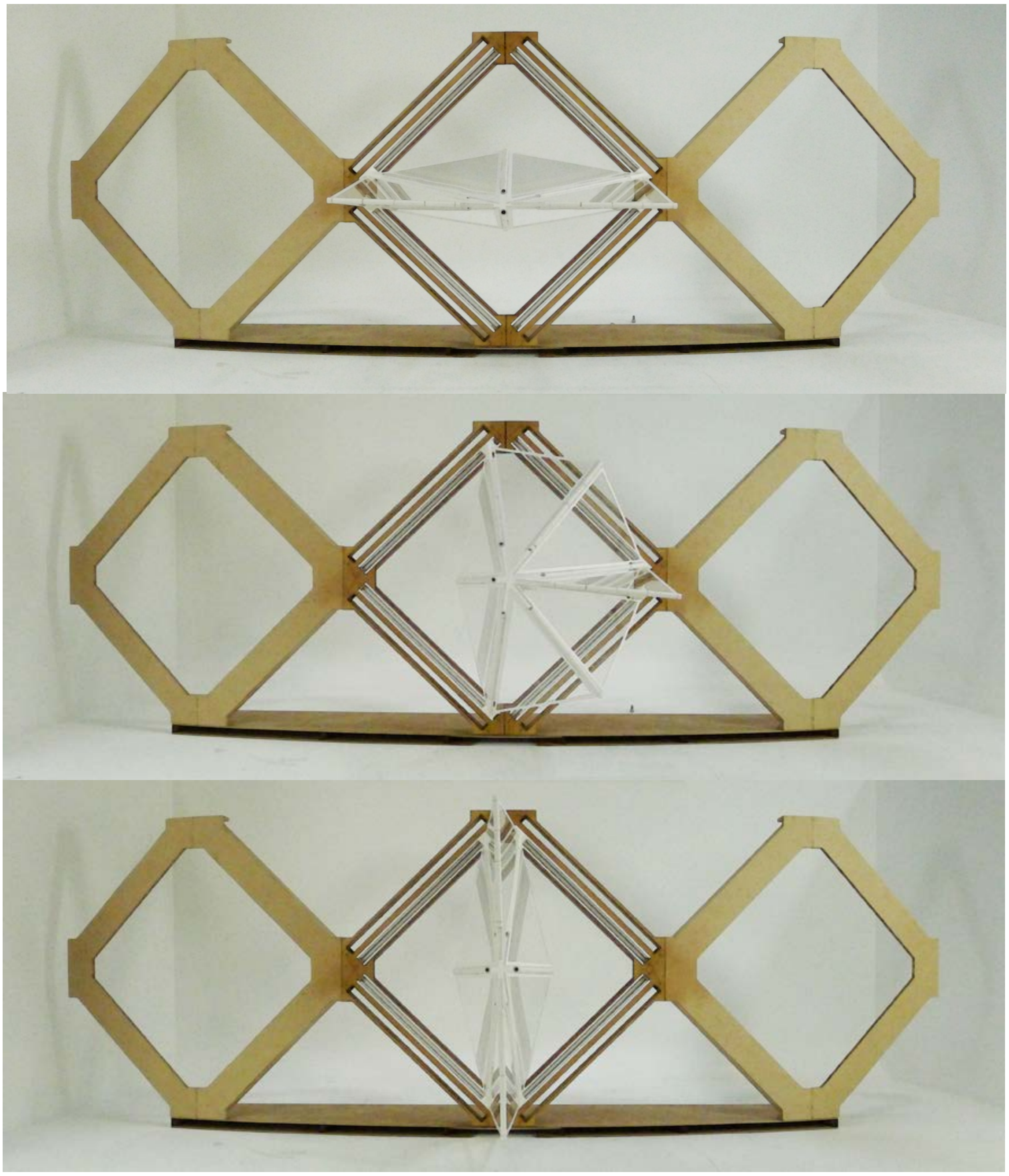

Fig 7.29: Final mock-up model with movement

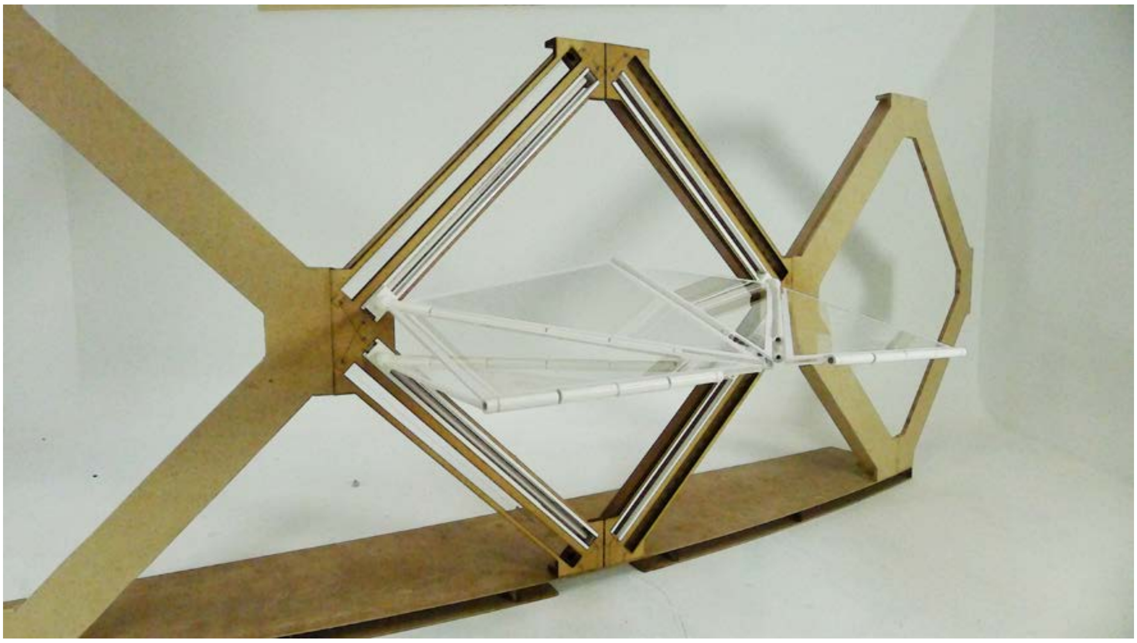
Fig 7.30: Final mock-up model


Fig 7.31: Final mock-up model – frontal fin detail

Fig 7.32: Final mock-up model – ball joints

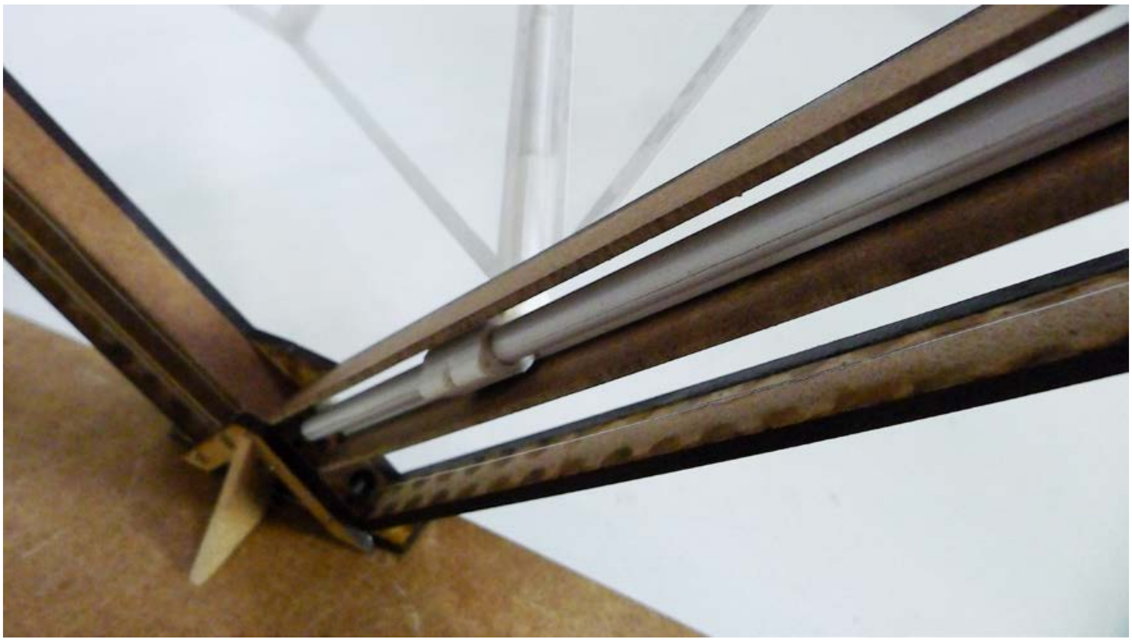

Fig 7.33: Final mock-up model – back structure tube and sliding part

8

Construction method and maintenance

Because of the main objective of wind responded adaptive façade is to reduce the effect of the wind load to the building which results in reduction of material used for handle wind load. However, as the size of structure is smaller means that the original load that can be handled is smaller as well. For example, if the façade was designed to reduce windload by 40% from 2kN/m^2, the high-rise structure definitely would be designed to receive wind load only at 1.2kN/m^2 (40% is taken by the façade). If the adaptive façade works properly, there will be no problem occur. On the other hand, if there is any malfunction or the building is under construction which the façade is not activated yet, the building structure will have to receive the load than that it was designed for. In order to prevent the damage to life and properties, the safety methods should be drafted.

8.1Building construction method

If the building construction process is divided into two main part, construction of building structure and construction of building envelope, the assembling of adaptive façade would be in between two of them.

As the building structures which include building core, column and floor plates are built up, it can be assumed that the load from the wind is lower than the complete building because the wind can flow through gaps between structures such as space between floor plates and columns. During this process, the need of the adaptive façade is not essential. However, the decision should base on structure calculation for the construction stage or the adaptive façade can be applied for the extra safety.

The adaptive façade that are installed during the building structure construction period might not need to be adaptable. From the research, shows that with only original position or horizontal position of the fin can reduce the load to almost haft of that can be reduced by adaptive one. The non-adaptive façade can be fixed in the horizontal position during this construction stage and being built up in the same speed of the increasing of the structure height.

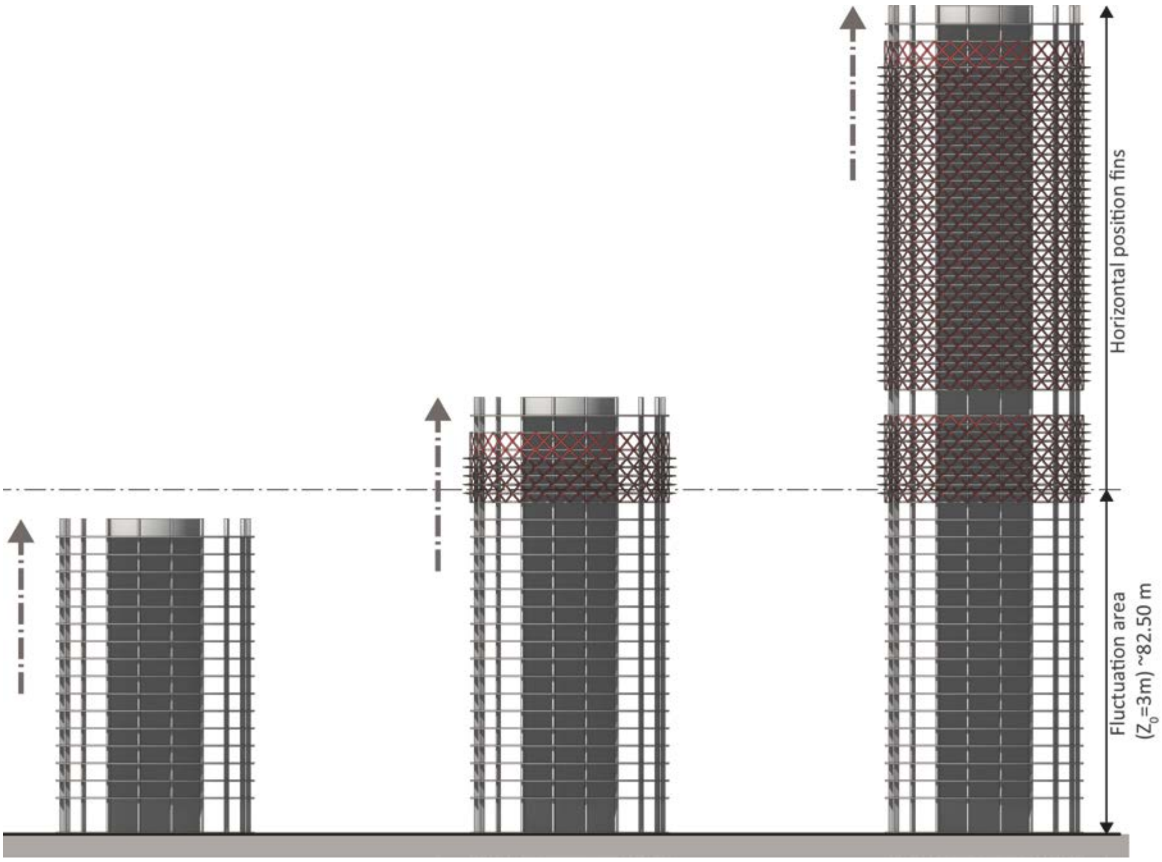

Fig 8.1: Construction sequence of the building structure and adaptive façade during the process before installing glazing and cladding. The fins stay in horizontal position without being adaptable at this moment.

At the stage where building envelope is being installed, the building will start to receive full windload. Before starting this stage, the adaptive façade should be adaptable and working during the construction of building envelope such as installing cladding or glazing. The installing of the envelope is not very complex because of the possibility of using service corridor outside the building (behind adaptive façade), however, lifting the envelope component from outside to inside of the building through the adaptive façade is not recommended. Those building surface need to be prepared inside or use other method of transporting them without chances of damaging the adaptive façade.

8.2Façade maintenance

The adaptive façade contain many moving mechanism that allow the façade to be adapted. These mechanisms, in order to maintain their durability and their functionality, the façade require maintenance frequently, especially the location with frequent strong wind. These maintenances can be referred to cleaning, fixing or replacing some parts of the façade. It is unavoidable for the need of working from outside the building. In normal highrise, the façade are maintained by using building maintenance unit (BMU) which mostly it is a lifting platform or cleaning personnel.

For the building that the wind responds adaptive façade is installed, BMU would be able to be applied to the system as well. However, with the cantilever of façade element can create some difficulty as the BMU cannot attach itself to building surface. At high altitude and strong wind according to the height, stand alone BMU can be a dangerous place to work.

The solution can be simply done by adding elements for BMU to attach itself and avoid being swung. These elements can be thin cantilever beams or cables that are located further than the length of cantilever of the façade fin.

Fig 8.2: Building maintenance unit (BMU) (S.A., 2014)

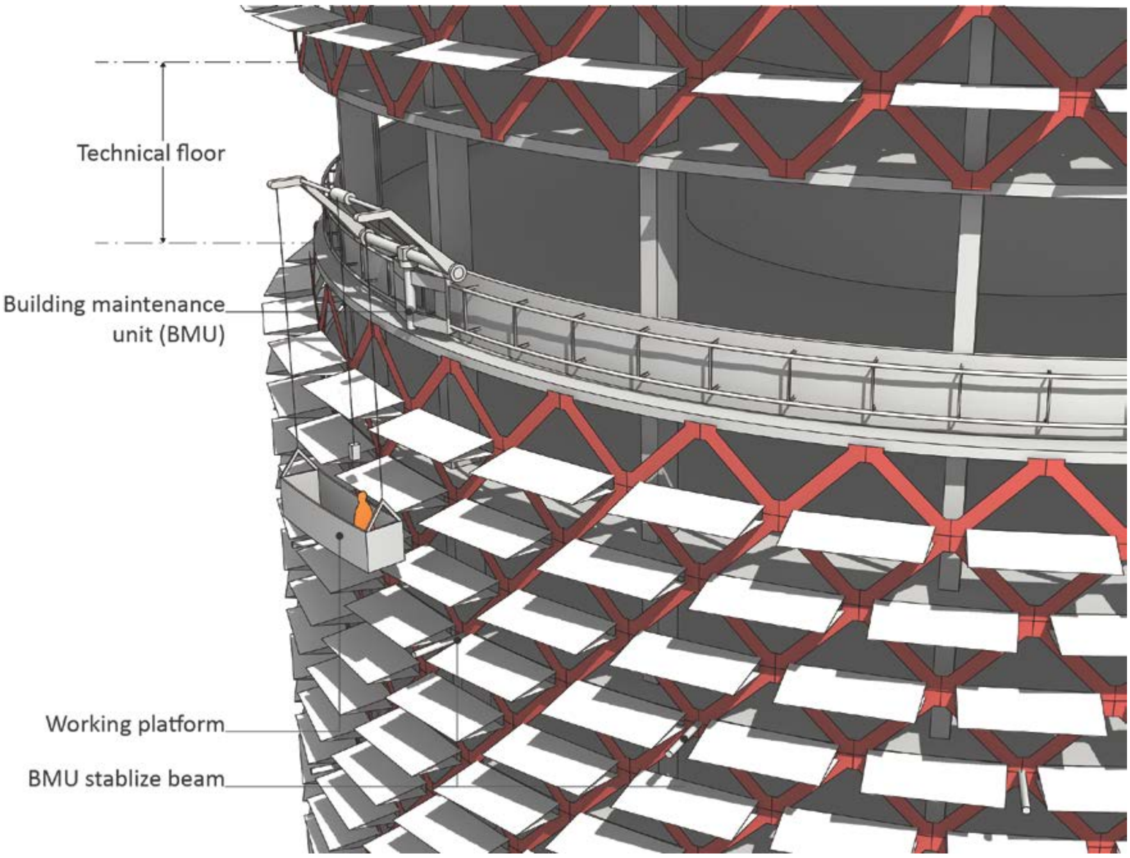

Fig 8.3: Suggested position of BMU during operating

The storage area of BMU as well as its lifting crane should be located in all technical floor which in those floor can be the exception of installing the adaptive fins and it provide the opening for the BMU to be lifted from inside to outside of the building.

8.3Safety criteria

With air pressure operating system, the failing of the façade is possible in a small scale with only one or two façade component that does not work. In this case, there will be only small effect to the ability to reducing wind load and those components can be replaced without any difficulty. These malfunctioning can be occurred because leakage in air pressure tube, obstacle in the fins mechanism, broken down of the pneumatic switch and error in controlling software.

However, there are also some possibilities that the system is the malfunction one. For example, if the whole building façade system or only one or two adaptive sets do not work properly, it will have big effect in wind load reduction and it can cause damage to building structure. It can be occurred when the system is completely lack of electricity, broken down of the software or terrorism.

If this situation is occurred, the façade control system should automatically turn the fin into horizontal position which can still reduce wind load. The setting of automatic reposition of the fin can be programmed in pneumatic switch to turn all the façade position to the horizontal position when the power supply is off. During this stage where the whole façade is malfunction and all the fin stay in the horizontal position, the building still can receive wind load at low to medium wind velocity (0-35m/s) which is the minimum velocity of typhoon wind speed. If the wind speed seems to reach the critical velocity, the whole building needs to be evacuated.

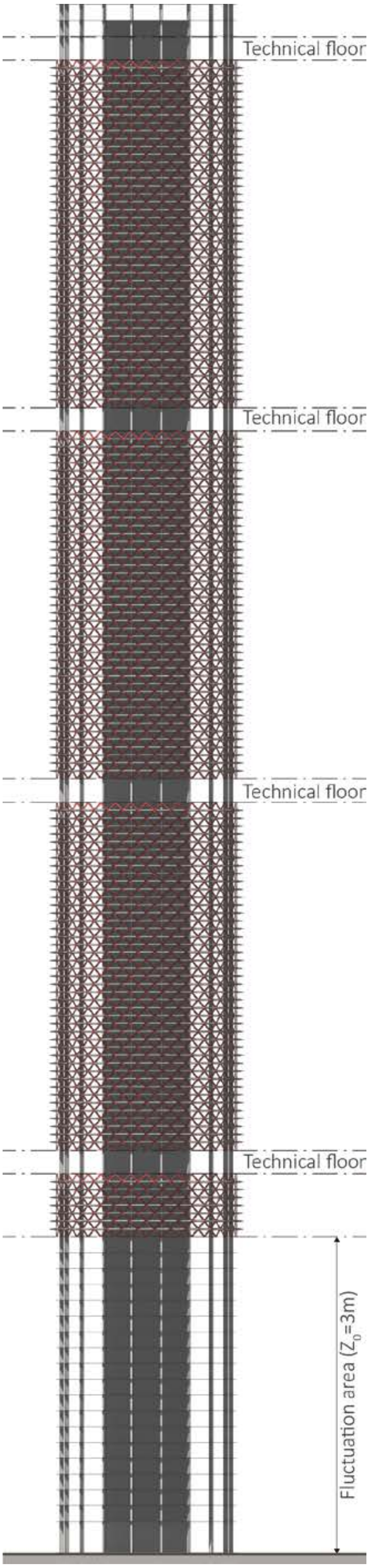

9

Conclusion

9.1 Visualization

The wind responded adaptive façade was applied to the mock-up building as in figure 9.1. The installation of the façade starts above the wind fluctuation area which is caused by the turbulence from buildings surrounding. The fluctuation area depends on the roughness length of the area (Z_0). The reason of exposing this area is that the wind in this area approach the building in the form of gust which is unstable and in the low velocity, also with low altitude the bending stress that is caused from this area is quite low.

Also the technical floors were left open without being covered with the adaptive façade because they are the area where the BMUs are located and they require the access to outside.

Top part of the building to the roof of the building is also left out because the flow there is different from the flow on other part of the building. Which in this part, it requires different approach in designing which is not included in this project.

The final building is 403.20m height with 94 floors above ground. The adaptive façade start from floor 19th to floor 92nd. The floor plate area in each floor is 1754 m^2.

There are 2,520 units of façade frame which is 10,080 frame elements and 5,112 fins installed in this building. All façade components can be divided into 6 control set along the height.

Fig 9.1: Mock-up building with adaptive facade

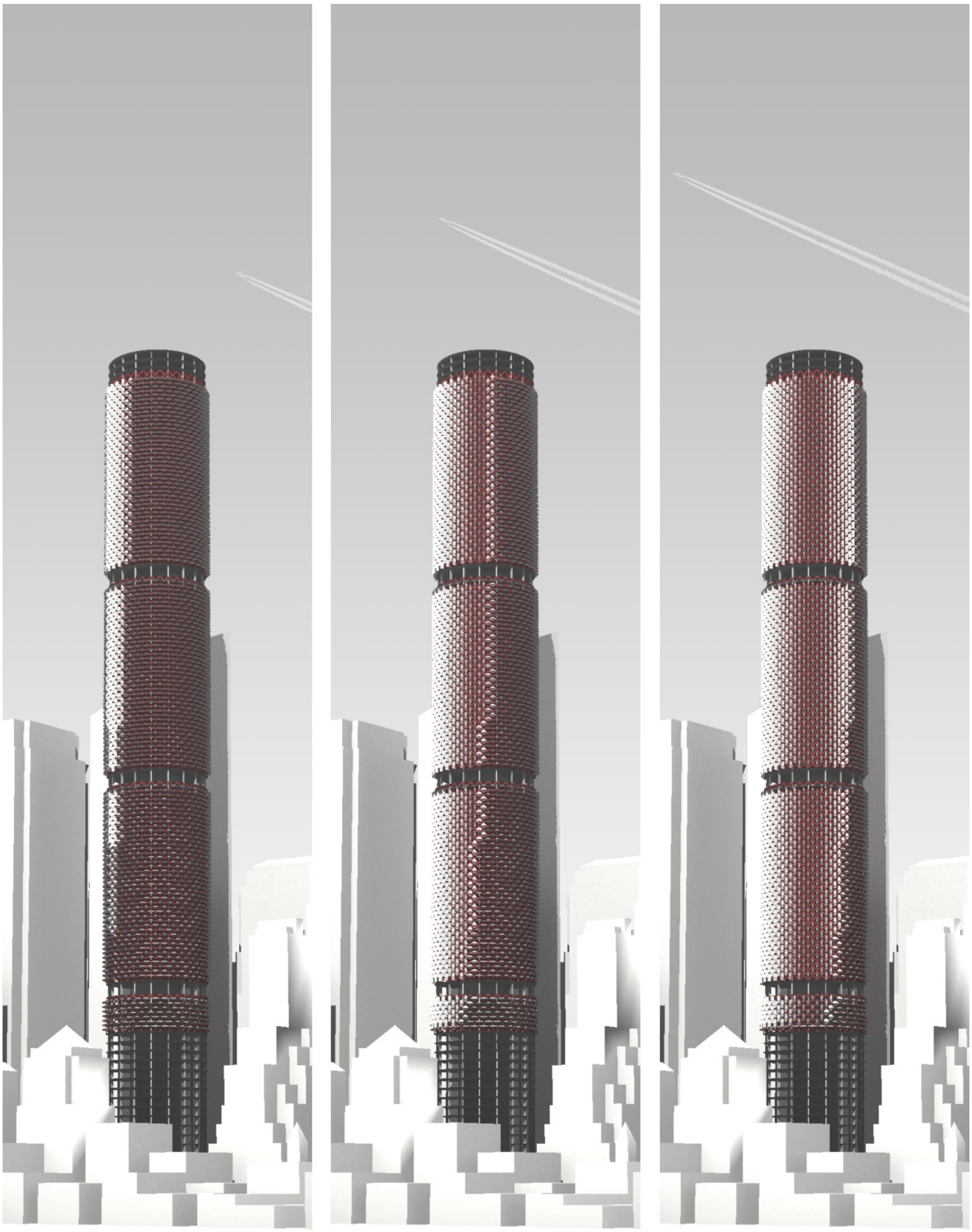

Fig 9.2: Morphing of the façade during the time of impact of the wind. (Left) is the moment when the wind is approaching the building and low velocity wind is occurred around the building. (Right) is fully adapted position.

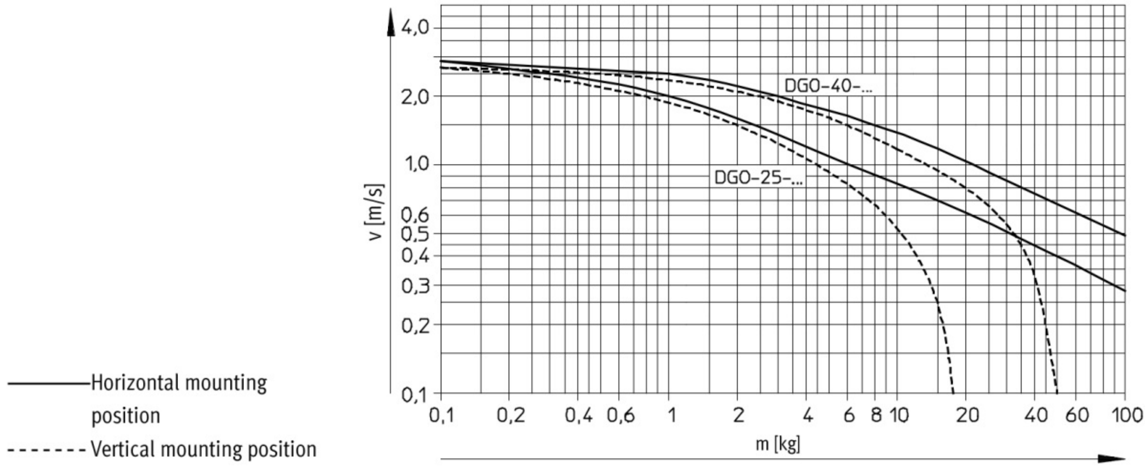

Fig 9.xx: Pneumatic tube DGO Max. piston speed (v) dependent on the moving mass (m) ("Festo: Linear drive units DGO," 2012) With the mass of the fin per one support = 204N (20kg), the 40mm pneumatic tube can finish the stroke in 2.5 second. If the whole system works continuously, the transformation can reach the widest point of the building in 25 second which is faster than the movement of separation flow area.

9.2Drag reduction and reduction in structure

9.2.1 Drag reduction

Drag force reduction according to the performance is divided in to two situations, the situation where the façade is non-adaptable which all the fins are in horizontal position and the situation where the façade is adaptable. The force reduction is show in figure 9.3 which is the result from computational fluid dynamic (CFD) software. The reduction values that the result from adaptive façade is not yet maximum because it is lack of horizontal and vertical fins optimizing. The optimized one would probably able to have better reduction performance.

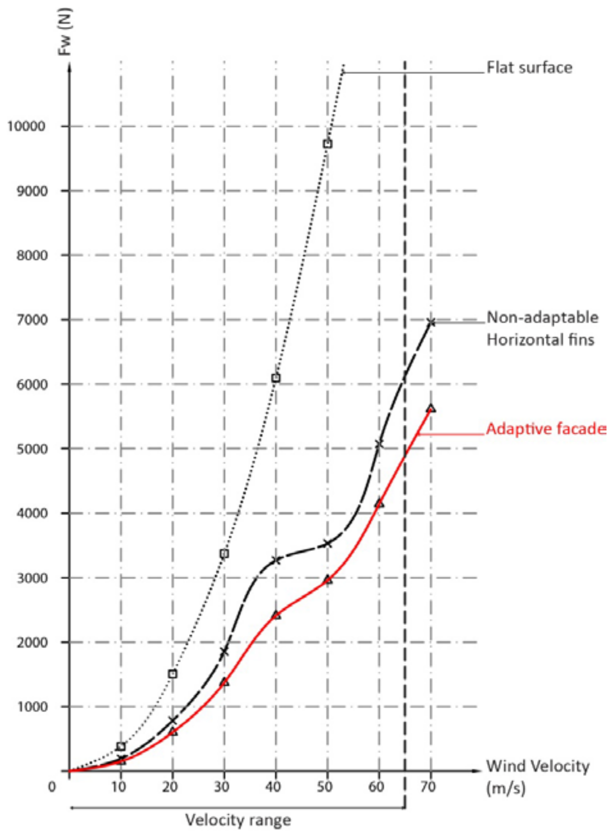

Fig 9.3: Comparison of drag force (Fw) reduction between three type of façade surface on circular cylinder object (building) with radius of 50m and 100m in height with the flow that only pass through the object on its sides but not over the object. (redraw of figure 5.7)

However, the force reduction in figure 9.3 was done with computer models that have been simplified and not yet included the final design where all the ribs are cut in small pieces as adaptive fins. In this conclusion stage, the computer models were remade and test in the same software to find exact reduction value and to investigate if the gaps between façade components have effect to the flow.

Multiple models were made again as 1) a smooth surface circular cylinder object with 48m diameter and 21m high, 2) an object in the same size with horizontal fins around it and 3) seven objects with horizontal fins in the front where the wind approach and vertical fin at the back of the object. For the third type of the object the numbers of adapted fins are different as part of optimization to find the best performance that the adaptive facade can be. The fins were made in the same shape with the final design also with the same gaps size between each of them. The size of the object were smaller than the previous experiment (chapter 5) because the size of the building change from 50m diameter to 48m and the height of the objects were reduce because with high detail model, it require a lot of time time to analyze. The analysis was done with 150% mesh quality which is 50% better than the previous experiment. The testes were done at wind velocity = 60m/s which is the highest speed calculated at 400m above ground

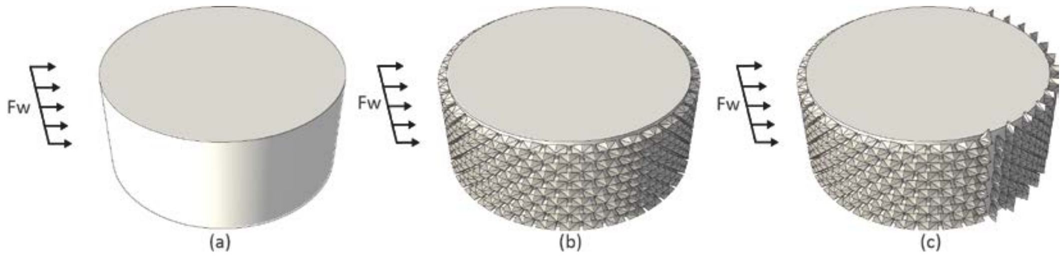

Fig 9.4: Final test models. a) the smooth surface model. b) the model with only horizontal fins. c) the one of seven optimized models which has the best performance in drag reduction

	Drag force (kN)	Drag force/area (kN/m^2)	Drag reduction (%)
Smooth surface	3941.84	3.91	-
Surface with horizontal fins	2326.35	2.31	40.92
Adaptive façade with horizontal + vertical fins	2063.37	2.05	47.57

Table 9.1: Drag force and drag reduction of the final designs compare to drag force of the smooth cylinder building surface at the wind velocity = 60m/s (Autodesk Flow Design, 2015)

9.2.2 Reduction in structure

The reduction of drag force should smaller the requirement of the structures that are designed for handling windload. The result from the experiment assume to be the wind speed on the top part of the building which the value can be used to estimate the wind speed at the bottom part of the building and also the load for both parts by standard calculation (EUROCODE, 1995).

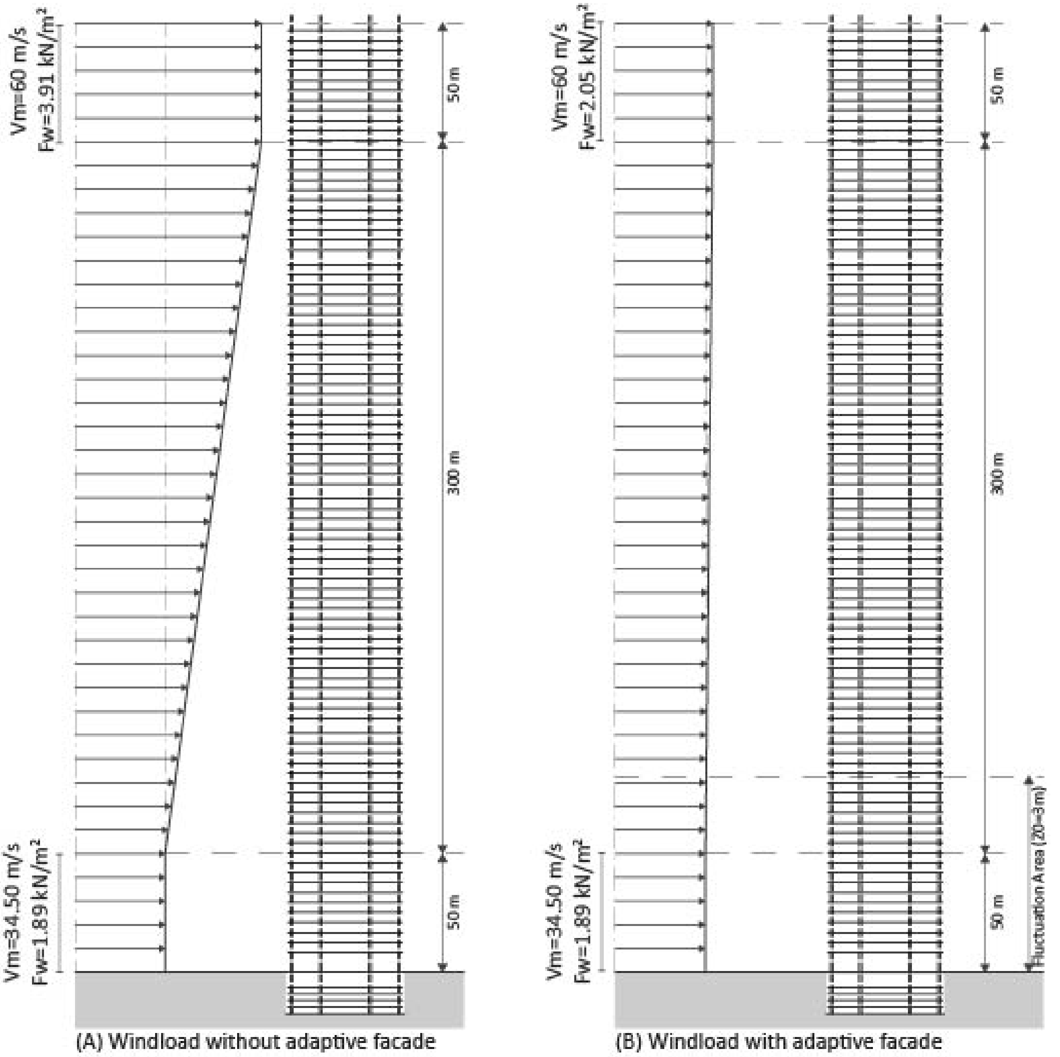

Fig 9.5: Wind load comparison. (A) is the load for the circular cylinder building with smooth surface façade and (B) is the building with adaptive façade. The loads at the bottom part of the façade are presumed to be the same because they are under the fluctuation area where the adaptive façade is not installed.

The windload reduction decreases the bending stress of the building core. The structure calculations were repeated as the same method in chapter 4. However, the size of the core of the building with smooth surface is slightly different from chapter 4 because the load in this conclusion part is from the CFD software but not from the standard calculation because for the comparison the values should come from the same source.

By the calculation, it shows the reduction in bending moment and increasing in the building load because the additional weight of the adaptive façade. The optimization of the calculation was done by modifying the inner radius of the core while keep the thickness of the wall as 1 meter. The result of the normal smooth façade shows that the requirement of the core should be 14.05m for diameter of the outer surface with 1 meter of wall thickness, while the building with adaptive façade requires only 8.80m for diameter of the outer surface. As consequence, even though both buildings are stable against the wind, on the other hand, the stresses in the core of the building with adaptive façade are more than 64% higher than the normal one. The detail of calculation can be found in Appendix D.

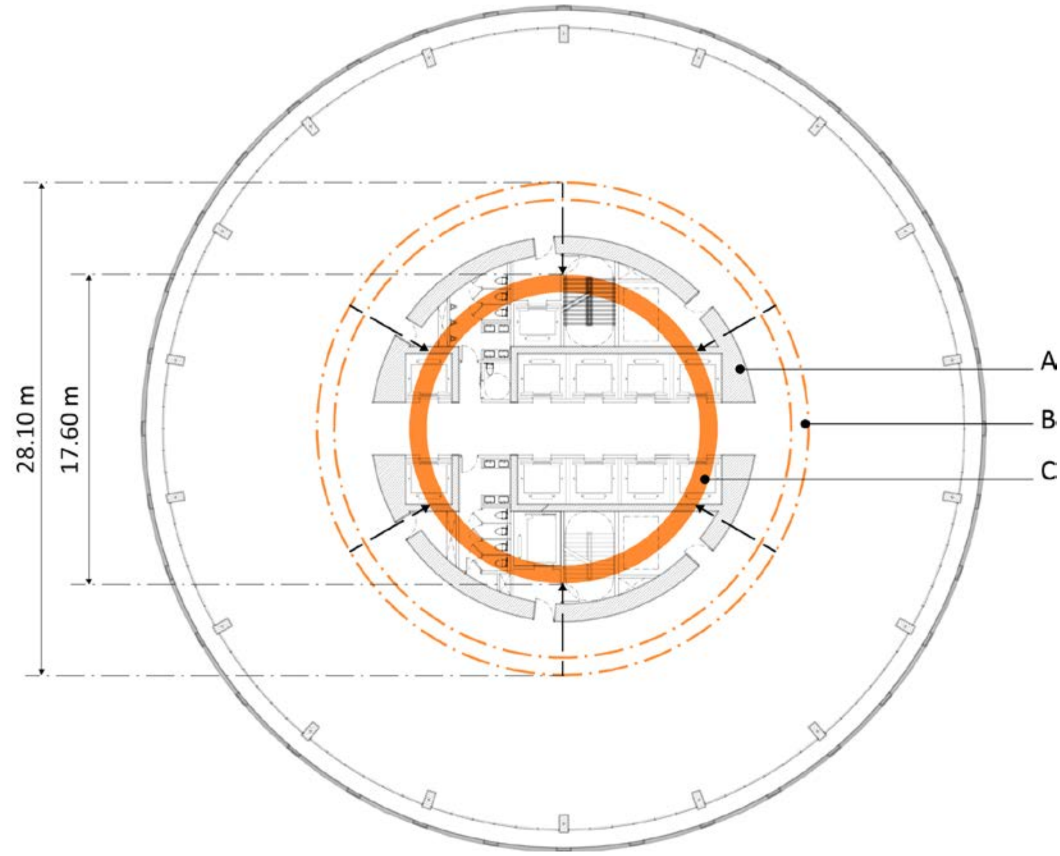

Fig 9.6: Reduction of building core. (A) is the original size from chapter 4 which handle wind load on the top part of the building at ~49.53m/s. (B) is the core size with the load from the wind at 60m/s on the top part without adaptive façade. (C) is the core size that the building requires after applying the adaptive façade.

The reduction of the core size can increase the usable area of each floor and also reduce the overall load of the building. In this case, the original net rental area per floor is 1133.59m^2 with the normal building envelope, but with applying of adaptive façade that net area is increased to 1510.62m^2 which can be the benefit to building owner by 33%.

9.3Feasibility

The feasibility of the product was analyzed by the comparison in two aspects. First aspect is the cost calculation of construction process between additional cost for adaptive façade and cost reduction due to the core size decreasing. And second is the cost calculation of the payback period by the comparison of energy requirement for adapting the façade to the increasing in rental price due to the increasing of rentable area. The detail of calculation can be seen from Appendix F.

<u>Additional adaptive façade cost vs. core material reduction cost</u>

The estimation of the material costs was done by using value from CES Edupack software for non-standard material such as aluminum profile, concrete as price per kilogram. And for standard components such as pneumatic tube, pneumatic switch and polycarbonate sheet, the price was referred to the cost in supplier websites.

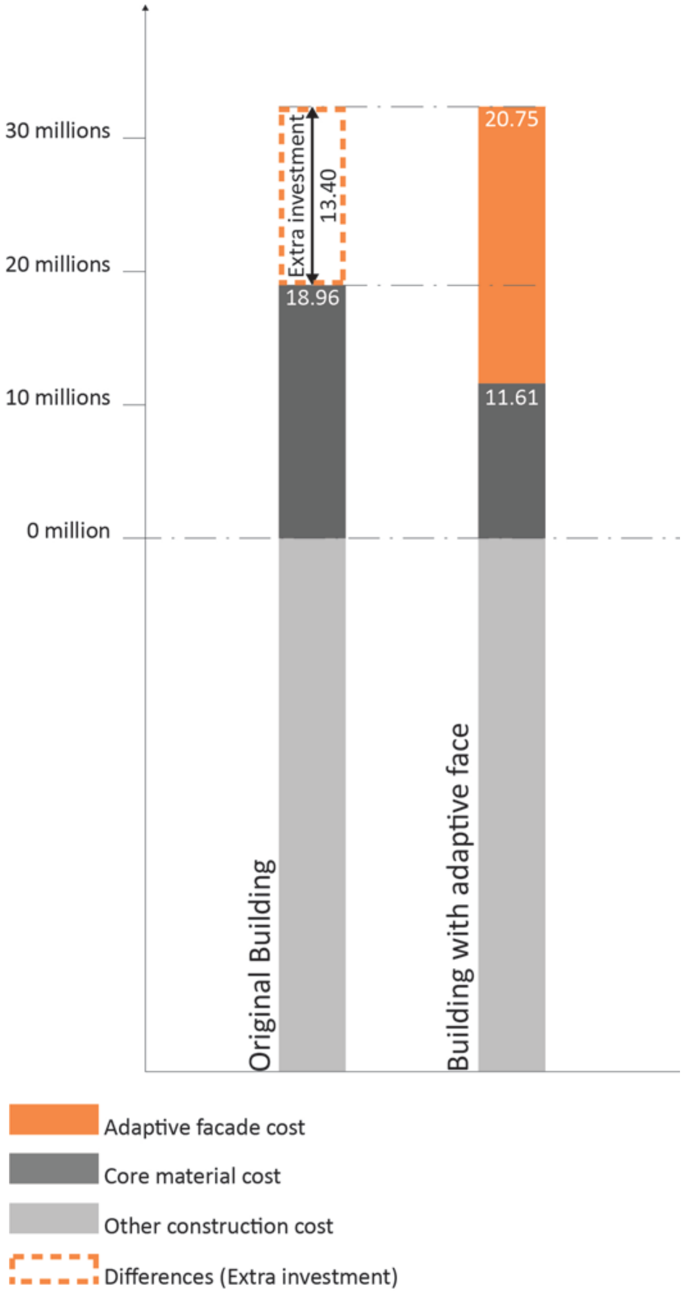

Fig 9.7: Construction cost comparison between original building and building with adaptive facade

The adaptive façade is considered to be additional element which is not for replacing any original building component. The building still requires normal glazing façade as usual. The estimated price of the adaptive façade for the whole building, which include the fins, façade frames, support system (pneumatic switch, pressurized tube, air pump and air tank etc.) and 30% of assembling and construction, is 20,749,642.51 EUR.

While the calculation for the material reduction of the core shows the result of the differences in price in EURO of the original core size (radius=14.05m, thickness=1m) and new core size (radius=8.80m, thickness=1m). The calculation was presumed that the core remain in the same thickness all the way from the ground to the top floor of the building. The concrete used for the core was reduced by 13,305.60m^3 which is approximately as 7,344,691.20 EUR.

It can be seen that the price of the façade is almost three times higher than the money that the owner will save from the reduction of core size. The differences of these two values shows how much money the building owner has to spend in order to use the adaptive façade, which is approximately 13,404,951.31 EUR.

Energy requirement vs. increasing of rentable area

This comparison shows the benefit during the operating period of the building. The calculation shows the expenses of energy usage for the adaptive façade in order to be operated and the income from the increased rental area. The comparison will shows the extra income per month and per year, and also show the payback time for the extra payment that is happened during the construction period.

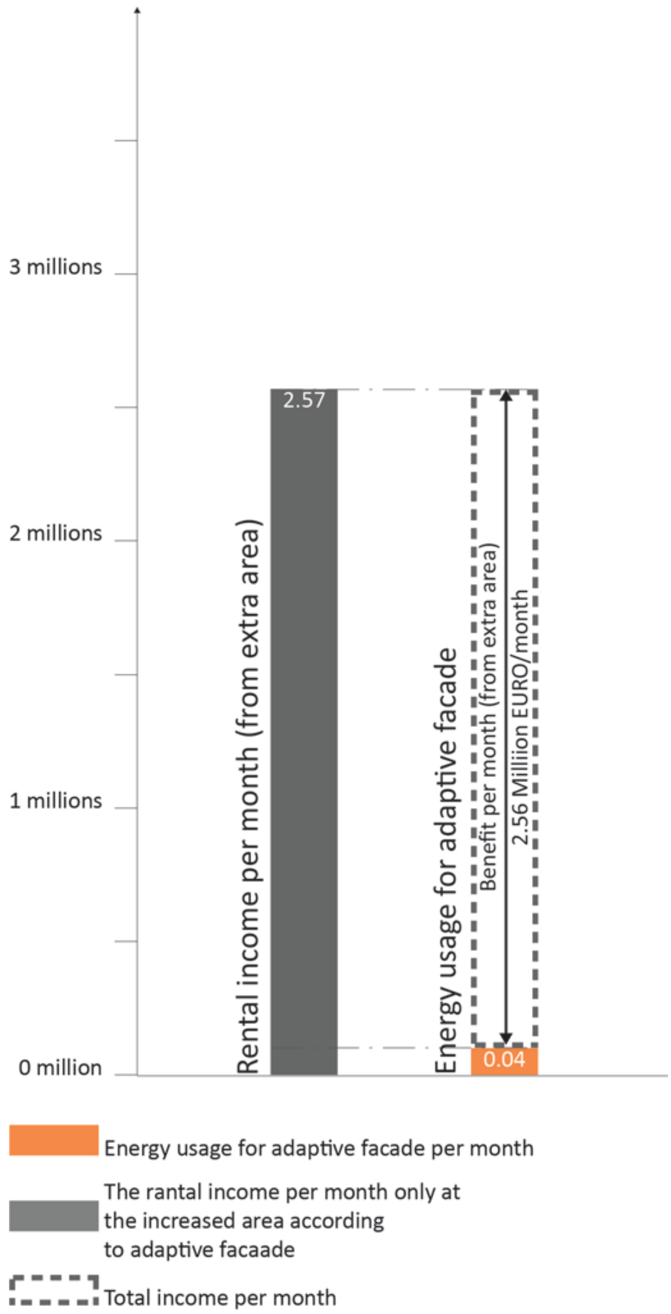

Fig 9.8: Comparison of rental income from the increased area to energy cost for façade operating. The graph shows the benefit per month from the extra area that is increased

The energy usage mainly comes from the air pump and operating system of the façade. There are 36 units of air pump and air tank which can provide 4680 liter/hour at maximum air pressure = 7 bars. The energy requirement for the adaptive system for the whole building is 463.97 kW per day (24 hours operated). If calculating with energy price per kWh at 0.26 EUR (the Netherlands), the energy cost per month is 3,618.95 EUR and 44,030.56 EUR per year. In this case, the maintenance cost was not put into consideration which in reality this amount of money should be added to the expense cost.

The rentable area increases 33,178.20m^2 from decreasing of core size from the radius at 14.05m to 8.80m. The smaller core has the effect on function arrangement inside the core. The 8.80 core is practically too small for all functions that it needs, however, in this case, the comparison is only concerned in structure aspect. In reality, the increased rental area should be smaller than 33,178.20m^2 because of the need of the toilet and support areas which have to be located outside the core. The rental price is the average value from 6 case studies of highrise in different locations, Hong Kong, Singapore, Bangkok and Dubai, which is 70.94-

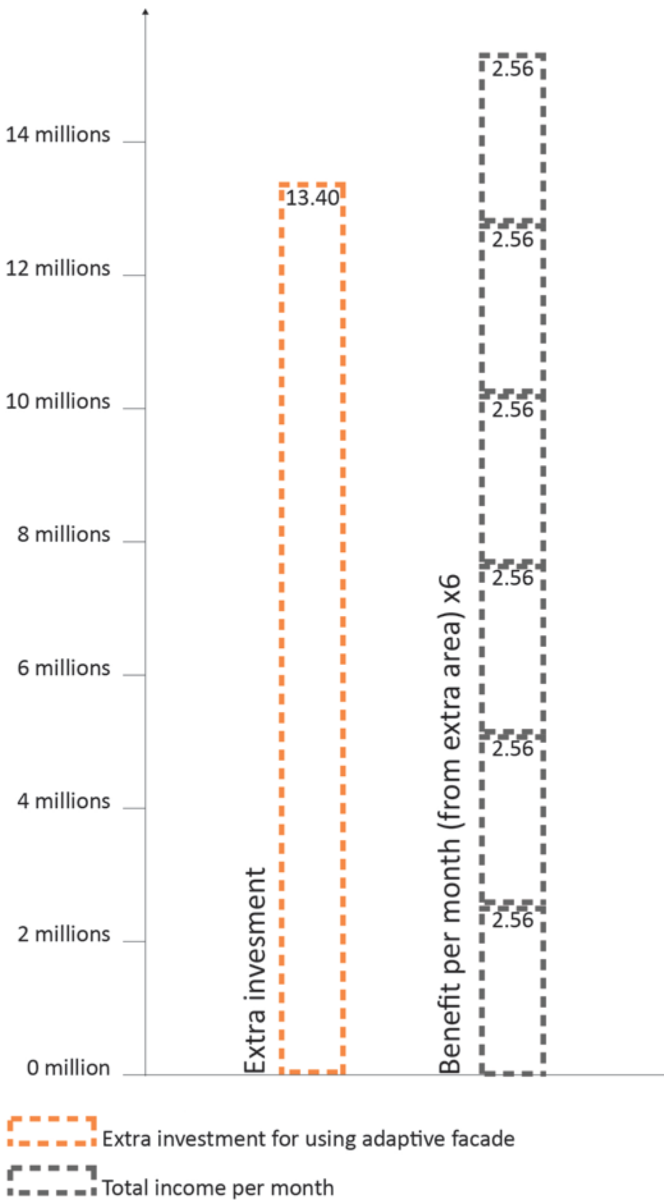

184.96 EUR/m^2 per month. The income from the increased area in this building is 30,807,490.00 EUR/year (80% rented).

Comparing to the additional structure cost (13,404,951.31 EUR), the payback period only for the façade is around 6 months. The benefit for the first year is 17,358,508.35 EUR, and 30,763,459.66 EUR from the second year onward.

Fig 9.8: Payback period graph shows the time required for the income from extra rentable area to compensate the extra construction cost.

9.4Reflection

The working on the adaptive façade for windload reduction in highrise was done with the approach to cover all the aspect as much as possible, which in this case, include aerodynamic engineering, structure engineer, construction, detailing, assembling, system design, maintenance and aesthetic look of the product. Along the progress, it shows many problems, issues and challenge as expected. However, the solutions for all the problems that visible in the progress were suggested as good as the knowledge of the designer can provide.

The windload reduction by wind responded adaptive façade is possible in theory. However, the product is involved, not just the look of the building, but also the safety the user and people who passing by. With this reason, using this façade still require higher and deeper investigate in most parts. In this stage some of the possible further developments are suggested.

1. Wind behavior analysis need to be done in more realistic way with full building analyzing in higher accurate CFD software and physical wind tunnel. The accurate CFD calculation requires a model with very high mesh quality, more complicate software that require specialist knowledge in aerodynamic or hydrodynamic engineering which will consume a lot of time in progress. The physical wind tunnel test require full height scale model of the building with optimizable (adaptable) façade with proper measuring equipments that can give value in bending stress and displacement of the building. The tunnel itself should be big enough for not create an effect of the flow from the tunnel wall the test model.

2. The optimization of the fin position is still required. In this case, it is the optimizing of the number of fins that will be transformed in each specific wind velocity from 0-60m/s. It is necessary to find the location of separation flow and program the fins that will be adapted to delay the separation. The record and statistic of the locations of the separation flow can be store in database and be used for creating the command script of façade controlling.

3. Because the use of the adaptive façade, the building requires only small core size compare to the one without the façade, which means that the building is weaker than the normal building and it require the façade to operate all the time. The system, as the design, relies on the supplying of electricity in order to pressurize the pneumatic system and to control the system. Electricity black-out can causes a fetal damage to building structure, users and people around the area. The system needs an emergency energy supply or self-sustain energy source by using wind energy or integration of polymer solar cell film (PV). The façade that is driven by the pressure from the wind itself is too complicate in this research but it can be possible with combination of wind catcher and the shape of the building which can be the further development.

4. Because the drag reduction of the model with horizontal fins compare to model with adaptable fins is quite small (~11%). The decision of using only horizontal fins is possible and effective enough for windload reduction which it will require no energy for operating, less complex in detail and assembling, and also possibility of easier maintenance. However, it will reduce the aesthetic and attractive value of the building.

10

Bibliography

. (2015, Jan 13). *NASA*. Retrieved from http://www.grc.nasa.gov/WWW/K-12/airplane/shaped.html

Barry Bergdoll, D. G., Philip Ursprung. (2007). Speedo, Fastskin FSII *Nature Design: From Inspiration to Innovation* (pp. 74-75). Zurich: Lars Muller Publishers.

CTBUH (Producer). (2015, 1 14). *Council on tall buildings and urban habitat*. Retrieved from http://www.ctbuh.org/

Drag (physics). (2015, 05 15). Retrieved from Wikipedia: http://en.wikipedia.org/wiki/Drag_(physics)

Drag coefficient. (2015, 05 15). Retrieved from Wikipedia: http://en.wikipedia.org/wiki/Drag_coefficient

Dean, B., & Bhushan, B. (2010). Shark-skin surfaces for fluid-drag reduction in turbulent flow: a review. *Philos Trans A Math Phys Eng Sci, 368*(1929), 4775-4806. doi: 10.1098/rsta.2010.0201

Dr Patrick TEUFFEL, D.-I. F. D. A. (2007). *Development of a Shape Morphing Building Envelope*. Paper presented at the IASS Symposium 2007 "Structural Architecture - Toward the future looking to the past", Venice, Italy.

DuPont™ (Producer). (2015, 04 28). Fluoroplastic Comparison - Typical Properties. *DuPont*. Retrieved from http://www2.dupont.com/Teflon_Industrial/en_US/tech_info/techinfo_compare.html

E. Maruta, M. K., J. Sato. (1998). Effects on surface roughness for wind pressure on glass and cladding of buildings. *Journal of Wind Engineering and Industrial Aerodynamics*(74-76), 651-663.

Emil Simiu, R. H. S. (1996). *Wind effect on structures: third edition*: A Wiley-Interscience Publication.

Eurocode. (1995). NEN-EN 1991-1-4 (en) *Eurocode 1: Actions on structures - Part 1-4: General actions - Wind actions*. The Natherlands: ICS 91.010.30.

. Festo: Linear drive units DGO. (2012). In Festo (Ed.), *Linear drive units DGO*.

Gladwell, M. (Producer). (2015, Jan 14). Max Gladwell: Entreprenurship and Adventure Sports. *The Coefficient of FastSkinz*. Retrieved from http://www.maxgladwell.com/2009/01/coefficient-fastskinz/

Hansen, F. V. (1993). Surface Roughness Length. *Army Research Laboratory*.

Irwin, P. A. (2009). Wind engineering challenges of the new generation of super-tall buildings. *Journal of Wind Engineering and Industrial Aerodynamics, 97*(7-8), 328-334. doi: 10.1016/j.jweia.2009.05.001

Lorenzo Lignarolo, C. L., Patrick Teuffel. (2011). Shape morphing wind-responsive facade systems realized with smart materials.

Mook, F. J. R. v. (Producer). (2015, April 24). Wind. *Driving rain on building envelopes*. Retrieved from http://sts.bwk.tue.nl/drivingrain/fjrvanmook2002/node7.htm

Oeffner, J., & Lauder, G. V. (2012). The hydrodynamic function of shark skin and two biomimetic applications. *J Exp Biol, 215*(Pt 5), 785-795. doi: 10.1242/jeb.063040

P. Mendis, T. N., N. Haritos, A. Hira, B. Samali, J. Cheung. (2007). Wind Loading on Tall Buildings. *EJSE Special Issue: Loading on Structures*, 41-54.

Polygal. (2011). *Polygal Polycarbonate Multiwall Sheets: Technical Specifications*.

Roughness length. (2015, 04 18). *Wikipedia*. Retrieved from en.,.wikipedia.org/wiki/Roughness_length

S.A., T. S. (Producer). (2014). Permanent Suspended Access : Building Maintenance Units - Monorails - Gantries.

Taranath, B. S. (2012). Wind Loads. In T. F. Group (Ed.), *Structural Analysis andDesign of Tall Buildings: Steel and Composite Construction* (pp. 211-244): CRC Press.

Tetuya KAWAMURA, H. T., Kunio KUWAHARA. (1985). Computation of high Reynolds number flow around a circular cylinder with surface roughness. *Fluid Dynamics Research 1 (1986)*, 145-162.

Velo, A. (Producer). (2015, Jan 14). Q&A: Why doesn't AeroVelo's speedbike use Golf Ball Dimples? *Youtube*. Retrieved from https://www.youtube.com/watch?v=ZXpZy_A7mMk

Yann (Producer). (2015, Jan 14). Skin reduces drag: shark. *Ask Nature*. Retrieved from http://www.asknature.org/strategy/038caf2e453c09b3016465cc6ca93605#.VLZAsek5DI

11

Appendix A

Standard wind calculation for Wind Force (Fw) NEN-EN 1991-1-4

Basic wind velocity:	40	m/s
Building height:	400.00	m
Building width:	50.00	m

Fw=C_sC_dxc_fx$q_{p(ze)}$xA_{ref}

at height 5om = 971.58 N/m^2

at height 400m = 2085.48 N/m^2

Calculated from

q_p: peak velocity pressure (expression a)

C_f: Force coefficient (expression b)

C_sC_d: structure factor (expression c)

A_{ref}: reference area of the structure (in this case use 1m^2)

$$q_p(z) = [1 + 7.I_v(z)].\frac{1}{2}.\rho.v_m^2(z) \quad \text{(a.)}$$

at 50m = 1659.16 N/m^2

at 400m = 3356.80 N/m^2

Calculated from

I_v: turbulence intensity (expression a.1)

$V_m(z)$: Mean velocity at height = z (expression a.2)

ρ: air density (1.173 kg/m^3 at 50m, 1.126 kg/m^3 at 400m at 25^o Celsius and 0 relative humidity

$$I_v(z) = \frac{k_I}{c_o.\ln\left(\frac{z}{z_0}\right)} \quad \text{(a.1)}$$

at 50m = 0.355

at 400m = 0.204

Calculated from

K_I: turbulence factor, the recommended value = 1

C_o: Orography factor = 1

z: Height above ground with the same distance with building width

z_0: roughness length =3m (as very high density city)

$v_m(z) = c_r(z).c_o(z).v_b$ (a.2)

at 50m = 28.48 m/s

at 400m = 49.53 m/s

Calculated from

V_b: Basic wind velocity

C_r: Roughness factor (expression a.2.1)

$c_r(z) = k_r.\ln\left(\frac{z}{z_0}\right)$ (a.2.1)

at 50m = 0.712

at 400m = 1.238

Calculated from

K_r: terrain factor (expression a.2.2)

$k_r = 0.19.(z_0/z_{0,II})^{0.07}$ (a.2.2)

$Z_{o,II}$: terrain categorie II = 0.05m

$c_f = c_{f,0}.\psi\lambda$ (b.)

c_f = 0.597

$c_{f,0}$: force coefficient of circular cylinder (NEN-EN 1991-1-4 figure 7.28)
at 50m = 0.878
at 400m = 0.889

$\psi\lambda$: end-effect factor for elements with free-end flow = 0.68
(NEN-EN 1991-1-4 table7.16 and figure 7.36)

$C_sC_d = \frac{1+2.k_p.I_v(z).\sqrt{B^2+R^2}}{1+7.I_v(z_s)}$ (c.)

at 50m = 0.981

at 400m = 1.041

Calculated from

R^2: Resonance response factor, allow for turbulence in resonance with the vibration mode (expression c.1)

B^2: Background factor, allowing for the lack of full correlation of the pressure on the structure surface (expression c.2)

k_p: peak factor defined as the ratio of the maximum value of the fluctuating part of the response to its standard deviation (expression c.3)

$R^2 = \frac{\pi^2}{2.\delta}.S_L(z_s, n_{1,x}).K_s(n_{1,x})$ (c.1)

at 50m = 0.918

at 400m = 0.969

Calculated from

K_s: size reduction function (expression c.1.1)

δ: total logarithmic decrement of damping (expression c.1.2)

S_L: Non-dimensional power spectral density function (expression c.1.3)

$$K_s(n) = \frac{1}{1+\sqrt{(G_y.\emptyset_y)^2+(G_z.\emptyset_z)^2+(\frac{2}{\pi}.G_y.\emptyset_y.G_z.\emptyset_z)^2}} \quad \text{(c.1.1)}$$

at 50m = 0.090

at 400m = 0.154

Calculated from

G_y: 5/18 (NEN-EN 1991-1-4 Table C.1)

G_z: ½ (NEN-EN 1991-1-4 Table C.1)

$\emptyset_y$: $\emptyset_y = \frac{c_y.b.n}{v_m(z)}$

$\emptyset_z$: $\emptyset_z = \frac{c_z.h.n}{v_m(z)}$

C_z: Decay constants = 11.5 (NEN-EN 1991-1-4 Page 109)

b: Building width

h: Building height

$$\delta = \delta_s + \delta_a + \delta_d \quad \text{(c.1.2)}$$

at 50m = 0.085

at 400m = 0.088

Calculated from

δ_s: logarithmic decrement of structure damping = 0.08 (NEN-EN 1991-1-4 Table F.2)

δ_a: logarithmic decrement of aerodynamic damping for the fundamental mode (expression c.1.2.1)

δ_d: logarithmic decrement of damping due to special devices =0

$$\delta_a = \frac{c_f.\rho.v_m(z)}{2.n_1.\mu_e} \quad \text{(c.1.2.1)}$$

at 50m = 0.005

at 400m =0.008

Calculated from

n_1: fundamental frequency of along wind vibration = 46/h

μ_e: equivalent mass per unit area of the structure =pb.b

pb: volumetric mass of the building = 347.4 kg/m^3

$$S_L(z,n) = \frac{6.8\ .f_L(z,n)}{(1+10.2.f_L(z,n))^{5/3}} \quad \text{(c.1.3)}$$

at 50m = 0.175

at 400m = 0.113

Calculated from

$f_L(z,n)$: Non-dimensional frequency determined by the frequency $n=n_{1,x}$ (expression c.1.3.1)

$$f_L(z,n) = \frac{n.L(z)}{v_m(z)} \quad \text{(c.1.3.1)}$$

at 50m = 0.443

at 400m = 1.151

Calculated from

L(z): turbulent length at height (expression c.1.3.2)

$L(z) = L_t.(\frac{z}{z_t})^{\alpha}$ (c.1.3.2)

at 50m = 109.82

at 400m = 495.85

Calculated from

z_t: = 200m

L_t: = 300m

A = 0.67+0.05.ln(z_0)

$B^2 = \frac{1}{1+0.9\,.(\frac{b+h}{L(z_S)})^{0.63}}$ (c.2)

at 50m = 0.314

at 400m =0.542

$k_p = \sqrt{2.\ln{(v.t)}} + \frac{0.6}{\sqrt{2.\ln{(v.t)}}}$ (c.3)

K_p at 50m = 3.069

K_p at 400m = 3.045

Calculated from

t: Averaging time for the mean wind velocity = 600 second

v: Up-cross frequency (expression c.3.1)

$v = n_{1,x}\sqrt{\frac{R^2}{B^2+R^2}}$ (c.3.1)

v at 50m =0.099

v at 400m =0.092

Calculated from

$N_{1,x}$: natural frequency of the structure =46/h

Appendix B

Building load estimation

Floor plate area	1754.0	m^2
Floor thickness (post-tension concrete floor)	0.25	m
Number of floors	92	floor

Live load

Load per area	1	kN/m^2	
Load per floor	1753.996	kN	
Total live load	161367.61	kN	(a)

Dead load

Floor plate:	Concrete volume per floor	438.50	m^3	
	Concrete mass	2400	kg/m^3	
	Floor mass	1052397.43	kg	
	Load per floor	10313.49	kN	
	Total floor load	948841.52	kN	(b)
Installation:	Load per area	0.50	kN/m^3	
	Load per floor	877.00	kN	
	Total installation loads	80683.80	kN	(c)
Separation wall:	Load per area	1.2	kN/m^3	
	Load per floor	2104.79	kN	
	Total installation load	193641.13	kN	(d)
Façade load:	Normal façade			
	load per length	1	kN/m (estimation)	
	Length	150.86	m	
	Load per floor	150.86	kN	
	Total normal façade load	13878.86	kN	(e)
	Adaptive façade (not included)			
	Load per length	1	kN/m (estimation)	
	Length	150.86	m	
	Load per floor	150.86	kN	
	Total normal façade load	13878.86	kN	(f)
Structure load:	Calculated at outer core surface radius = 10.8 m			
	Inner core surface radius = 10.0 m			
	Assume that core thickness is equal all the height of the building			
	Total core load	4920.11.52	kN	(g)
	Column size 0.80x0.40 =	0.32	m^2	
	Number of columns	18	columns	
	Total columns load	54190.08	kN	(h)

Total building load (exclude (f))	**1944615.51**	**kN**
Total building floor area	**161367.61**	**m^2**
Building load per area	**12.05**	**kN/m^2**

Appendix C

Design choices comparison

The comparison table is on next page.

System	Design	Testing time (00.00 minute)	Result			
			Possitive peak pressure (pa)	Negative peak pressure (pa)	Highest velocity (m/s)	Drag coefficient
0 Circular building with second skin	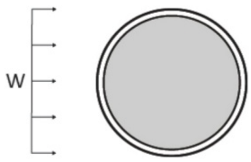	00.04	724.131	-1002.685	63.427	2.250
		00.08	795.220	-1234.066	57.663	1.680
		00.12	847.218	-917.309	50.127	1.830
		001.6	832.406	-799.699	50.357	1.720
1 Shape changing envelope	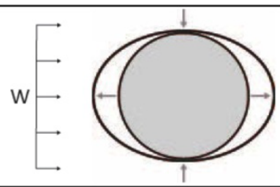	00.04	589.869	-713.649	68.578	1.440
		00.08	704.225	-899.610	70.026	1.290
		00.12	736.986	-1251.849	70.889	1.060
		001.6	757.348	-1208.508	66.257	1.120
2 Rotatable aerodynamic shape envelope	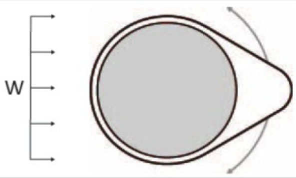	00.04	588.204	-830.256	63.731	1.590
		00.08	665.621	-949.792	66.486	1.440
		00.12	694.376	-1098.631	53.613	0.930
		001.6	657.007	-1507.728	56.498	0.600
3 Adaptable fins outer envelope 1 (two directions)	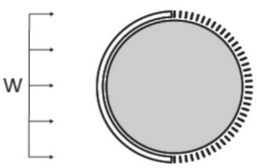	00.04	662.678	-932.782	65.674	0.190
		00.08	790.809	-1239.290	60.053	0.140
		00.12	839.304	-888.135	49.734	0.140
		001.6	822.325	-775.536	50.253	0.130
4 Adaptable fins outer envelope 2 (horizontal directions)	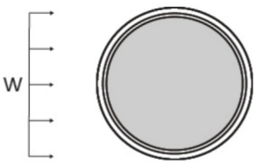	00.04	694.525	-790.782	82.919	0.200
		00.08	879.972	-1228.723	79.939	0.180
		00.12	845.762	-1063.581	69.424	0.140
		001.6	862.510	-941.902	69.382	0.140
5 Adaptable surface roughness by using membrane	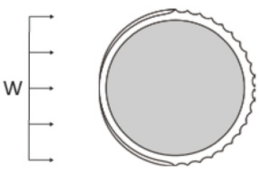	00.04	671.297	-940.604	71.098	1.920
		00.08	804.011	-1183.865	60.039	1.550
		00.12	824.068	-1115.886	49.937	1.400
		001.6	834.649	-903.878	49.643	1.480
6 Virtical axis wind turbine envelope	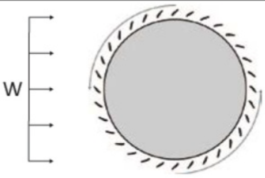	00.04	662.352	-933.667	65.486	1.280
		00.08	790.073	-1206.572	58.593	0.980
		00.12	841.876	-943.068	50.680	1.050
		001.6	817.566	-991.029	50.467	0.950

Development of negative pressure	Aerodynamic property	Assumption						Note
		Material cost	Construction difficulty	Maintenance aspect	Mechanical requirement	Energy requirement	User disturbance	
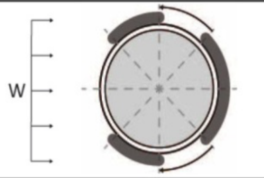 	I	IIIIII	IIIIII	IIIIII	IIIIII	IIIII	IIIIII	
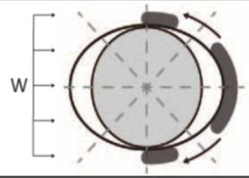 	II	IIII	IIII	IIII	IIII	IIII	IIIII	
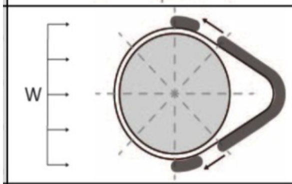 	IIIII	I	I	I	I	IIIII	II	- Presume that it is rotated by flow of the wind
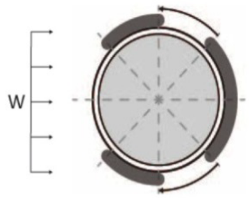 	IIIIII	IIIII	IIIII	IIIII	IIIII	II	III	
	IIIII	IIIII	IIIII	IIIII	IIIII	III	IIII	
	III	II	III	III	III	I	IIIII	
	IIII	III	II	II	II	IIIIII	I	- the analysis has been done without moving components - might be able to produce energy
	more (**I**) means better aerodynamic property	more (**I**) means cheaper	more (**I**) means easy to be built	more (**I**) means less maintenace	more (**I**) means less technology	more (**I**) means low energy needed	more (**I**) means more comfort	

Appendix D

Building core size reduction calculation

Bending moment calculation from point load

$M = FL$

M: Bending moment

F: Point load

L: Distance to suppor

Normal load

$F_{fl} = q.A_{fl}$

F_{fl}: Floor load

q: Distribute load (building load/m^2)

A_{fl}: Floor area

Bending stress

$\sigma_m = \frac{M_{max}.Z}{I}$

σ_m: Bending stress

M_{max}: Maximum bending moment

Z: Radius of the structure (core)

I: Second moment of area $I = \frac{\pi}{64}.(r_{out}^4 - r_{in}^4)$

Normal stress

$\sigma_n = F_{total}/A_{core}$

σ_n: Normal stress

F_{total}: Sum of all floor normal force

A_{core}: Cross-section area of the core

The calculation was done in excel sheet with optimizing the value of inner radius of the core (r_{in}) by keeping the thickness of the core =1m. From figure 4.6, combination of normal stress and bending stress should be zero or negative as compression at the base of the structure in the side where it receive the wind.

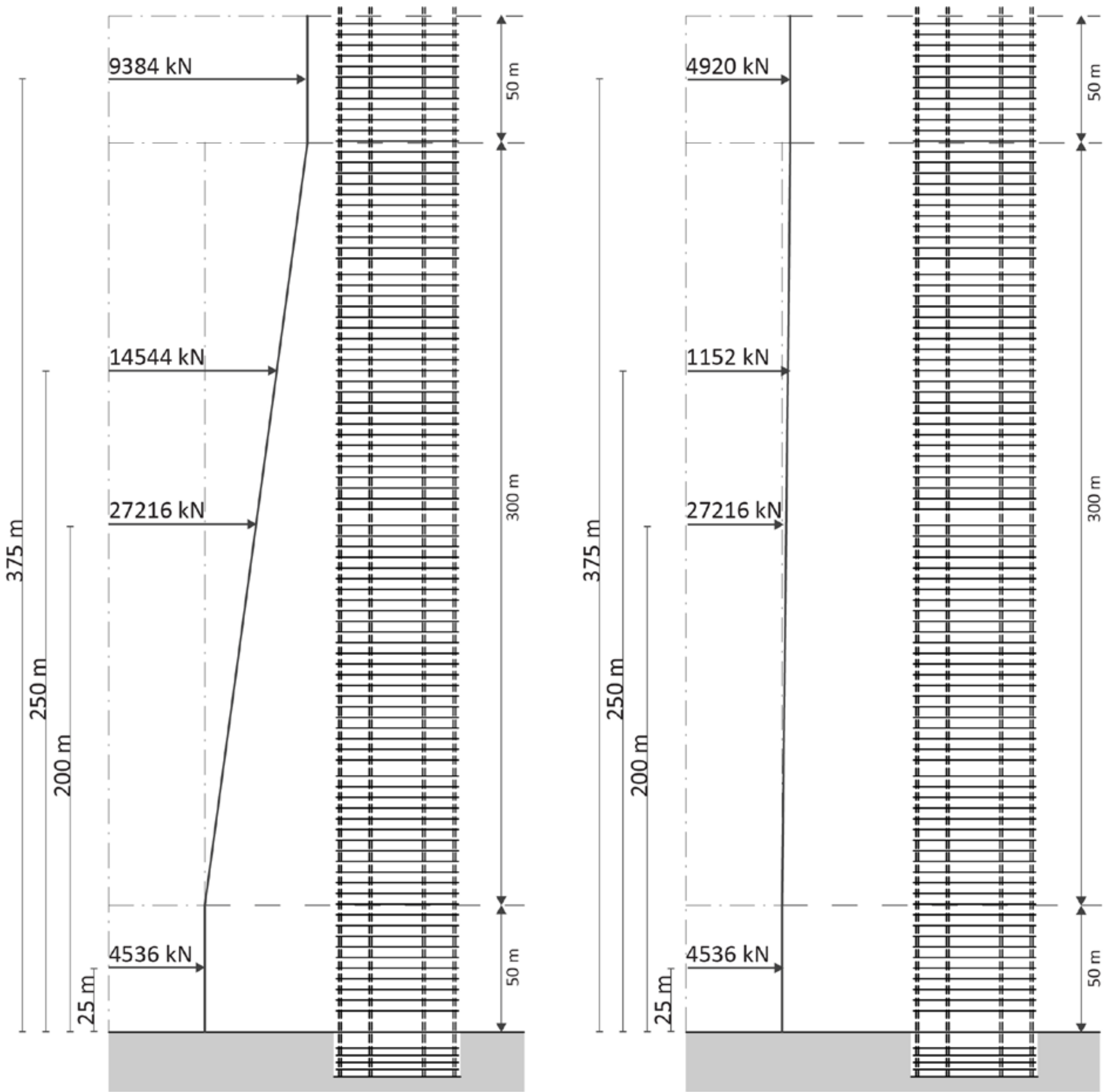

(A) Windload without adaptive facade (B) Windload with adaptive facade

Fig D.1: point loads translated from wind distributed loads

Smooth surface building			Adaptive facade building			Note
Bending Moment			**Bending Moment**			
M(A) :maximum M from load A	3519000	kNm	M(A) :maximum M from load A	1845000	kNm	
M(B) :maximum M from load B	3636000	kNm	M(B) :maximum M from load B	288000	kNm	
M(C) :maximum M from load C	5443200	kNm	M(C) :maximum M from load C	5443200	kNm	
M(D) :maximum M from load D	113400	kNm	M(D) :maximum M from load D	113400	kNm	
M(total)	**12711600**	**kNm**	**M(total)**	**7689600**	**kNm**	
Normal force			**Normal force**			
q : distributed load	12.05	kN/m^2	q : distributed load	12.14	kN/m^2	
A(fl) : floor area	1754	m^2	A(fl) : floor area	1754	m^2	
n(fl) : floor number	92	floor	n(fl) : floor number	92	floor	
F(fl)=q*A(fl)	21135.7		F(fl)=q*A(fl)	21293.56		
F(total)	**1944484.4**	**N**	**F(total)**	**1959007.52**	**N**	
Stress			**Stress**			
r(in)	13.05	m	r(in)	7.8	m	Note (a)
r(out)	14.05	m	r(out)	8.8	m	Note (b)
I=¶/64*((r(out)*2)^4-(r(in)*2)^4)	7829.490036		I=¶/64*((r(out)*2)^4-(r(in)*2)^4)	1803.566286		
σ(m)=M(total)*Z(core)/I	**22810.9339**	**kN/m^2**	**σ(m)=M(total)*Z(core)/I**	**37519.2642**	**kN/m^2**	
	22.81093394	kN/mm^2		37.51926421	kN/mm^2	
A=¶(r(out)^2-r(in)^2)	85.17142857	m^2	A=¶(r(out)^2-r(in)^2)	52.17142857	m^2	
σ(n)=F(total)/A(core)	**22830.2429**	**kN/m^2**	**σ(n)=F(total)/A(core)**	**37549.4322**	**kN/m^2**	
	22.83024287	kN/mm^2		37.5494322	kN/mm^2	
σ(n)>σ(m)			σ(n)>σ(m)			
A=σ(m)-σ(n)	-0.01930893	kN/mm^2	A=σ(m)-σ(n)	-0.030167988	kN/mm^2	Note (c)
B=-σ(m)-σ(n)	-45.64117681	kN/mm^2	B=-σ(m)-σ(n)	-75.06869641	kN/mm^2	

Optimization (Smooth) r(out)	σ(m)	σ(n)	σ(m)-σ(n)	Optimization (Adaptive) r(out)	σ(m)	σ(n)	σ(m)-σ(n)	Note
13.15	236581.6828	236144.9	436.8043	7.9	399557.7976	397019.5	2538.323	Range of optimizing
13.25	117830.8708	117623.5	207.3762	8	198466.9721	197253.3	1213.626	
13.35	78245.20218	78118.63	126.5681	8.1	131427.6994	130675.2	752.5265	
13.45	58450.9128	58367.89	83.02772	8.2	97902.02146	97393.84	508.1817	
13.55	46573.2478	46518.77	54.48225	8.3	77782.32017	77431.13	351.1929	
13.65	38653.95385	38620.45	33.50555	8.4	64366.03478	64127.63	238.4037	
13.75	32996.63523	32979.72	16.91339	8.5	54780.62159	54629.32	151.2987	
13.85	28753.09287	28749.98	3.1123	8.6	47589.79386	47509.19	80.60373	
13.95	25452.10397	25460.89	-8.78417	8.7	41995.60173	41974.45	21.15227	
14.05	22810.93394	22830.24	-19.3089	8.8	37519.26421	37549.43	-30.168	
14.15	20649.65992	20678.46	-28.802	8.9	33856.09283	33931.44	-75.3484	

Table D.1: Core size optimization calculation. The values of r(in) and r(out) are the radius of the inner surface and outer surface of the core relatively.

(a): r(in) is the optimizing input

(b): r(out)=r(in)+1meter

(c): A value should be close to zero but remain negative as compression in stress.

Range of optimizing shows that the thickness can be smaller in case of 14.05m radius core

Appendix E

Calculation for pneumatic tube extra support

Load from gravity per panel 102.10N

Load from gravity per support 204.20N

Bending moment

$M = F \cdot L = 204.20N \cdot 900mm = 183781.7Nmm$

Load and bending moment from wind per support in different position

$M = F \cdot L$

		Load at position (F) (N)	Half-length between support (L) (mm)	Bending moment (M) (Nmm)
0%	Horizontal	0	986.5	0
10%	movement	259.2	1067.85	276786.72
20%	movement	518.4	1149.2	595745.28
30%	movement	777.6	1230.55	956875.68
40%	movement	1036.8	1311.9	1360177.92
50%	movement	1296	1393.25	1805652
60%	movement	1555.2	1474.6	2293297.92
70%	movement	1814.4	1555.95	2823115.68
80%	movement	2073.6	1637.3	3395105.28
90%	movement	2332.8	1718.65	4009266.72
100%	half transformed	2592	1800	4665600

Lateral load to the pneumatic tube

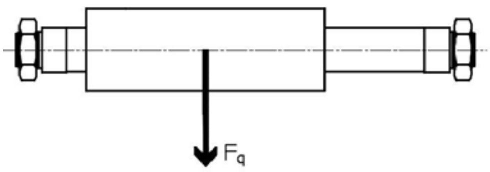

Load (Fq) from gravity

Fin position	Half-length between supports (mm)	**Force (Fq) (N) from bending moment from gravity load**
Horizontal position	173	**1062.32**
10% transformed	336	**547.46**
20% transformed	498	**368.74**
30% transformed	661	**277.99**
40% transformed	824	**223.09**
50% transformed	987	**186.30**
60% transformed	1149	**159.92**
70% transformed	1312	**140.09**
80% transformed	1475	**124.63**
90% transformed	1637	**112.25**
Vertical position	1800	**102.10**

Load (Fq) from windload

Fin position	Half-length between supports (mm)	Bending moment (Nmm) from windload	**Force (Fq) (N) from bending moment from windload**
Horizontal position	1800	0.00	**0.00**
10% transformed	1637	276786.72	**169.05**
20% transformed	1475	595745.28	**404.00**
30% transformed	1312	956875.68	**729.38**
40% transformed	1149	1360177.92	**1183.59**
50% transformed	987	1805652.00	**1830.36**
60% transformed	824	2293297.92	**2783.80**
70% transformed	661	2823115.68	**4270.33**
80% transformed	498	3395105.28	**6812.01**
90% transformed	336	4009266.72	**11943.00**
Vertical position (half transformed)	173	4665600.00	**26968.79**

H beam second moment of area

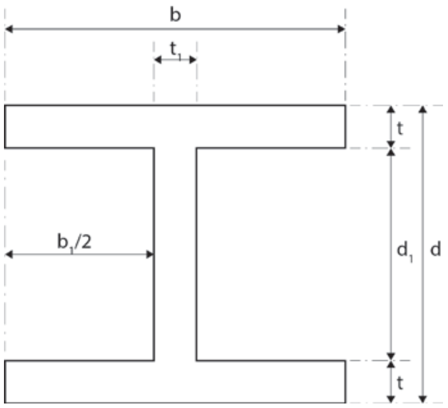

Width (b): 40mm
Height (d): 35mm
Horizontal plate thickness (t): 5mm
Vertical plate thickness (t_1): 5mm

$$I = \frac{bd^3}{12} - \frac{b_1 d_1^3}{12} = 97343.75$$

Elastic modulus (Young's modulus)

Aluminum: 69 GPa
Stainless steel: 180 GPa

Displacement Calculation

Option one: Pin support

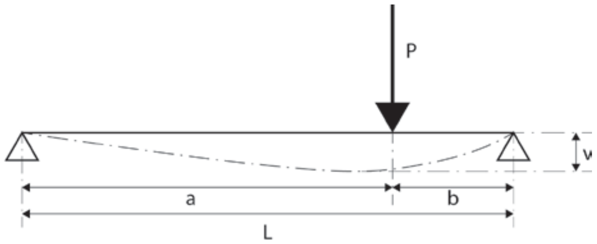

$$v = \frac{Pb(L^2 - b^2)^{3/2}}{9\sqrt{3}IEL}$$

Fin position	Displacement from gravity load (mm)	Displacement from wind load (mm)	Total displacement (mm)
10% transformation	1.54	0.48	1.53
20% transformation	1.98	2.17	3.82
30% transformation	2.07	5.43	7.35
40% transformation	1.97	10.43	12.36
50% transformation	1.73	17.00	18.73
60% transformation	1.41	24.52	25.93
70% transformation	1.04	31.81	32.85
80% transformation	0.67	36.65	**37.32**
90% transformation	0.32	33.65	33.97

Option two: Clamp support

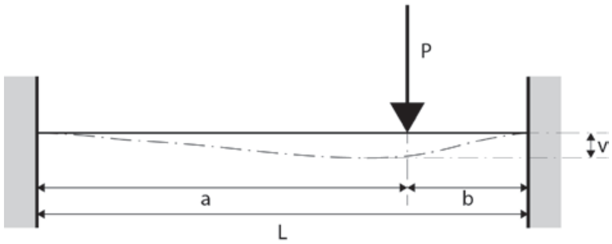

$$v = \frac{126Pb^2a}{3EI(L + 2a)}$$

Fin position	Displacement from gravity load (mm)	Displacement from wind load (mm)	Total displacement (mm)
10% transformation	0.03	0.01	0.03
20% transformation	0.07	0.07	0.14
30% transformation	0.11	0.29	0.40
40% transformation	0.15	0.77	0.92
50% transformation	0.17	1.71	1.89
60% transformation	0.10	1.82	**1.92**
70% transformation	0.06	1.68	1.73
80% transformation	0.02	1.26	1.28
90% transformation	0.01	0.58	0.58

Appendix F

Additional adaptive façade cost vs. core material reduction cost

Additional adaptive façade cost

	Items	amount	units	price(€)/unit	price (€)
1	**Single fin**				
	Panels	8	pieces		
	Polycarbonate 10mm 1.37m^2/piece				
	2.1x6m = 6 pieces	1.33	pieces	99.00	132.00
	Aluminum structure volume	129.60	kg	1.70	220.32
	Aluminum 2d hinge volume	17.28	kg	1.70	29.38
	Ball joint + U profile	6.48	kg	1.70	11.02
	Total per one fin				392.71
	Total fins	**5112**	**units**		**2007543.74**
2	**Single frame side**				
	Polyester composite	79.20	kg	2.40	190.08
	Steel connection to structure	30.00	kg	1.53	45.90
	40mm Pneumatic tube	2	units	560.00	1120.00
	Total per one frame				1355.98
	Total frame	**10080**	**units**		**13668278.40**
3	**System**				
	pneumatice switch	2520	units	65.00	163800.00
	Pressurised tube Ø 65mm (tube thickness = 2.9mm)	147.71	m/floor		
		10340.00	m total	1.85	19092.83
	Main pressurised tube (set 1) 4 floors Ø 400mm	16.80	m	11.74	197.30
	Main pressurised tube (set 2) 7 floors Ø 400mm	29.40	m	11.74	345.27
	Main pressurised tube (set 3) 10 floors Ø 400mm	42.00	m	11.74	493.24
	Main pressurised tube (set 4) 13 floors Ø 400mm	54.60	m	11.74	641.21
	Main pressurised tube (set 5) 18 floors Ø 400mm	75.60	m	11.74	887.83
	Main pressurised tube (set 6) 22 floors Ø 400mm	96.60	m	11.74	1134.45
	Air pump	18	units	3150.00	56700.00
	Air tank (2.00m^3)	18	units	900.00	16200.00
	Total				259492.12
	other equipment	10	% of total		25949.21
	Total system cost				**285441.33**
4	Total additional façade material cost				15961263.47
	Construction cost	30	% of total		4788379.04
5	**Total additional façade cost**				**20749642.51**

Building core material reduction

	Items	amount	units	price(€)/unit	price (€)
1	**Original core**				
	Outter radius	14.05	m		
	Inner radius	13.05	m		
	cross-section area	85.17	m^2		
	total concrete volume	34341.12	m^3		
	total concrete mass	82418688.00	kg	0.23	18956298.24
2	**New core**				
	Outter radius	8.80	m		
	Inner radius	7.80	m		
	cross-section area	52.17	m^2		
	total concrete volume	21035.52	m^3		
	total concrete mass	50485248.00	kg	0.23	11611607.04
3	**Total material & cost reduction**	**13305.60**	**m^3**		**7344691.20**

Comparison of additional adaptive façade cost and core structure material reduction

	Items	price (€)
1	Total additional adaptive façade cost	20749642.51
2	Total core material & cost reduction	7344691.20
3	**Differences**	**13404951.31**

Energy requirement vs. increasing of rentable area

Pneumatic system sizing calculation

	Item			Note
1	**Pneumatic tube**			
	Diameter Ø	0.04	m	(1.1)
	Length	2.50	m	(1.2)
	Operation presure	1.3-7	bar	
	Air volume (1.1)x(1.2)	0.003	m^3/unit	(1.3)
2	**floor presurised tube**			
	Number of façade frame per floor	144	units	36x4
	Number of pneumatic tube per floor	144	pairs	(2.1)
	Required presurised air volume for adapting façade per floor : volume of presurised tube each floor (1.3)x(2.1)	0.453	m^3	(2.2)
	Tube length	147.714	m	(2.3)
	Tube cross-section area (2.2)x(2.3)	0.003	m^2	(2.4)
	Tube diameter	0.062	m	
		65.00	mm	
	Total tube length (2.3)xno.floor	**10340**	**m**	
3	**Main presurised tube**			
	set 1: 4 floors			
	height	16.80	m	(3.1)
	Floor pressurized tube volume (2.2)xno.floor	1.81	m^3	(3.2)
	Tube cross section area (3.2)/(3.1)	0.10	m^2	
	Tube diameter	0.37	m	
		40	**mm**	

	Item			Note
	set 2: 6 floors			
	height	29.40	m	(3.3)
	Floor pressurized tube volume (2.2)xno.floor	2.72	m^3	(3.4)
	Tube cross section area (3.4)/(3.3)	0.09	m^2	
	Tube diameter	0.34	m	
		40	**mm**	
	set 3: 10 floors			
	height	42.00	m	(3.5)
	Floor pressurized tube volume (2.2)xno.floor	4.53	m^3	(3.6)
	Tube cross section area (3.6)/(3.5)	0.11	m^2	
	Tube diameter	0.37	m	
		40	**mm**	
	set 4: 12 floors			
	height	54.60	m	(3.7)
	Floor pressurized tube volume (2.2)xno.floor	5.43	m^3	(3.8)
	Tube cross section area (3.8)/(3.7)	0.10	m^2	
	Tube diameter	0.36	m	
		40	**mm**	
	set 5: 17 floors			
	height	75.60	m	(3.9)
	Floor pressurized tube volume (2.2)xno.floor	7.69	m^3	(3.10)
	Tube cross section area (3.10)/(3.9)	0.10	m^2	
	Tube diameter	0.36	m	
		40	**mm**	
	set 6: 21 floors			
	height	96.60	m	(3.11)
	Floor pressurized tube volume (2.2)xno.floor	9.50	m^3	(3.12)
	Tube cross section area (3.12)/(3.11)	0.10	m^2	
	Tube diameter	0.35	m	
		40	**mm**	

Air pump calculation

	Air pump		Unit	air tank size	Unit
	Air volume required by adaptive system to chang 2/3 of all façade per one floor	0.30	m^3/floor	0.50	m^3/floor
	Adapting speed	30	second		
1	set 1: 4 floors				
	air volume required	1.21	m^3	2.02*	m^3
	Air providing by pump	0.04	m^3/second	1unitx2.00	m^3
		40.23	litre/second		
2	set 2: 6 floors				
	air volume required	1.81	m^3	3.02*	m^3
	Air providing by pump	0.06		2unitsx2.00	m^3
		60.34	litre/second		
3	set 3: 10 floors				
	air volume required	3.02	m^3	5.04*	m^3
	Air providing by pump	0.10	m^3/second	3unitsx2.00	m^3
		100.57	litre/second		
4	set 4: 12 floors				
	air volume required	3.62	m^3	6.05*	m^3
	Air providing by pump	0.12	m^3/second	3unitsx2.00	m^3
		120.69	litre/second		
5	set 5: 17 floors				
	air volume required	5.13	m^3	8.57*	m^3
	Air providing by pump	0.17	m^3/second	4unitsx2.00	m^3
		170.97	litre/second		
6	set 6: 21 floors				
	air volume required	6.33	m^3	10.58*	m^3
	Air providing by pump	0.21	m^3/second	5unitsx2.00	m^3
		211.20	litre/second		
7	**Total number of air tank (2 m^3)**			**18**	**units**
	Total number of air pump (Speed: 4680 litre/hour, Max pressure: 7 bar)			**36**	**units**

*air tank size that is calculated from air volume require is the size of the tank where the air is used and still have the pressure that is high enough to operate the façade for couple of time more. In this case, it is 1.67 times the required air which can be used approximately 3-4 times without adding new air.

Energy requirement

Energy requirement		
Input power per one air pump	530	W
Total power need for air pump	19.080	kW
Controller energy used per unit	0.014	kW
Total controller energy used (~18units)	0.252	kW
Presume that the system work	24	h/day
Energy price per kWh (the Netherlands)	0.26	EUR
Energy cost per day	120.63	EUR
Energy cost per month	3618.95	EUR
Energy cost per year	**44030.56**	EUR

Increasing of renting income

Floor plate radius	23.00	m
Floor plate area	1662.57	m^2
Original core radius	14.05	m
Original core area	620.41	m^2
Original rentable area	**1042.16**	**m^2**
New core radius	8.80	m
New core area	243.38	m^2
New rentable area	**1419.19**	**m^2**
Rentable area increase	377.03	m^2/floor
Total rentable area increase	**33178.20**	**m^2**

Rental price examples	area (m^2)	Price (EUR)/month	Price/area/month
Hongkong International Finance Center II	2196.00	406177.85	184.96
Singapore One Raffles Quay (D01)	2879.97	305891.00	106.21
Singapore Premium Office New Downtown	2229.65	252607.27	113.29
Bangkok Park Ventures Ecoplex			33.99
Dubai Office Commercial in Downtown Burj Dubai	5202.57	369072.70	70.94
Shell and core office in Downtown Burj Dubai	10405.14	738145.40	70.94
Average office rental price			**96.72**

Average rental increased income per year = 96.72x33178.2x12 = 38509362.78 EUR
Presume that the 80% of the area is rented, income per year = 30807490.00 EUR

Payback period

Additional cost for façade - core material reduction	13404951.31	EUR	(1)
Energy consumtion from façade	44030.56	EUR/year	(2)
Average rental gain per year (from the increased area)	38509362.78	EUR/year	
Presume 80% of area is rented (from the increased area)	30807490.23	EUR/year	(3)
Benefit for first year = (3) - (1) - (2)	17358508.35	EUR	
Benefit after payback time = (3) – (2)	30763459.66	EUR/year	
Payback time (only for façade part) = (1)x12/((3)-(2))	**5.24**	**months**	

Appendix F references

Cellular Polycarbonate. (2015, 06 17). Weisa. Retrieved from http://www.weisa.lv/en/polikarbonats/sunu-polikarbonats/

Magnetically Coupled Rodless Cylinder-CY1B series Rodless cylinder-CY1B40-H-1000mm. (2015, 06 17). AliExpress. Retrieved from http://www.aliexpress.com/item/Magnetically-Coupled-Rodless-Cylinder-CY1B-series-Rodless-cylinder-CY1B40-H-1000mm/1942462187.html

Pneumatic Directional Control Valves, 2-way, 3-way or 4-way air or solenoid operated. (2015, 06 17). AliExpress. Retrieved from http://www.omega.com/pptst/V60_Series.html

Foshan Hongke air compressor. (2015, 06 17). Alibaba.com. Retrieved from http://www.alibaba.com/product-detail/Foshan-Hongke-air-compressor-europe_1684947365.html

FRP Pressure Tank, Pentair FRP tank. (2015, 06 17). Alibaba.com. Retrieved from http://www.alibaba.com/product-detail/FRP-Pressure-Tank-Pentair-FRP-tank-_60085702761.html

Pendular piston pump / air. (2015, 06 17). Direct Industry. Retrieved from http://www.directindustry.com/prod/knf-neuberger/product-9163-61755.html

Electricity pricing. (2015, 06 17). Wikipedia. Retrieved from https://en.wikipedia.org/wiki/Electricity_pricing

2 International Financial Center. (2015, 06 17). Primeoffice.com.hk. Retrieved from http://www.primeoffice.com.hk

2 International Financial Center. (2015, 06 17). Primeoffice.com.hk. Retrieved from http://www.primeoffice.com.hk

For Rent - One Raffles Quay (D01). (2015, 06 17). Commercial Guru.com.sg. Retrieved from http://www.commercialguru.com.sg

For Rent – Premium Office Grade A Infrastructure New Downtown (D01). (2015, 06 17). Commercial Guru.com.sg. Retrieved from http://www.commercialguru.com.sg

Park Ventures Ecoplex. (2015, 06 17). CBRE Thailand. Retrieved from http://www.cbre.co.th

Office Commercial in Downtown Burj Dubai. (2015, 06 17). Just Rentals.com. Retrieved from http://www.justrentals.com

Shell and core office for rent in Downtown Burj Dubai. (2015, 06 17). Dubizzle. Retrieved from http://dubai.dubizzle.com